Comparison of Frost Heave Prediction Models

by

NEIL A. CHANDLER

A thesis
presented to the University of Manitoba
in partial fulfillment of the
requirements for the degree of
Master of Science
in
Civil Engineering

Winnipeg, Manitoba

ISBN 0-315-33961-6

COMPARISON OF FROST HEAVE PREDICTION MODELS

BY

NEIL A. CHANDLER

A thesis submitted to the Faculty of Graduate Studies of the University of Manitoba in partial fulfillment of the requirements of the degree of

MASTER OF SCIENCE

ACKNOWLEDGEMENTS

I would like to acknowledge the guidance of Dr. L. Domaschuk during the preparation of this thesis. I would also like to thank Dr. Sven Knutsson from the Division of Soil Mechanics, University of Luleå, Sweden, for his assistance during his stay in Canada.

ABSTRACT

The objective of this study was to compare the accuracy and ease of use of published frost heave models. The six models investigated were those developed by: Konrad and Morgenstern; Sheriff,Ishibashi and Ding; Arakawa; Knutson; Penner and Walton; and Takashi, Yamamoto, Ohrai and Masuda. The report first examines the basic mechanisms of frost heaving and outlines the factors that influence its magnitude. Published theories are then explained in terms of these influencing factors. The study goes into detail on how the soil parameters or relationships required for each of the various theories were obtained and the statistical accuracy of these parameters. The models were used to predict the frost heaving during freezing tests carried out at the University of Manitoba between 1974 and 1983. No one theory provided consistently accurate results but the models outlined by Konrad and Morgenstern, Penner and Walton, and Takashi et al. were recommended for use under specific conditions.

CONTENTS

LIST OF TABLES

LIST OF FIGURES

Chapter I

INTRODUCTION

Frost action and its destructive nature are of concern to engineers in northern climates throughout the world. The destructive aspect may be heaving of roadways and buried pipelines, frost jacking of piles, forces against buried structures and thaw-weakening of the soil. Extensive research facilities exist in such countries as Canada, U.S.A., Norway, Sweden, Japan, Russia, and Great Britain and are presently being used to study the soil freezing phenomenon. Researchers have developed several theories and models for the prediction of frost penetration and frost heaving since early in the century, but it has not been until recent years that models for the prediction of ice lensing have gained a good deal of acceptance. These models may range in complexity from a simple freezing index solution to a sophisticated computer simulation which involves coupled heat and moisture flow relationships. Many of these solutions are discussed in the body of this thesis.

When a frost susceptible soil freezes the downward progression of the freezing front is normally accompanied by an upward heaving of the surface of the soil. This heaving is the result of the combined effects of the expansion of water at phase change and the segregation of freezing moisture into discreet bands of massive ice known as ice lenses. In order for ice lenses to form there must be sub-zero temperatures, available moisture and a frost susceptible soil. The degree to which a soil will heave under given conditions depends upon its frost susceptibility. The frost susceptibility of a particular soil type has until now only been defined in very general terms.

The purpose of this study was to examine some of the accepted theories and to compare methods of predicting the degree of frost heaving with the results of frost heave experiments carried out in the laboratory. It is hoped that from these comparisons an acceptable method of predicting the frost heave of a given soil can be recommended.

Chapter II

THE MECHANICS OF FROST HEAVING

The three conditions that must be met before frost heaving will occur are:

1. subfreezing temperatures;
2. available moisture;
3. a frost susceptible soil.

These conditions alone are not enough to ensure that heaving will indeed happen. The degree to which heaving will occur and, in fact, if it will occur at all, depends on many factors. The important factors are: the rate of frost penetration, the rate of heat removal, subsurface temperature gradients, frozen and unfrozen hydraulic conductivities, the depth to the water table, overburden stresses, the pore structure of the soil and degree of saturation. Most of the conditions affecting the degree of frost heave are interelated, that is if one is changed others are affected.

2.1 CAPILLARY THEORY

When the temperature of the surface is lowered below the freezing point an unsteady heat flow situation is created. The heat imbalance will result in the progression of the freezing front into the unfrozen soil. The rate of this frost penetration is largely dependant upon the rate of heat removal and hence the thermal conductivity of the soil. Ice crystals will begin to form in the pores of the soil matrix. Once this occurs a suction potential is established which may be sufficient to draw moisture towards the freezing front. This suction is the driving mechanism behind the phenomenon of frost heaving.

The cause of the suction potential which exists in a freezing soil has been under investigation for many decades. Taber(1929) felt that the water migration was due to "molecular cohesion" and was related to void ratio, particle sizes and rate of cooling. Beskow(1935) stated that the suction was due to capillary rise and therefore related to grain size and depth to the water table. Penner(1957) concluded that the magnitude of suction depended on the pore geometry, smaller pore sizes resulting in higher suctions. The works of researchers such as Miller, Gold, Penner, Everett and Haynes, during the early 1960's, established that the suction is related to the ice/water interfacial energy and the radii of the pores in the soil matrix. Everett(1961) described the relationship using the following equation:

$$Pi - Pw = 2\sigma iw / Riw \quad (1)$$

in which:

P_i = the pore pressure in the ice

P_w = the pore water pressure (or suction)

σ_{iw} = the ice/water interfacial energy

R_{iw} = the ice/water interfacial radius.

The value of Riw (the radius of the ice/water interface) becomes the radius of the pore necks, as shown in Figure 1.

The relationship between pore size and capillary suction is the basis of what is now known as the capillary frost heave model. This process is similar to capillary rise due to surface tension at an air/water interface. Heaving, for this model, is related not only to the pore geometry but to several other factors. The permeability of the unfrozen soil will affect the flow of moisture through the soil to the ice lens. The rate of heat extraction will influence the rate at which the segregated moisture can freeze, and the stress above the growing ice lens will have the effect of reducing the suction immediately below it. All these variables together, however, are not enough to explain the thickness to which an ice lens will grow in a freezing soil.

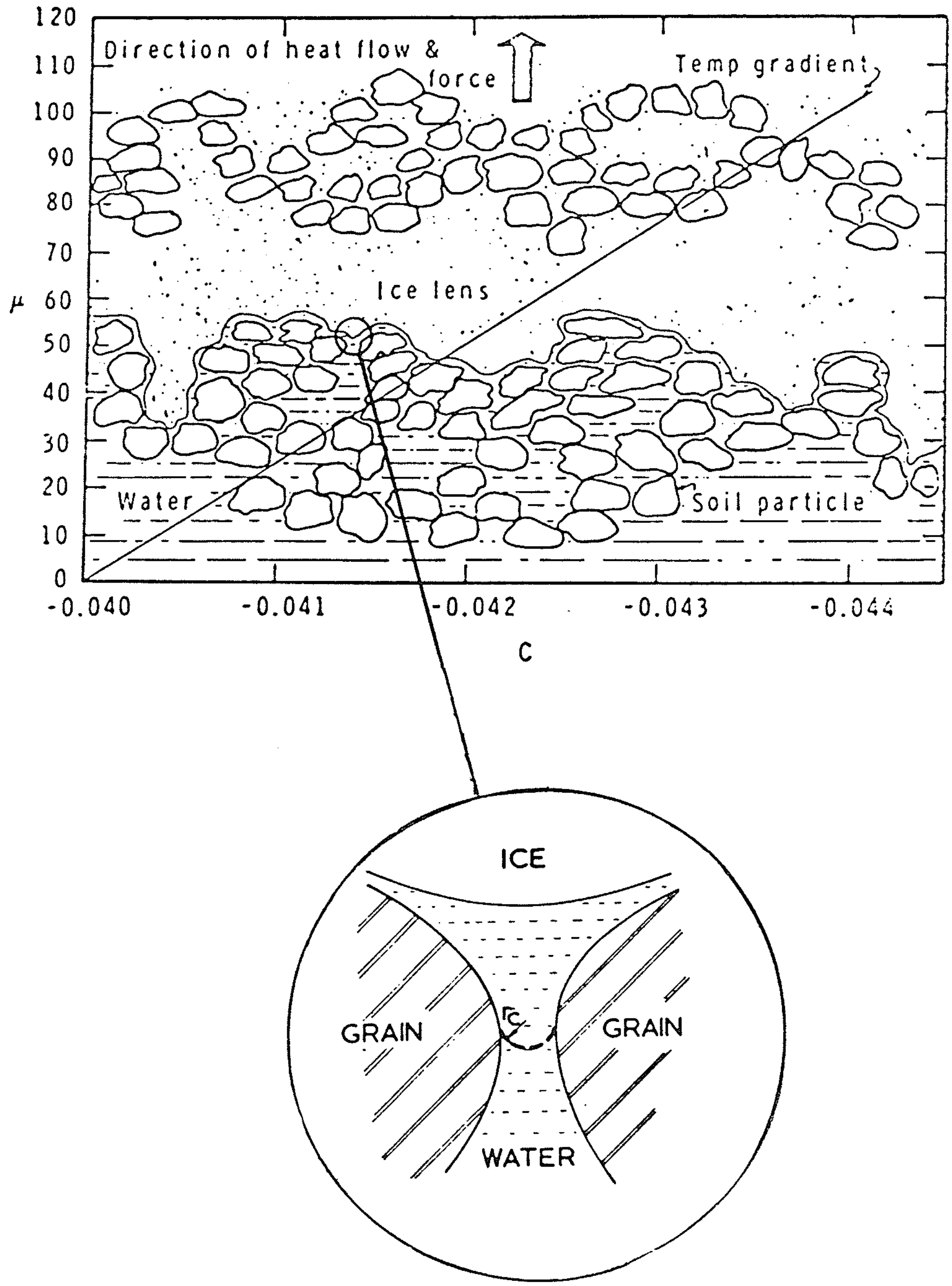

Figure 1: Source of capillary suction potential (after Penner 1972, above, and Holden, Jones and Dudek 1981, below)

2.2 SECONDARY HEAVE THEORY

Experimental results appeared to show some discrepancies between the laboratory heaving pressures and those calculated using Equation 1. This discrepancy was explained by Penner(1973) who stated that an ice lens would begin to form immediately above the smallest pores producing the large suctions that were being experienced. Miller(1972) explained that the capillary theory alone would only produce needle ice and was not sufficient to generate thick ice lenses. Miller's solution to this problem, which is termed the theory of secondary heaving, has now gained general acceptance.

An integral part of the theory of secondary heaving is the existence of a partially frozen zone just above the freezing front and below the ice lens. In this region, termed the "frozen fringe", both ice and liquid water are being transported. Researchers have since noted the existence of the frozen fringe which has been stated to be anywhere from a millimeter to several centimetres in thickness (Loch 1979,Horiguchi 1978). The rate at which water travels through the frozen fringe towards the ice lens is the limiting factor to its rate of growth.

Konrad and Morgenstern(1980) describe the freezing process of a soil based on a continuously advancing frost front and unsteady heat flow within the frozen fringe itself. Capillary suction will initiate the movement of moisture upwards through the frozen fringe. After a sufficient amount of moisture is accumulated a discreet ice lens may form. Since the frost front is still advancing, the temperature within the frozen fringe will continue to decrease with time and the thickness of the zone of partially frozen moisture will increase. Figures 2 and 3 show the temperature gradient profile, the suction potential profile, and the permeability profile within the frozen fringe and the changes of each of these characteristics with the advance of the frost front. As the temperature of the frozen fringe decreases ice will begin to form in the pores of the soil matrix and the formation of ice will reduce the permeability of the partially frozen soil. As the flow of moisture becomes restricted due to the decreased permeability, the suction potential will be increased. This suction is therefore related to the ice content of the soil pores and hence to the soil temperature. This pressure to temperature relationship can be closely modelled by the Clausius Clapeyron equation:

$$\frac{Pw}{\rho w} = \frac{Pi}{\rho i} = \left(\frac{L}{K}\right) T \qquad (2)$$

in which:

Pw = the water pressure (or suction)

Pi = the ice pressure

ρw and ρi = the densities of water and ice respectively

L = the latent heat of fusion

K and T = the temperatures in °K and °C respectively.

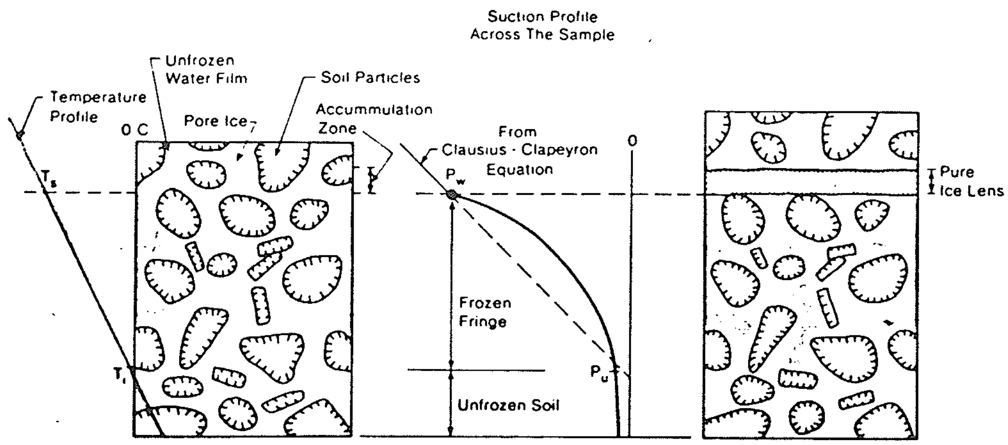

Figure 2: Temperature gradient and suction potential in a freezing soil (from Konrad and Morgenstern 1980)

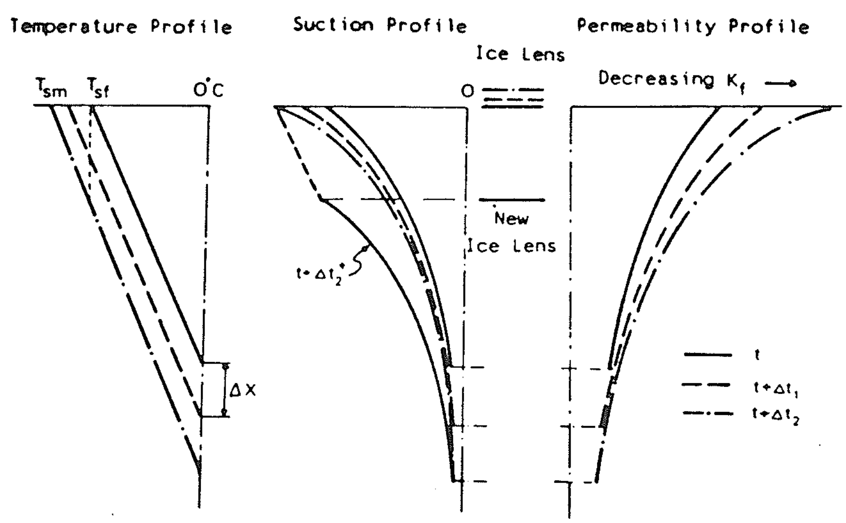

Figure 3: Variation of temperature, suction and permeability with time (from Konrad and Morgenstern 1980)

Since a temperature gradient exists across the frozen fringe, so does a hydraulic gradient. The hydraulic gradient will draw moisture up from the unfrozen soil to the ice lens.

As the frost front advances, the temperature of the frozen fringe will drop and the permeability below the ice lens will decrease. At a temperature which is sufficiently low, the soil will become impermeable and the flow is stopped. An ice lens will begin to form at a greater depth, its position depending on local permeability and the temperature at which ice will begin to form in the pores of the soil matrix. This process will be repeated as the freezing front advances and successive ice lenses are formed in a process known as rythmic banding.

2.3 ADSORPTION FORCE THEORY

The theory as put forward by Takagi in 1977, varies significantly from the capillary and secondary heave theories. The driving force for the flow of water towards a growing ice lens is the tension that exists in the unfrozen film of water between the ice and the soil particles. This theory is illustrated in Figure 4. As the film of water is being turned into ice just below the ice lens, loss of thickness of this film water generates a tension that draws moisture up from the unfrozen soil. The suction created is related to the tension gradient in the film water. Similar to the

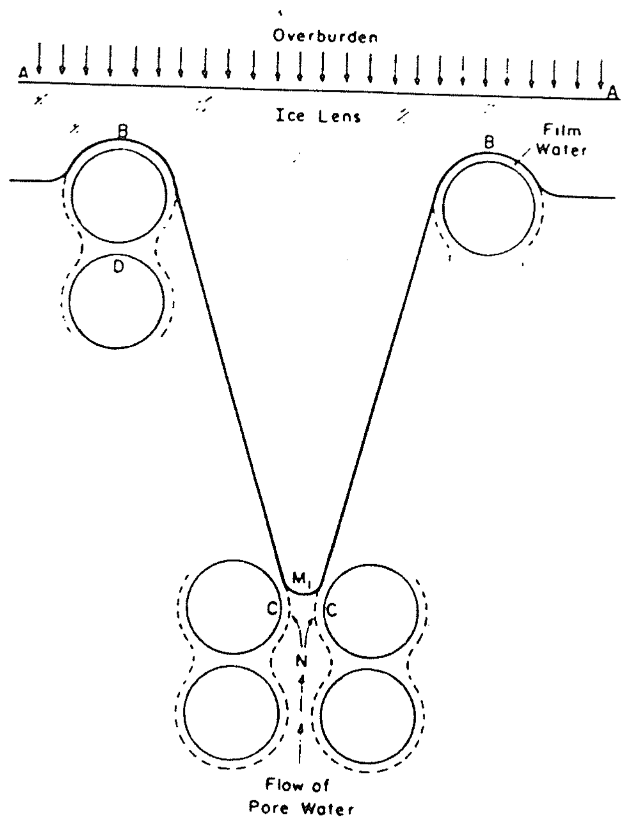

Figure 4: Adsorption force frost heave theory (from Takagi)

secondary heave theory, Takagi suggests that there is a zone of partially frozen soil, which he terms the zone of diffused freezing, where the flow of water will be affected by the temperature gradient. This theory is related to the amount of unfrozen water and hence will be related to the specific surface area of the soil particles. The rate of heat removal will govern the freezing of the soil moisture. The temperature gradient within the zone of diffused freezing and the thickness of this zone will affect the flow of water to the ice lens. The theory as yet has no simple solution and will not be discussed in the following chapters.

2.4 FACTORS AFFECTING FROST HEAVE

The various factors that influence the degree to which heaving will occur have already been mentioned. These factors and their significance are summarized below.

2.4.1 The Rate of Frost Penetration

The rate of frost penetration is the rate at which the freezing front (or the 0° isotherm) moves into the unfrozen soil. When the freezing front moves quickly through the soil mass there is little time for the moisture to flow to the ice lens before the pores of the soil become frozen and the frozen fringe is rendered impermeable. For a slow moving frost front the rate of cooling of the frozen fringe is much less and as a result, more time is available for moisture to flow to the ice lens.

The rate of cooling is a term which can be related to the rate of frost penetration. The rate of cooling is defined as the temperature drop of the soil per unit time. The rate of frost penetration multiplied by the temperature gradient in the frozen fringe will yield the rate of cooling of the frozen fringe.

Researchers (Carlson et al. 1983, Kaplar 1970, Takashi et al. 1978) have investigated the effect of the rate of frost penetration on the amount of frost heave. Konrad and Morgenstern refer to the rate of cooling, rather than the rate of frost penetration, as a factor influencing the potential for frost heave.

2.4.2 The Rate of Heat Removal

Penner(1972) stated that the rate of heat extraction is the basic variable in the frost heave process. This value can be defined as the rate of heat transfer in the frozen soil less the rate of heat transfer in the unfrozen soil. The difference between these two values is the latent heat of fusion given off as the moisture in the soil freezes. Analytically this can be represented by:

$$Q = L = kf\ dTf/dx - ku\ dTu/dx \qquad (3)$$

in which:

Q = the rate of heat flow

L = the total latent heat of fusion

kf and ku = the frozen and unfrozen thermal conductivities respectively

dTf/dx and dTu/dx = the temperature gradients at the frost front of the frozen and unfrozen soils respectively.

The rate of heat extraction is related to the rate of cooling by the following equation :

$$dT/dt \times C = dQ/dx \qquad (4)$$

where:

dT/dt = the rate of cooling

C = the volumetric heat capacity of the soil

dQ/dx = the derivative of the heat flow rate with respect to depth.

Increasing the frost penetration rate, and hence the rate of cooling, will lead to a greater amount of latent heat being extracted. Researchers have tried to relate the rate of heat removal to the rate of frost heaving. Beskow(1935) and Loch(1977) felt that the rate of heave was independent of the rate of heat removal, but their tests were conducted over only a narrow range of heat extractions (Charleson 1981). Kaplar(1970) and Freden(1965) felt that the rate of heaving was directly proportional to the rate of heat extraction. Horiguchi(1978) and Loch(1979) said that there was a non-linear relation between frost heave and heat extraction, and that for small values of heat flow rates the rate of frost heaving is related to the rate of heat extraction. The theories presented above are expanded upon in the section dealing with heat flow prediction models.

2.4.3 Temperature Gradients

The temperature gradient of a freezing soil is an integral parameter in most of the mechanisms contributing to the frost heave process. The temperature gradient directly controls the thickness of the frozen fringe (Konrad and Morgenstern 1980). The rate of cooling of the partially frozen zone is dependent upon both the temperature gradient and the rate of frost penetration. The rate of heat flow is analytically described as the temperature gradient times the thermal conductivity. This will again indicate an interrelationship between the various parameters involved in the frost heave process.

As mentioned in the section on secondary heaving, the soil suction potential and the hydraulic conductivities are temperature dependent. This will establish a hydraulic gradient from warm to cool within the frozen fringe, which will increase or decrease as the temperature gradient changes. This will in turn increase or decrease the flow of moisture to the ice lens. Freden(1965) and the segregation potential theory of Konrad and Morgenstern(1980,1981,1982a,1982b) describe the effect of temperature gradient on the suctions induced. These researchers propose that the moisture flux is directly proportional to this temperature gradient.

2.4.4 Overburden Pressure

Taber(1929) was probably the first to realize that increasing the pressure on a freezing soil had the effect of decreasing the amount of heave. It wasn't until researchers (such as Penner and Ueda, 1978) began to investigate models that related pressure to the total amount and rate of frost heave that this idea was developed. Konrad and Morgenstern(1982) and Carlson et al.(1982) suggested that by increasing the overburden pressure the pressure in the ice is increased as well. From Equation 1, increasing the ice pressure will reduce the capillary suction in the freezing soil. The relationship between applied pressure and frost heave is important when considering a frost heave model.

There is some debate as to the existence of a theoretical "shut-off" pressure. This is the pressure exerted on the ice lens at which moisture flow towards the ice lens is stopped or perhaps reversed. McRoberts and Morgenstern(1975) stated that this pressure exists and is a function of soil type. The applied pressure neccessary to stop the flow of moisture to the ice lens would be close to zero for granular soils. It was proposed that the effective stress below an ice lens is a constant for any given soil type. Higher applied pressures would result in higher pore pressures in order to keep the effective stress at a constant value. This pore pressure increase would be accompanied by an expulsion of water away from the frost front. In opposition to this theory, Penner and Ueda(1978) found that no shut-off pressure existed below 465 KPa for clays,silts or sands. They demonstrated that the expulsion of water is followed by intake if a sufficient amount of time is allowed. Konrad and Morgenstern(1982) stated that if the rate of cooling is kept low (0.01 °C/hr) the shut-off pressure, should it exist, would be beyond the engineering range of applied pressures.

The expulsion of water away from the frost front has been observed when both the overburden pressure and the rate of frost penetration were increased (Takashi et al. 1978, Penner and Ueda 1978, McRoberts and Morgenstern 1975). This is a consideration that may become important when modelling the amount of frost heave of a granular material or when the rate of cooling is expected to be large.

2.4.5 Soil Moisture Conditions

The potential for frost heave will increase with an increase in the availability of soil moisture. As the degree of saturation increases and the height above the water table decreases, the possibility of generating thick ice lenses will become greater. Flow of water to the freezing front will be reduced if the suction potential has to overcome interparticle and gravitational forces. Theories are available which relate the depth to the water table to the magnitude of frost heave (see for example Chalmers and Jackson 1970). The degree of saturation, moisture content, and the density of the soil not only affect the magnitude of the suction which draws water to the ice lens but also the amount of heave that will occur due to expansion of the 'in-situ' water as the soil is frozen.

The physical and thermal factors mentioned in this chapter are all very much interrelated. There is no one solution that rigorously models all the processes involved. Other factors, such as freeze-thaw cycling, have been said to be of significance but are not well understood. Many of these processes are difficult to model accurately and involve relationships that are not easily determined, such as the variation of unfrozen water content or the permeability of the frozen fringe with changes in temperature. Some researchers have attempted to more rigorously model the soil freezing problem with the use of computer simulations, while others have aimed towards making a simpler solution based on easily determined soil characteristics.

Chapter III

FROST HEAVE PREDICTION MODELS

The extent that a freezing soil would heave was originally indicated by classifying the soil as having a high or low degree of frost susceptibility. The classification of frost susceptible soils was first carried out by Casagrande(1931). Improvements to this classification have been attempted by too many workers to mention, but Casagrande's grain size definition is still used with considerable success by many highway construction authorities as the basis for determining a frost susceptible soil. Until the 1960's, researchers had not attempted to make actual predictions based on one or more aspects of the soil freezing mechanism (such as pore sizes, surface temperature, or rate of heat transfer). The prediction models examined in this section range from completely empirical to rigorous computer simulations based on coupled heat and moisture flow.

3.1 EMPIRICAL MODELS

The empirical models for ice lensing generally relate an easily determined soil characteristic to the total amount of frost heaving or to the heaving rate. These soil characteristics may include pore size or grain size distribution, or perhaps liquid limit (Rieke et al. 1983), or a combination of these. Although these models show a good experimental fit with the published data, they may or may not be applicable to all soil types or tests carried out under dissimilar conditions.

3.1.1 Sheriff, Ishibashi and Ding (1976)

A quantitative relationship between values of freezing temperature, freezing time, percent fines and the total heave was established. This involved the freezing of five blends of silty Ottawa sands at three constant freezing temperatures. The samples were prepared at their optimum moisture content and frozen in a 300 mm freezing cell for roughly 72 hours. The test results were used to empirically determine a frost heave equation relating total heave to percent fines, time and a constant subzero temperature. This relationship was:

$$H = F^{0.61}\, t^{0.83-0.063\,\theta}\, J \qquad (5)$$

in which:

H = amount of heave (mm)

F = percent finer than 0.02 mm by weight

t = freezing time (days)

θ = absolute value of surface freezing temperature (°C below zero)

J = a factor depending upon θ (refer to Figure 5).

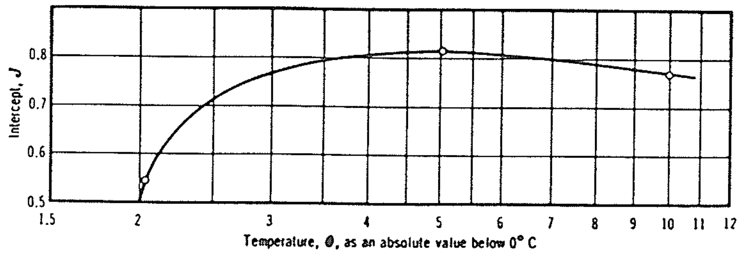

Figure 5: The variation of J with θ

3.1.2 Reed, Lovell, Altschaeffle and Wood (1979)

In the theory put forward by Reed et al., the total heaving rate of silty soils was related to the pore size distribution. Three clays and three clayey silts were tested under rapid freeze, constant temperature heaving tests. A constant rate of frost heave was experienced to the end of the 48 hour tests. This justified the use of relating the pore size distribution to the frost heave rates. Pore sizes were felt to control the migration of water in the soil and would also provide a description of the soil fabric. A regression analysis was carried out between the heave rates and cumulative porosities, and pore size distribution indicators. This method of analysis provided a reasonably good fit with the experimental data.

$$Y = -0.3805 + 1.6940(D_{40}/D_{80}) \tag{6}$$

or

$$Y = -5.46 - 29.46(X_{3.0})/(X_0-X_{0.4}) + 581.1(X_{3.0}) \tag{7}$$

where:

Y= frost heave rate (mm/day)

D_{40} = pore diameter where 40% of the pores are larger

D_{80} = pore diameter where 80% of the pores are larger

$X_{3.0}$ = cumulative porosity for pores > 3.0 μm but < 300 μm

$X_{0.4}$ = cumulative porosity for pores > 0.4 μm but < 300 μm

X_0 = total cumulative porosity.

3.1.3 Knutson (1973)

In this model frost heave data was collected from field observations and then related to the freezing index, moisture content, and the degree of frost susceptibility. This was achieved by the use of a soil factor 'β' which could be chosen from a table which uses frost suceptibility and freezing index as input (from Saetersdaal 1980). The values of β are summarized in Table 1. The relation (Equation 8) is very simple:

$$\Delta H = \beta \cdot Wf \cdot \Delta X \qquad (8)$$

where:

ΔH = increase in heave

ΔX = increase in frost penetration

Wf = frozen moisture content

β = soil factor relating to freezing index.

TABLE 1

Values of β to be used in equation 8

(from Saetersdaal 1980)

	Freezing Index (°C hrs)		
	10,000	20,000	30,000
Very Frost Susceptible	0.4 - 0.7	0.3 - 0.4	0.2 - 0.3
Medium Frost Susceptible	0.2 - 0.4	0.2 - 0.3	0.15 - 0.2
Low Frost Susceptible	0.1 - 0.2	0.1 - 0.2	0.1 - 0.15
Water	0.09		
Sand	0 - 0.2		

3.2 ICE SEGREGATION RATIO

The rate of increase of total heaving has, in many cases, been related directly to the rate of frost penetration. Knutson's work (Equation 8) could be rewritten so that the ratio of ΔH to ΔX can be determined. The ratio of ΔH to ΔX is termed the Ice Segregation Ratio (or ISR). In other words it is the ratio of the total heave to the depth of frost penetration. This parameter will not be constant throughout any single experiment but may be easilly related to other parameters such as frost penetration rate and over-burden pressure.

$$\text{Heave} = \Sigma\ (\Delta ISR(\dot{X},P)\ \Delta X) \qquad (9)$$

in which:

ΔISR = Ice Segregation Ratio for a specific time increment

$\dot{X}$ = frost penetration rate

P = pressure above the growing ice lens

ΔX = increase in depth of frost penetration.

This relationship should be consistent for a soil type and independent of testing procedure. Once the relationship between Ice Segregation Ratio and the parameters which affect it is known, then the heave can be determined, but first the amount of frost penetration must be known or predicted.

3.2.1 Carlson, Ellwood, Nixon and Slusarchuk (1982)

A frost heave test facility in Calgary has generated considerable frost heave data. The total heave was plotted from these results against the frost penetration and the plot was divided into straight line sections (see Figure 6). The slope of these lines appear to be directly related to the rate of frost penetration. The ice segregation ratio can be defined as a function of two parameters: the rate of frost penetration and the overburden pressure at the frost front (as indicated in equation 9). The amount of heave is then equal to the ISR multiplied by the increase in frost depth. The authors of this paper provide no relationship but state that such a solution would be empirical and could be derived from both field and laboratory tests.

3.2.2 Takashi, Yamamoto, Ohrai and Masuda (1978)

These researchers carried out several experiments at constant frost penetration rates under different overburden pressures. The two soil types used in this experiment were both undisturbed, overconsolidated blends of silt and clay cut into 100 mm diameter samples. The observed total frost heave was found to be inversely proportional to both the square root of the rate of frost penetration and to the overburden stress. These basic relationships were used to derive a formula, using empirically determined soil constants, for the rate of moisture flowing to or from the freezing front. Figure 7 compares the Takashi's experimental results to the values obtained from the following relationship:

$$\frac{\Delta w}{\Delta X} = \frac{1}{1.09} \frac{P_0}{P} \left(1 + \sqrt{\frac{U_0}{\dot{X}}} \right) - nf \frac{0.09}{1.09} \qquad (10)$$

The ratio of the total heave to the depth of frost penetration (ISR) are:

$$ISR = P_0 / P \left(1 + \sqrt{U_0 / \dot{X}} \right) \qquad (11)$$

in which:

$\Delta w/\Delta X$ = moisture flux to the frost front

nf = porosity of the frozen soil

ISR = Ice Segregation Ratio

P_0 , U_0 are soil constants

P = overburden pressure

$\dot{X}$ = frost penetration rate.

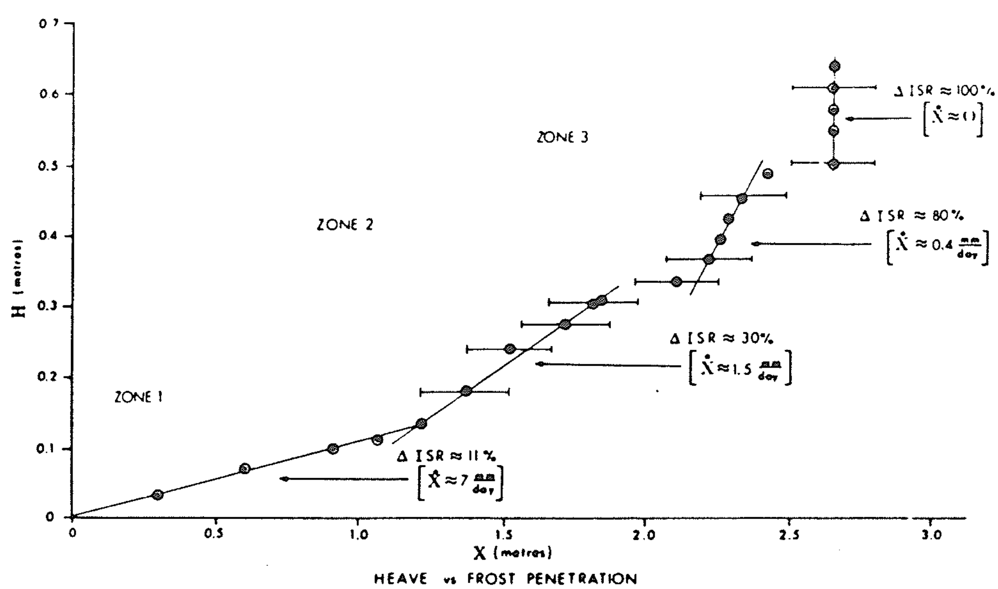

Figure 6: Ice segregation ratio plot (from Carlson et al. 1982)

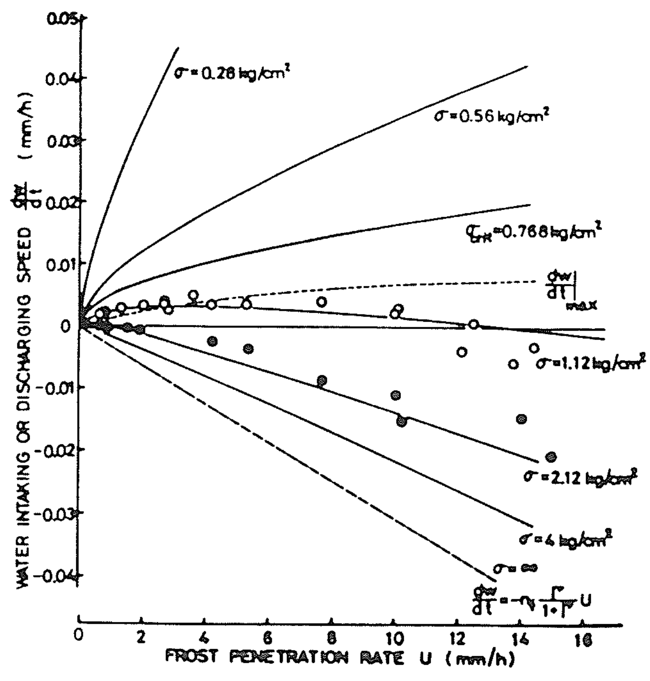

Figure 7: Relation between moisture flux, frost penetration rate and pressure (from Takashi et al. 1978)

3.2.3 Penner and Walton (1979)

The influence of overburden pressure and cold side freezing temperature was recognized by Penner and Ueda (1978). They conducted extensive laboratory frost heave experiments on eight various soil types ranging from clay to silty sand. All the tests were carried out under constant freezing temperatures between -0.3 and -3.95 °C and under applied vertical pressures between 10 and 400 KPa. Penner and Ueda concluded that:

1. heaving occurred at a constant rate for the initial stages of freezing and
2. the rate of heaving was related to the pressure to temperature ratio (P/T) in accordance with Equation 11:

$$\Delta H/\Delta t = a \exp\{ -b\ P/T \} = R_0 \qquad (12)$$

where:

R_0 = the initial heaving rate

$\Delta H/\Delta t$ = the rate of frost heaving

a , b = soil parameters

P = external pressure

T = cold side freezing temperature (°C).

Penner and Walton carried out three long term experiments and found that the heave rate decreased from this initial value with an increase in time and depth of frost penetration. This was said to be due to an accumulating percentage of ice in the frozen soil. The ice segregation ratio was related to time, the initial heave rate (R_0 calculated from Penner and Ueda), and the depth of frost penetration.

$$ISR = 1 - \exp \{ -R_0 \, t/X \} \qquad (13)$$

in which:

t = time

X = frost penetration

R_0 = the initial heave rate.

3.3 HEAT FLOW MODELS

Beskow (1935) wrote that the rate of frost heaving was independent of the rate of heat exchange. Since Beskow's article the effect of heat flow on the rate of frost heaving has been investigated with many different results. Important research relating heat flow to frost heave was carried out by Horiguchi (1978) and Loch (1979). The conclusion was that as the rate of heat removal from the freezing front increased, the rate of heaving would increase, reach a maximum, and then decrease. The maximum heave rate was found to be dependent upon soil particle size and soil chemistry (see Figure 8). It is important to look at a wide range of heat flow rates when studying its relationship to frost heaving. The conclusion drawn from a set of tests carried out at low rates of heat extraction could be that the heave rate is proportional to heat flux, but at high rates it may be that heat flux and heave rate are independent of each other. This may explain some of the discrepancies between the works of different researchers. Still, the relationship between heat flux and rate of heaving is an important one and the prediction models which use this theory should be investigated.

3.3.1 Segregation Efficiency (Arakawa 1965)

The segregation efficiency is the ratio of the heat flow required to freeze segregational ice (which is the ice that makes up the ice lenses) to the total heat flow at the frost front. When the rate of frost penetration has diminished and only heaving is occurring, the efficiency ('E') is said to be perfect and its value is equal to one. When a non frost susceptible soil is being frozen without ice segregation, 'E' is equal to zero. In most instances the efficiency lies between zero and one. It is neccessary to understand how the ice segregation efficiency is related to the frost heave process before a prediction model can be established.

Penner(1972) used Arakawa's efficiency theory to create a simple prediction model. He found that the value of 'E' was related to the frost penetration rate and that this relation was a characteristic of the soil. Penner went on to state that the segregation efficiency would decrease with increasing frost penetration rate. Using Penner's theory and Equation 2, the segregational frost heave can be determined by the following relation:

$$\Delta Hs = \frac{E(\dot{X})}{L} \left(kf \frac{dTf}{dx} - ku \frac{dTu}{dx} \right) \Delta t \qquad (14)$$

in which:

ΔHs = segregational heave

L = latent heat of fusion

$E(\dot{X})$ = the segregation efficiency as a function of the frost penetration rate ($\dot{X}$)

kf, ku = the frozen and unfrozen thermal conductivities

$dTf/dx, dTu/dx$ = the frozen and unfrozen temperature gradient at the freezing front.

3.3.2 Temperature Gradients (Freden 1965)

Freden proposed that the moisture migration towards an ice lens was proportional to the temperature gradient between the ice lens and the unfrozen soil. This zone, which is similar in definition to the frozen fringe, has a temperature dependent suction potential. A temperature gradient creates a corresponding pressure (or suction) gradient which induces moisture to flow to the ice lens. The rate of flow (or the rate of heaving) is linearly proportional to the temperature gradient in this "boundary layer" or frozen fringe. This is shown experimentally with tests on three soils: a silty fine sand; a clayey silt; and a heavy clay. Freden's results are presented in Figure 9. Since the temperature gradient is proportional to heat flow then it can be stated that the rate of heaving is linearly related to both the heat flow and temperature gradient. Freden's relationship can be simply expressed in the equation:

$$\Delta H = C \times dTf/dx \quad \Delta t \tag{15}$$

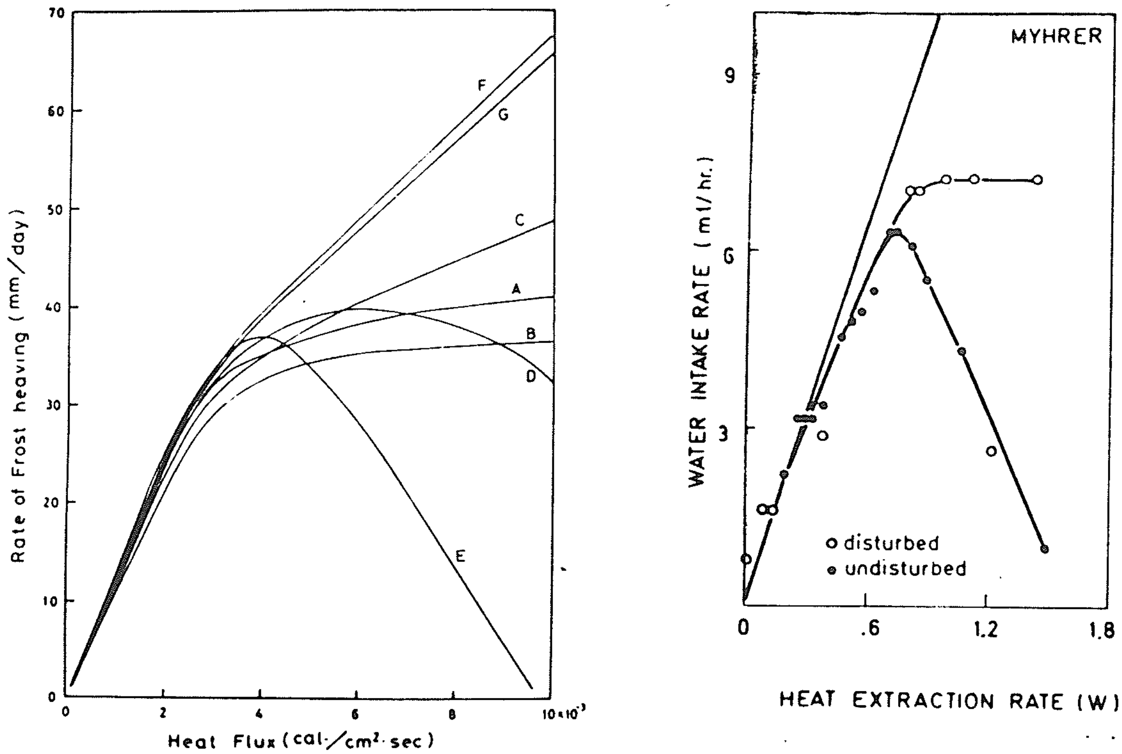

Figure 8: Relation between frost heave rate and heat flux for 7 powdered zeolites (Horiguchi 1978) and Myhrer silt (Loch 1979)

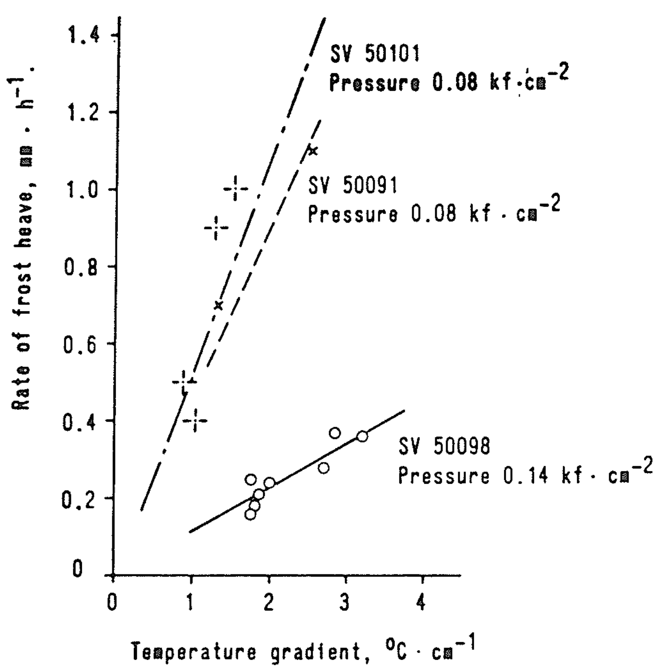

Figure 9: Relation between frost heave rate and temperature gradient (from Freden 1965)

where:

ΔH = incremental increase in total frost heave

dTf/dx = the temperature gradient in the frozen fringe

C = a constant of proportionality that is characteristic of soil type

Δt = time increment.

3.4 SEGREGATION POTENTIAL THEORY

The segregation potential theory was presented by Konrad and Morgenstern in a series of four articles between 1980 and 1982. The basic theory is similar to that of Freden(1965) where the moisture flux is directly related to the temperature gradient in the frozen fringe. Large suctions are created by large temperature gradients causing a greater flow of moisture to the ice lens. Konrad and Morgenstern go on to define the effect of applying an external load to a freezing fine-grained soil. An external pressure will have the effect of reducing the suction immediately below the warmest ice lens as well as increasing the unfrozen water content. The segregation potential theory defines the relationship between pressure and moisture flux and states that this relationship is a property of a certain type of soil.

The segregation potential ('SP') is defined as the ratio of moisture flow to the temperature gradient in the frozen fringe. The segregation potential can be derived from a small number of freezing tests conducted under different pressures. The following relationship can be developed between SP and external pressure (Pe):

$$SP = SP_0 \times \exp\{-a\ Pe\} \qquad (16)$$

where SP_0 is the segregation potential at zero applied load and 'a' is a soil constant.

The amount of heave can be computed by using:

$$\Delta H = (SP \times dTff/dx) \times 1.09\ \Delta t + 0.09\ \epsilon\ n\ \Delta X \qquad (17)$$

in which:

ΔH = the change in total heave

Δt = the time increment

ΔX = the increase in frost penetration

$dTff/dx$ = the temperature gradient in the frozen fringe

ϵ = factor accounting for unfrozen water

n = porosity.

3.5 COMPUTER SIMULATIONS

There have been several computer simulations developed to model the frost heave process. They are generally solutions to the coupled heat and moisture flux problem. Miller (1977) explains the processes involved by modelling the Clausius Clapeyron pressure temperature relation (Equation 2), the Laplace surface tension equation (Equation 1), the Terzaghi effective stress principle, Darcy's law for fluid flow and the Fourier equation for sensible heat flow. Application of the model cannot be carried out before several assumptions regarding the hydraulic and thermal properties are made(Guymon et al. 1981). These properties include the pore pressure to hydraulic conductivity relation, temperature effects on unfrozen water content, thermal conductivities, heat capacities, freezing point depression temperatures, unfrozen water content to pressure relation and the hydraulic conductivity in partially frozen soils as a function of temperature. Researchers who have provided finite difference and finite element solutions to this problem include Gilpin, Outcalt, O'Neal, Guymon, Hromodka, Berg and Johnson to name a few.

The present report will concentrate on simpler and more usable solutions. The prediction models investigated in this thesis will allow the heaving characteristics of any soil type to be determined by conducting a small number of frost heave experiments, and will involve only a few parameters or relationships.

Chapter IV

ANALYSIS OF FROST HEAVE EXPERIMENTS

The present report attempts to determine whether or not the amount of frost heave measured at the ground surface can be predicted using selected frost heave models. In this chapter the experimental procedure and the data are reviewed and the procedure for determining the soil parameters and relationships used in the various frost heave theories are outlined.

4.1 MEASURED FROST HEAVE DATA

Over thirty frost heave tests were carried out at the University of Manitoba between 1974 and 1983 and the results of these tests were summarized in two papers prepared by Domaschuk (1982,1984). The primary purpose of these tests was to measure frost heave forces on piles and buried structural elements. Surface heaving and the air and subsurface temperatures were measured in addition to the measurement of heaving pressures.

4.1.1 Test Apparatus and Procedures

A total of four different freezing chambers were used in the experiments. Their size ranged from a large scale pit to a small freezing cell. Their dimensions were as follows:

1. a 100 mm diameter by 125 mm segmented ringed cell;
2. an 800 mm deep by 600 mm square tank;
3. a 1.76 m by 2.40 m diameter circular tank; and
4. a 1.83 m by 2.40 m square pit.

The instrumentation is shown in Figures 10 to 13. The tests were carried out at either constant surface temperatures or constant rates of frost penetration. Since these tests were concerned with measuring frost heave pressures, information important for the purpose of evaluating the amount of surface heave was either not recorded or not adequately measured. No more than two dial gauges were used to measure surface heave for any one test. Frost penetration was assummed to be horizontal and soil temperature gradients were estimated from thermocouples spaced vertically at 25 or 50 mm. Soil densities and moisture contents were evaluated generally only before and not after the tests. Measurements of heat or moisture flow were not taken. These deficiencies are not serious but they could account for some scatter and low statistical confidence in the results.

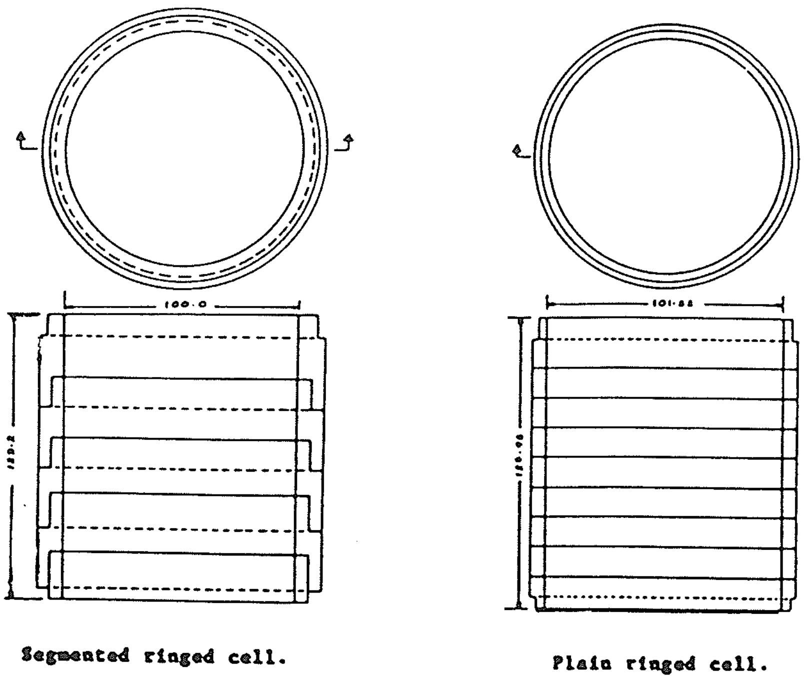

Figure 10: 100 mm diameter by 125 mm cylindrical cells

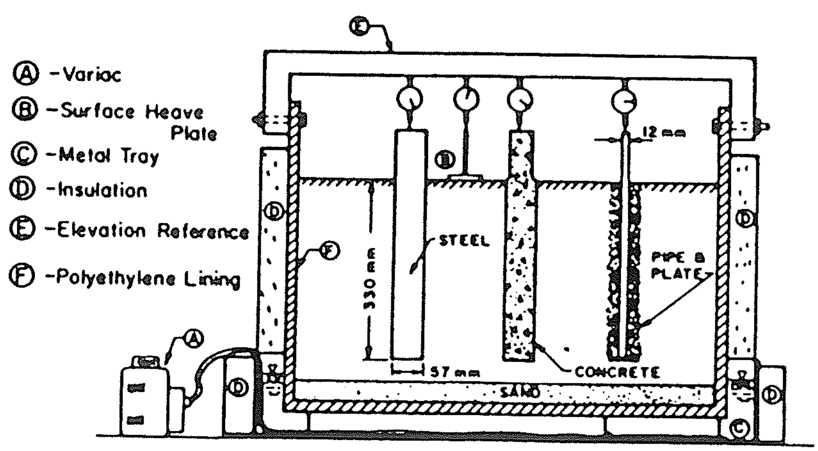

Figure 11: 800 mm deep by 600 mm square tank

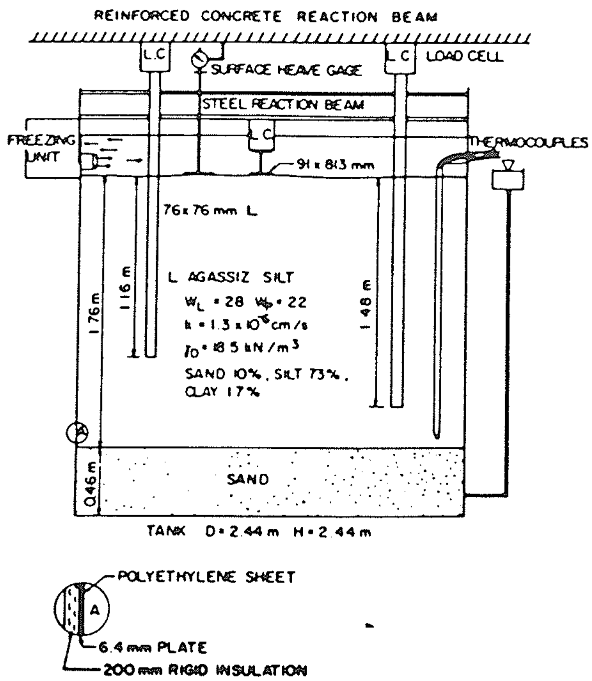

Figure 12: 1.76 m by 2.40 m diameter circular tank

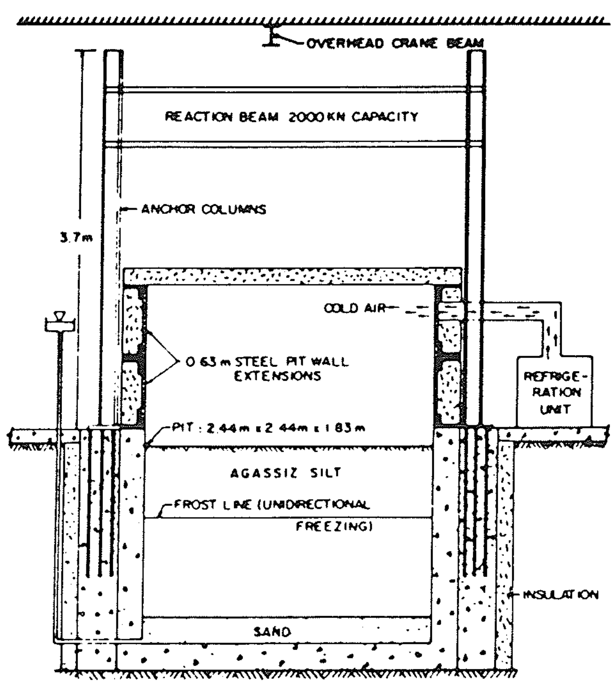

Figure 13: 1.83 m by 2.40 m square pit

4.1.2 Soil Types

Three types of soil were used in the experiments: a plastic silt (Agassiz silt); a non plastic silt (Piney silt); and a well-graded sand. Agassiz silt is a soil common to the Winnipeg area and is known to be frost susceptible. Piney silt is found in south eastern Manitoba and is highly frost susceptible. The sand which contains a small amount of silt was of low frost susceptibility. The soil properties and the grain size distributions are included in Appendix A. The densities and moisture contents of the soils varied from test to test. The majority of the experiments involved light compaction of the soil. In one of the small scale tests the soil was compacted to maximum dry density at the optimum water content.

4.1.3 Summary of Frost Heave Experiments

For the purpose of the writer's analysis, the laboratory frost heave tests were divided into two groups:

1. preliminary tests to be used for the determination of the soil parameters necessary for the frost heave equations; and
2. frost heave tests used to check the accuracy of the predictive models.

Four tests for each soil type were chosen arbitrarily to serve as the preliminary tests. Table 2 summarizes both the preliminary and predictive frost heave experiments analyzed in this study.

TABLE 2

Summary of Frost Heave Experiments

Test No.	Soil Type	Apparatus	Freezing Conditions	Test Length (hrs)
Preliminary Tests for Determining Model Parameters				
A1	Agassiz silt	1.83m x 2.40m square pit	Constant surface temp -7 °C	3600
A2	Agassiz silt	1.83m x 2.40m square pit	Constant freezing rate 4 mm/day	2400
A3	Agassiz silt	1.76m x 2.40m round tank	Constant freezing rate 28 mm/day	900
A4	Agassiz silt	1.76m x 2.40m round tank	Two stage freezing rate 68 mm/day and 14 mm/day	650
P1	Piney silt	800mm x 600mm square tank	Two stage surface temp -5°C and -10°C	191
P2	Piney silt	800mm x 600mm square tank	Two stage surface temp -9.5°C and -13°C	287
P3	Piney silt	800mm x 600mm square tank	Constant surface temp -15°C	120
P4	Piney silt	800mm x 600mm sqaure tank	Constant freezing rate 6 mm/day	290
S1	silty sand	800mm x 600mm square tank	Two stage freezing rate 75 mm/day and 8 mm/day	192
S2	silty sand	800mm x 600mm square tank	Two stage freezing rate 70 mm/day and 30 mm/day	192

S3	silty sand	800mm x 600mm square tank	Constant freezing rate 20 mm/day	398
S4	silty sand	800mm x 600mm square tank	Constant freezing rate 20 mm/day	398

Prediction Tests

1974-1	Agassiz silt	1.76m x 2.40m round tank	Constant freezing rate 40 mm/day	500
1974-2	Agassiz silt	1.76m x 2.40m round tank	Constant freezing rate 43 mm/day	860
1975-1	Agassiz silt	800mm x 600mm square tank	Constant freezing rate 25 mm/day	500
1975-2	Agassiz silt	800mm x 600mm square tank	Constant surface temp -4°C	690
1975-3	Agassiz silt	800mm x 600mm square tank	Constant freezing rate 20 mm/day	600
1978-1	silty sand	800mm x 600mm square tank	Constant freezing rate 40 mm/day	200
1978-2	silty sand	800mm x 600mm square tank	Constant freezing rate 18 mm/day	405
1978-3	silty sand	800mm x 600mm square tank	Average freezing rate of 7 mm/day	1200
1980-1	Piney silt	800mm x 600mm square tank	Constant surface temp -5°C	890
1981-1	Piney silt	125mm x 100mm diameter cell	Constant surface temp -12°C	250

1983-1	Piney silt	800mm x 600mm square tank	Constant freezing rate 9 mm/day	864
1983-2	Piney silt	800mm x 600mm square tank	Constant freezing rate 9 mm/day	768

4.2 PREDICTION MODELS USED

All frost heave prediction models require input information such as soil properties, freezing conditions, temperature gradients, heat flow, etc. Many of the models require one or two additional parameters which are constant for one particular soil type. In the laboratory frost heave studies, only very limited information was measured and collected. Consequently many of the available predictive models could not be used. The models used and the input information are described in the subsequent sections.

4.2.1 Sheriff Ishibashi and Ding (1976)

Sheriff et al. (Section 3.1.1) derived the following empirical formula for frost heave using the percent fines (F), the freezing time (t), the freezing temperature (θ), and a temperature dependent factor (J) as input:

$$H = F^{0.61} \, t^{0.83 - 0.063\,\theta} \, J \qquad (5)$$

The percent fines (less than 0.02 mm particle size by weight) for each of the three soils was:

Agassiz silt	50 %;
Piney silt	12 %;

Silty sand 3 %;

Hence only time and temperature are variables in this model. Refer to Figure 5 for the relation between J and temperature.

4.2.2 Knutson (1973)

The model presented by Knutson (Section 3.1.3) related the increase in frost heave (ΔH) to a soil parameter (β), the frozen moisture content (Wf) and the increase in frost penetration (ΔX) using the following relationship:

$$\Delta H = \beta \cdot Wf \cdot \Delta X \qquad (8)$$

The value of β is dependent upon the soil type and the freezing index. In this analysis β was determined using the total depth of frost penetration (X) and the total frost heave (H):

$$\beta = \frac{H}{X \cdot Wf} \qquad (18)$$

The relationship between β and the freezing index must be determined for each soil type. The parameter β can be calculated at any time during the freezing test using equation 18. This can be plotted against the freezing index. If this is done for 4 or 5 points during a test the results can be plotted on a log-log grid and a regression analysis can be used to obtain an empirical equation relating β to the freezing index for a particular soil type.

There were two difficulties involved in this method of correlation. Most of the tests were of limited total depth (less than 450 mm in depth) and were conducted over a short period of time (less than three weeks). In such tests the freezing index is not sufficient to predict the rate of freezing of the soil. For the tests of short duration the total freezing index was very small and there were not enough points generated to establish a good relationship between β and the freezing index. For these reasons, the preliminary analysis used only input from long term pit tests on Agassiz silt.

Two tests were used as preliminary freezing tests to determine the necessary parameters. The variation of β with freezing index is illustrated for both tests in Figure 14. For test number 2, β fell within Saeterdal's range for a medium frost susceptible soil (refer to Table 1), while for test number one, β was greater than the upper limit for a highly frost susceptible soil. This variation of results is excessive, but for the purpose of obtaining a relationship between β and the freezing index the average of the two tests was used. The error that occurs in this analysis suggests that more than two preliminary freezing tests are required to define the β to freezing index relation or to judge whether such a relationship exists. Figure 15 is a plot of the natural log of the average β values versus the natural log of the inverse of the corresponding values of

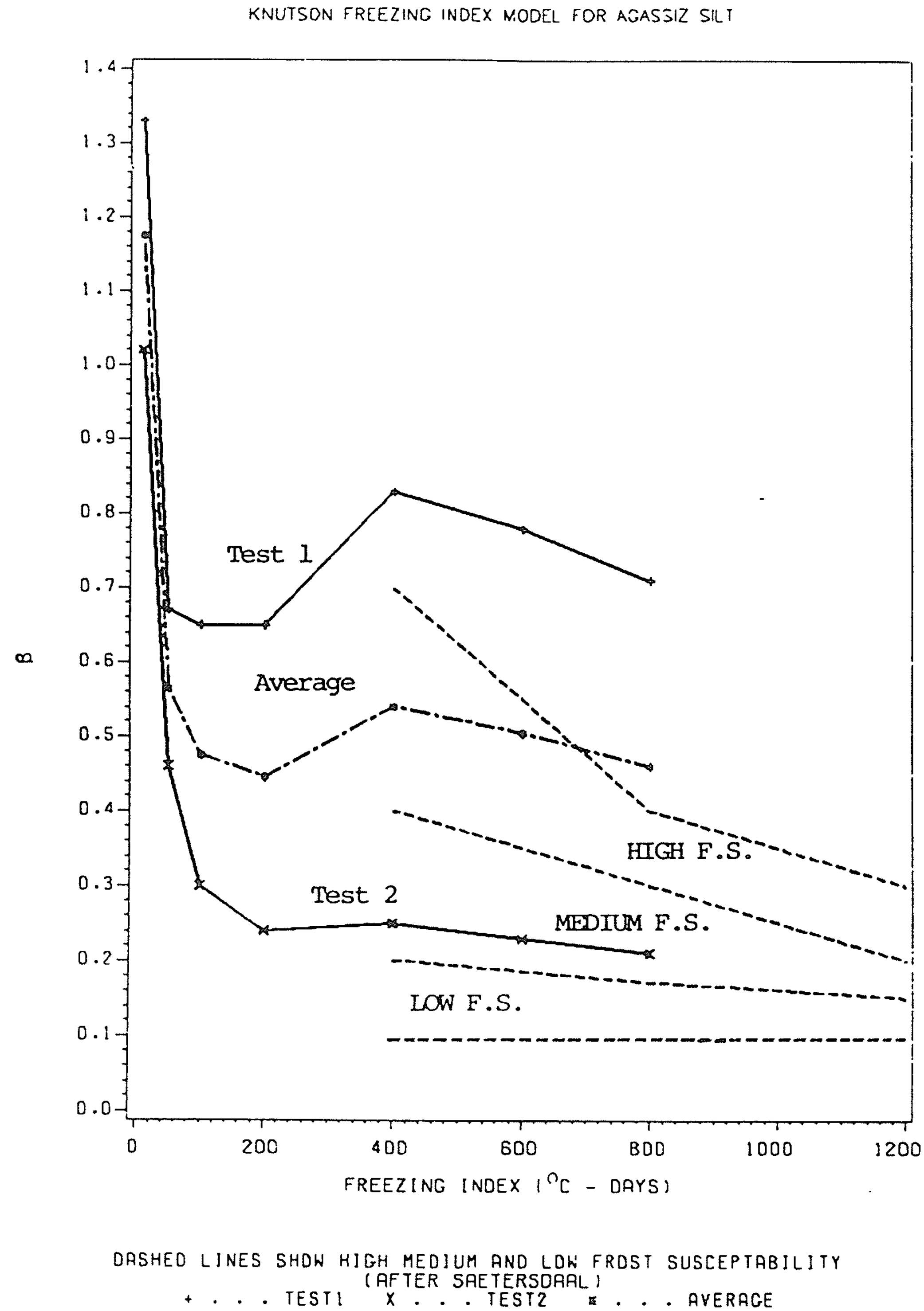

Figure 14: The relationship between β and freezing index for two tests on Agassiz silt

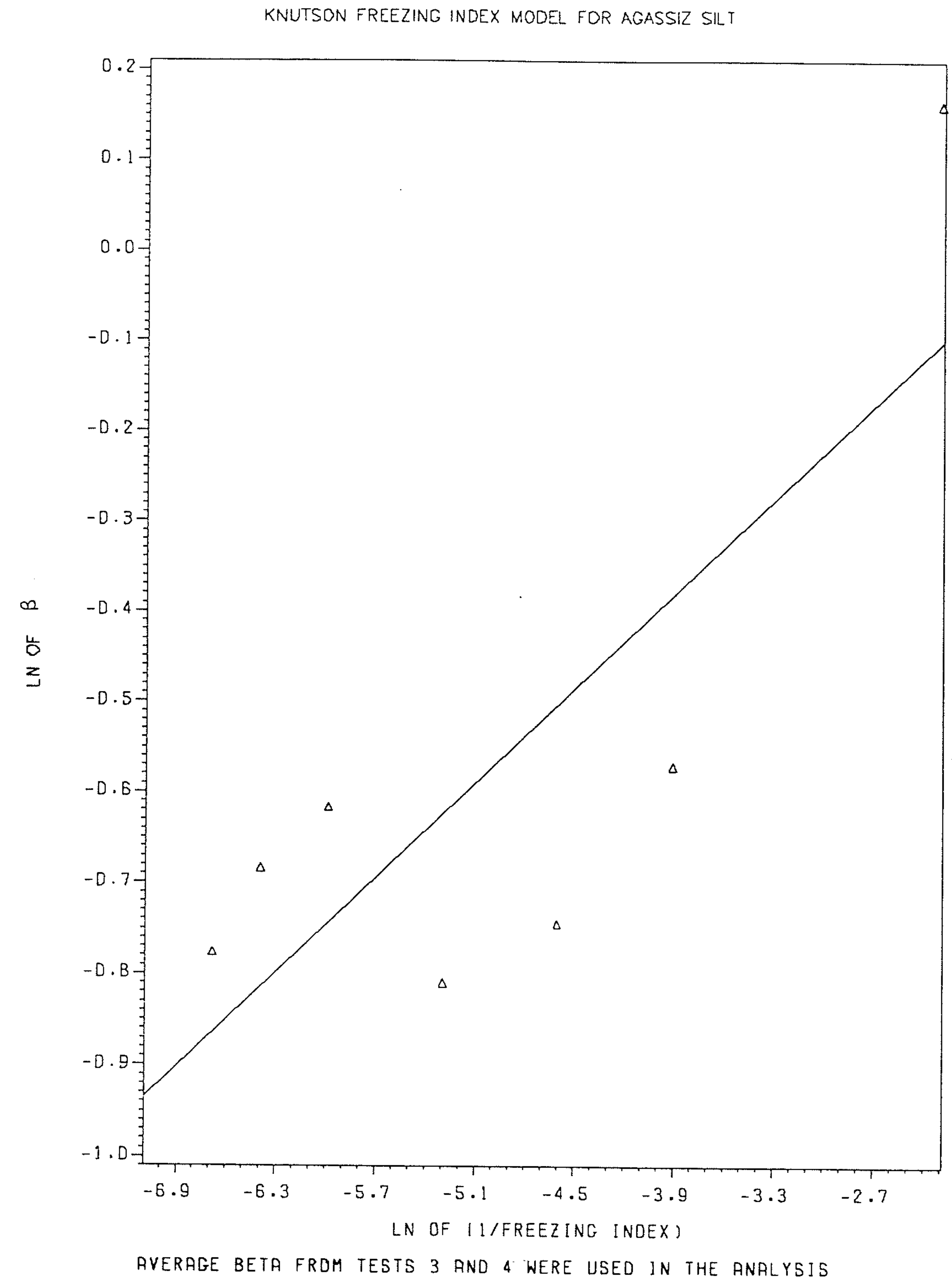

Figure 15: The relationship between the average β values and freezing index for Agassiz silt

freezing index. The equation of the regression line is of the form:

$$\beta = a \left(1/ FI \right)^{b} \tag{19}$$

where:

FI = freezing index

a and b are constants determined from regression analysis.

For Agassiz silt the values of a and b were found to be 1.350 and 0.174 respectively when the freezing index was measured in °C days. When compared with the two preliminary tests, the model provides a value of β which is 50 and 70 percent in error. However it does compare favourably with Saetersdaal's β values for a highly frost susceptible soil (refer to Table 1). The model also predicts the high β values experienced in both preliminary tests at a freezing index of less than 100 °C-days.

The total amount of frost heave at any point in time was determined for Agassiz silt using:

$$H = w/100 \times 1.35 \left(1/FI \right)^{0.174} \quad X \tag{20}$$

in which:

H = total frost heave

X = total frost depth

w = initial moisture content %

FI = total freezing index

The freezing index is the only variable required as input into this model. This relation was used to predict the amount of frost heave for two large scale tests and three smaller tests in which Agassiz silt was used.

4.2.3 Ice Segregation Ratio Theories

According to Carlson et al. (1982) the ISR is a function of pressure at the frost front and the rate of frost penetration. Such models, as outlined by Penner and Walton, Takashi et al. and a comparison model, are discussed in the following sections. There are two possible methods of describing the amount of frost penetration into a soil. The frost depth can be taken as either the depth of frozen soil below a stationary datum or the depth below the upward heaving soil surface. In both cases the amount of frost heaving is taken as the height above the original ground surface. When either definition of frost depth is used in the ISR models, the results are essentially equal. The only difference occurs when heat flow approaches steady state and the rate of frost penetration approaches zero. In laboratory tests it has been seen that although the frost line is stationary, ice lensing continues to occur. If the first definition is used in the equation:

$$\Delta ISR = \Delta H / \Delta X$$

then ΔISR will approach infinity as ΔX approaches zero. The second definition allows for continued heaving to be modelled under steady state conditions. This second method (which is defined as the "alternate" method) becomes difficult to use without the aid of a computer. Predictions based on both definitions were made.

4.2.3.1 Comparison Model for Frost Heave

Before developing any relation for the Ice Segregation Ratio it should be understood that by increasing either the frost penetration rate or the overburden pressure the rate of heaving will decrease. If the product of frost penetration ratio and overburden pressure is plotted against the ISR on a log-log grid, the resulting regression line will provide a relationship in the form:

$$ISR = a \times (\dot{X}P)^{-b} \qquad (21)$$

in which:

P = overburden pressure

$\dot{X}$ = frost penetration rate

a and b are soil constants derived from regression analysis.

This can be used as a comparison with published models.

The model was developed from tests on each of the three soil types. The a and b values in Equation 21 were determined from a log-log plot of ISR versus overburden pressure multiplied by the frost penetration rate. The results are shown in Figures 16 and 17. The values plotted in Figure 17 use the "alternate" method of determining the frost penetration, as was described previously. The results from the regression analysis, are summarized in Table 3 They are based on a frost penetration rate expressed in mm/day and on overburden pressure in KPa. The remaining variables in this

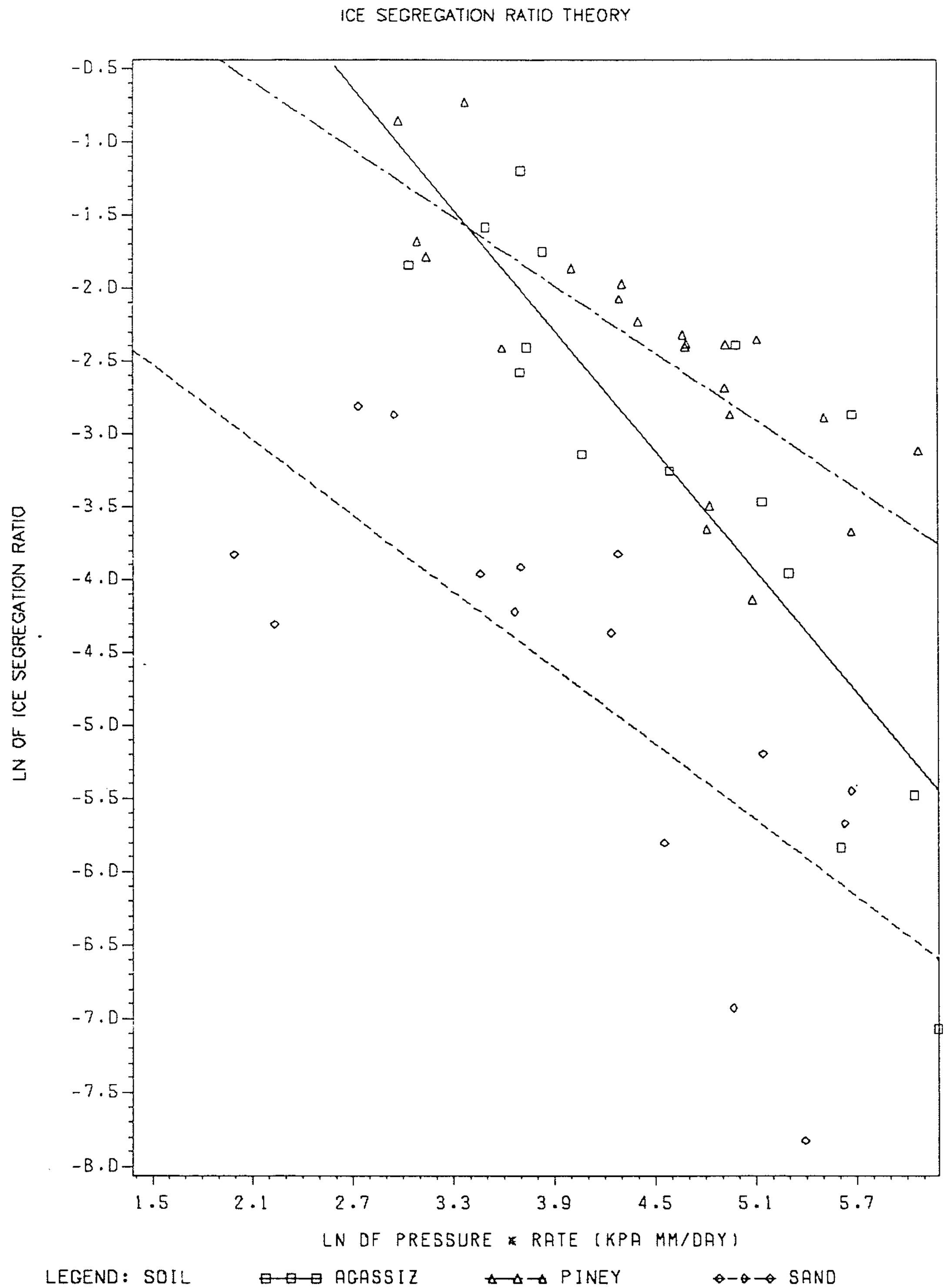

Figure 16: Plot of ISR vs. penetration rate x overburden pressure

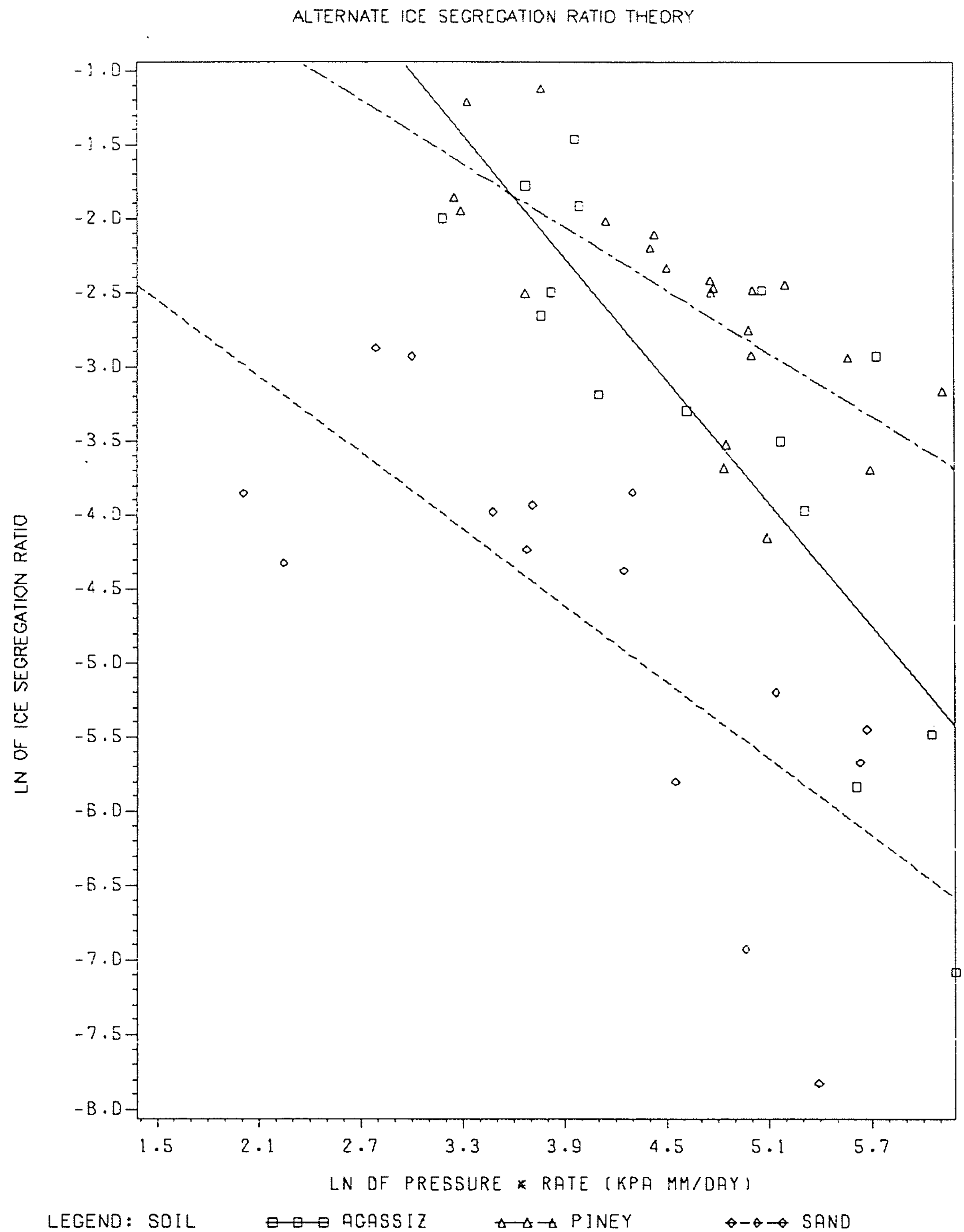

Figure 17: Plot of ISR vs. penetration rate x overburden pressure (alternate method)

TABLE 3

a and b values for ISR Equation 21

Soil	ISR Theory		Alternate ISR Theory	
	a	b	a	b
Agassiz Silt	22.20	1.381	22.48	1.378
Piney Silt	2.80	0.774	2.06	0.712
Silty Sand	0.296	0.870	0.287	0.862

model are the rate of frost penetration and the overburden pressure. Since there was no surcharge at the ground surface in the laboratory studies, the pressure applied on the ice lens can be calculated on the basis of the depth of frost penetration.

The degree of confidence in each of the frost heave parameters was evaluated before the prediction models were either supported or criticized. The statistical confidence with which each of the frost heave parameters were derived is presented for each model. Also the frost heave constants for Agassiz silt, Piney silt and the silty sand are compared with published parameters and comments are made on any similarities or discrepancies.

The regression coefficient "r" and the coefficient of variation "CV" are considered to be indicative of the closeness of the fit, or the scatter of the observations about the regression line. The coefficient of variation is the standard error of the regression divided by the average value of the independent variable. The closer r is to 1.0 and CV is to 0.0 the better is the fit of points to the regression line. The regression coefficient "r" is most commonly used, but the coefficient of variation is a good indication for comparing the various models since it is less influenced by sample size. The 90 percent confidence limits for all of the frost heave parameters were also derived.

A definition of reasonable values of r and CV is required. An acceptable range of 90 percent confidence limits must also be defined. The value of r can be used to determine the probability that a relationship exists, and that the relationship is closely defined by the resulting regression line. The probability depends upon the sample size, and in this analysis the number of observations used for any one model ranged from 6 to 22. Table 4 shows the r values that correspond to 99 % and 99.9 % probability that a relationship exists (or that the slope of the regression line is not equal to zero) for various sample sizes. A value of r corresponding to a probability of less than 99 percent can be used as an indication of a poor regression.

The value of CV is useful since it is less dependent upon the number of observations. Therefore this parameter can be used as a comparison from one model to the next. When CV is

TABLE 4

r values corresponding to regression probabilities

Sample size	99 %	99.9 %
5	0.936	0.980
10	0.754	0.865
15	0.637	0.754
20	0.559	0.675

less than 25 in this analysis, the regression appears reasonable. Values of CV greater than 100 are excessive. The 90 percent confidence range can be compared with the mean value. A range greater than ±20 % was arbitrarily considered excessive for this analysis.

Table 5 provides statistical information for the ISR model. The r and CV values indicate that the relationships are reasonable based on the previous discussion. There is little statistical difference between the two methods of calculating the depth of frost penetration. The 90 % confidence limits for the 'b' parameter indicate that only a ±6 to 11 % error exists while the 90 % confidence limits for the 'a' parameter are ±24 to 62 % away from the mean value. This error is excessive for all soil types and the inability to obtain a good 'a' value would make this a poor model for use.

TABLE 5

Statistical information for ISR Equation 21

Soil	r	CV	90 % confidence limits a	b	Sample size
Agassiz	0.834	29.7	12.92 - 38.15	1.266 - 1.496	15
(alt.)	0.816	29.3	12.49 - 40.46	1.255 - 1.501	15
Piney	0.773	22.4	2.21 - 3.55	0.722 - 0.826	22
(alt.)	0.726	21.0	1.59 - 2.66	0.657 - 0.767	22
Sand	0.744	20.7	0.195 - 0.447	0.791 - 0.988	15
(alt.)	0.739	20.6	0.189 - 0.436	0.763 - 0.961	15

4.2.3.2 Takashi, Yamamoto, Ohrai and Masuda (1978)

Takashi et al. (Section 3.2.1) provided a means of determining the ISR as a function of frost penetration rate and overburden pressure. The relationship presented by Takashi et al. could be rewritten to relate the Ice Segregation Ratio (ISR) to the applied pressure (P) and the frost penetration rate ($\dot{X}$) using parameters P_0 and U_0 which remain constant for a particualar soil type:

$$ISR = P_0/P \left(1 + \sqrt{\frac{U_0}{\dot{X}}} \right) \qquad (11)$$

If the product of ISR and overburden pressure is plotted against the inverse of the square root of frost penetration rate the regression line will produce an equation of the form:

$$ISR \times P = b / \sqrt{\dot{X}} - a \quad (22)$$

This can be rearranged into the form represented by Equation 11 where P_0 = a (the intercept of the regression line) and $U_0 = b^2/a^2$. The results from the four preliminary freezing tests for each of the three soil types, are shown in Figures 18 and 19. The frost penetration was determined using the alternate approach for data presented in Figure 19. The P_0 and U_0 values for each of the three soils are listed in Table 6.

TABLE 6

U_0 and P_0 values for Equation 11

Soil	ISR Theory		Alternate ISR Theory	
	P_0 (KPa)	U_0 (mm/day)	P_0 (KPa)	U_0 (mm/day)
Agassiz Silt	0.230	113.7	0.118	138.8
Piney Silt	0.485	83.7	0.293	114.6
Silty Sand	0.0554	61.5	0.0527	63.8

The variables required to calculate the frost heave using Equation 11 are the depth and rate of frost penetration and the applied pressure.

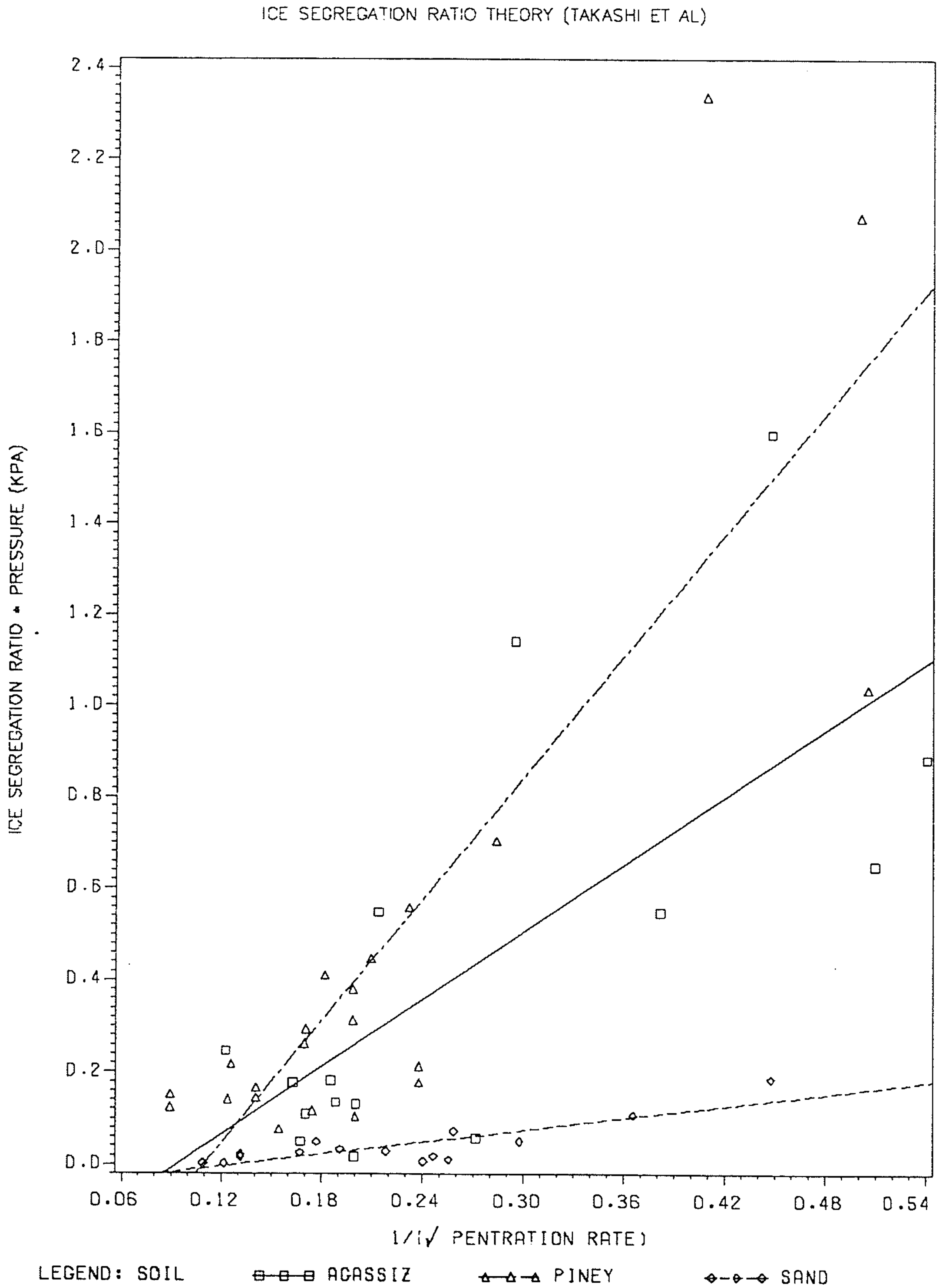

Figure 18: Plot of ISR x overburden pressure versus the inverse of the frost penetration rate (for Takashi et al.)

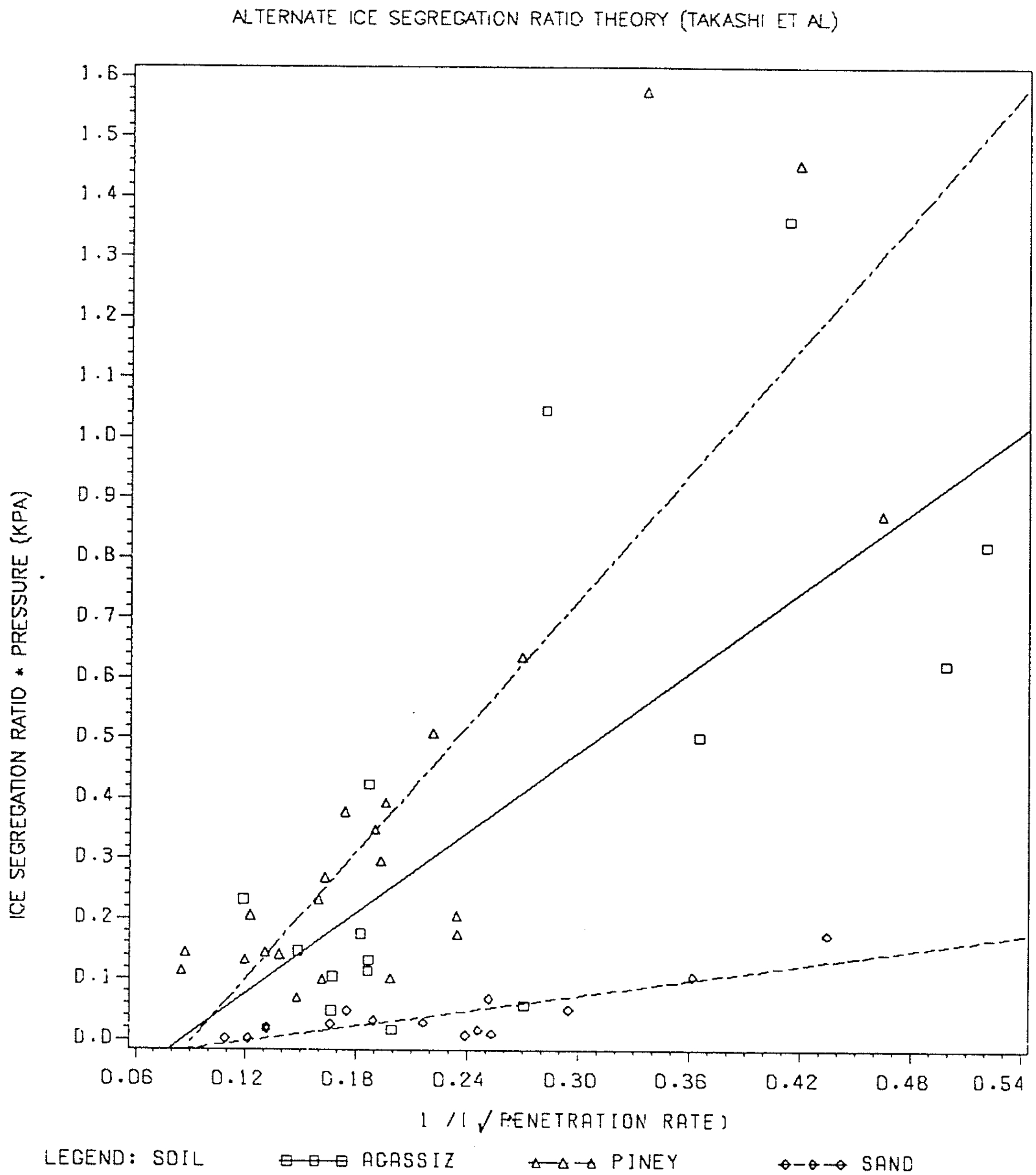

Figure 19: Plot of ISR x overburden pressure versus the inverse of the frost penetration rate (Takashi et al. alternate method)

The r values presented in Table 7 indicate that the fit again appears to be reasonable. The CV values illustrate a lesser statistical variation for this model than for the previous ice segregation ratio model. The 90 % confidence limits for U_0 and P_0 show an excessive error (greater than ±20 %) in the P_0 values for Agassiz silt and in the U_0 values for Piney silt and the silty sand. There is little statistical difference between the two methods of calculating frost penetration.

TABLE 7

Statistical information for the Takashi et al. model

Soil	r	CV	90 % confidence limits U_0	P_0	Sample size
Agassiz	0.710	79.0	102.6 - 124.8	0.138-0.322	15
(alt.)	0.704	78.1	126.7 - 150.9	0.107-0.270	15
Piney	0.844	70.2	66.7 - 100.7	0.429-0.541	22
(alt.)	0.873	53.6	97.8 - 131.4	0.258-0.328	22
Sand	0.845	64.8	44.4 - 78.6	0.047-0.064	15
(alt.)	0.838	64.6	46.2 - 81.4	0.045-0.061	15

U_0 and P_0 values were supplied by Takashi et al. for two samples of silty soils. U_0 was found to be 70.6 and 41.0

mm/day and P_0 was stated to be -2.5 and -6.53 KPa. The magnitude of U_0 for the soils presented by Takashi et al. were slightly lower than the values obtained for the University of Manitoba soils. The two published P_0 parameters were of the opposite sign and were roughly ten times larger than the values presented in Table 6. The soil used by Takashi et al. would experience much greater frost heave under similar pressures and frost penetration rates. The negative P_0 value indicates that ice lensing will occur even at extremely rapid rates of frost penetration.

4.2.3.3 Penner and Walton (1979)

Penner and Walton (Section 3.2.3) determined the Ice Segregation Ratio as a function of the time (t) and frost depth (X):

$$ISR = 1 - \exp\{ -R_0 \ t/X \} \qquad (13)$$

The initial rate of frost penetration (R_0) is a function of the pressure to temperature ratio (P/T) and is dependent upon soil type.

$$R_0 = a \ \exp\{ -b \ P/T \} \qquad (12)$$

The P/T ratio is zero for all our cases since there was no initial overburden pressure (P=0). Equation 12 indicates that R_0 is the same for all tests on the same soil type. R_0 can be derived from a plot of the ln of (1 - ISR) against the value of t/X where the regression line must go through the origin. The equation of this regression line is:

$$\ln (1 - ISR) = R_0 \ t/X \qquad (23)$$

where:

t = time

X = total frost depth.

This equation can easilly be transformed into the form of Equation 12. Figure 20 illustrates the plot of the above relation for each of the three soil types. The results can be summarized as follows:

Agassiz Silt R_0 = 0.997

Piney Silt R_0 = 3.078

Silty Sand R_0 = 0.379

The r, CV, and 90 % confidence limits for the R_0 values are presented in Table 8. The values of r and CV indicate that the fit of observations to Agassiz silt regression line is not reasonable. The Piney silt and silty sand relationships are reasonable and the ranges of values between the 90 % confidence limits are small.

R_0 values corresponding to a pressure to temperature ratio of zero can be taken from a figure published by Penner and Ueda (1978) for Leda clay and a silty test soil. The values are 8.3 and 6.3 mm/day respectively which are slightly higher than the R_0 values for Agassiz and Piney silt. For the silty sand the lower value of R_0 represents the material's low degree of frost susceptibility.

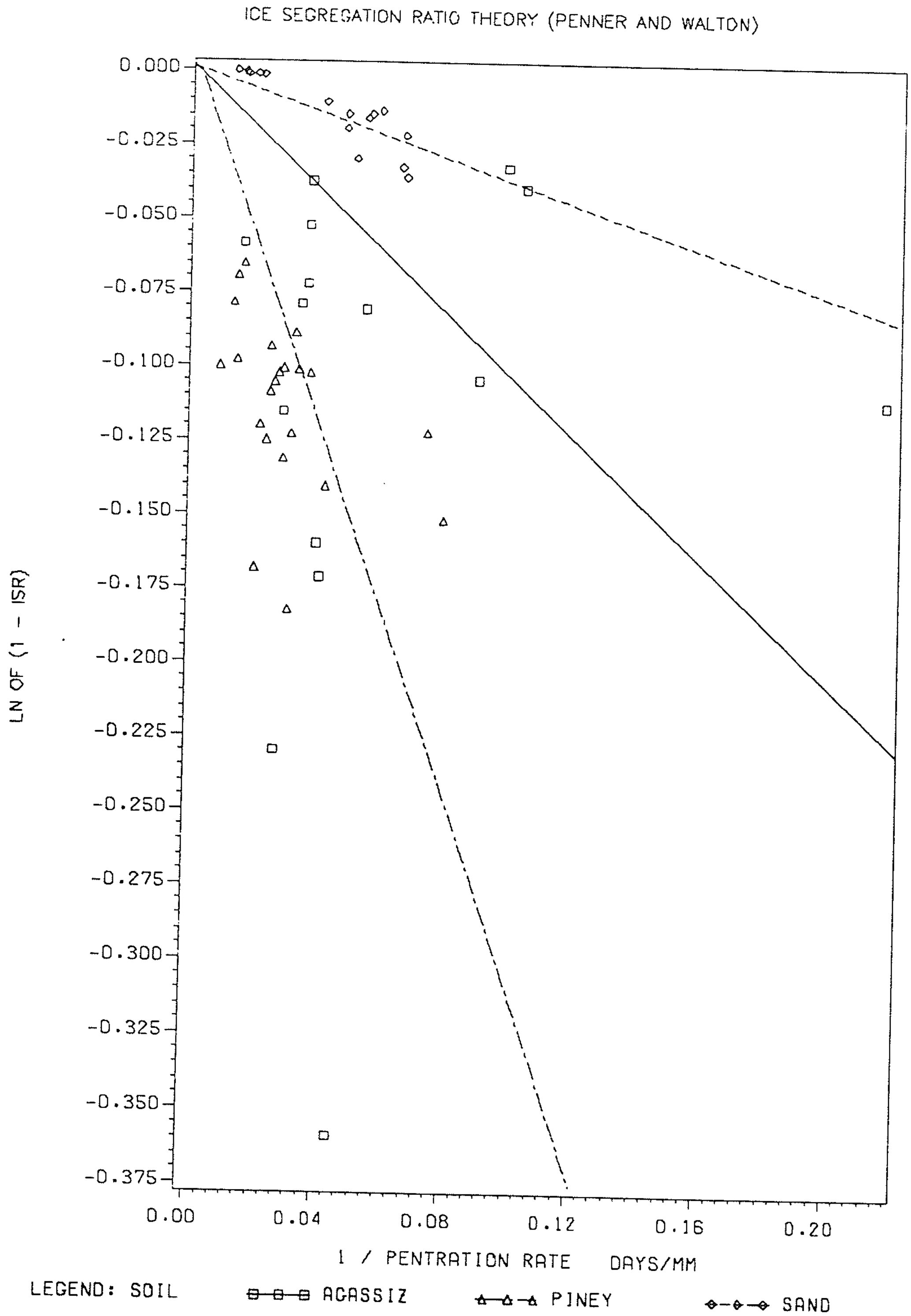

Figure 20: Plot of the ln of (1 - ISR) versus t/X for the Penner and Walton theory

TABLE 8

Statistical information of Penner and Walton's model

Soil	r	CV	90 % confidence limits for R_0	Sample size
Agassiz	0.597	105.5	0.877 - 1.117	16
Piney	0.888	49.8	2.98 - 3.18	22
Sand	0.940	46.8	0.366 - 0.392	15

4.2.4 Heat Flow Models

This procedure is difficult to accurately consider since no measurement of heat flow was taken. The heat flow at the frost front can be estimated if the frozen and unfrozen temperature gradients and the thermal conductivities are known. Time and the depth of frost penetration are the variables used as input into Equation 3.

$$\text{Heat Flow } (Q) = K_f\,(dT_f/dx) - K_u\,(dT_u/dx) \qquad (3)$$

The temperature gradients (both frozen and unfrozen) were calculated from temperatures measured in two of the tests on Agassiz silt. The thermal conductivities can be estimated from the Kersten diagrams. Arakawa's ice segregation efficiency 'E' (Section 3.3.1) was calculated and plotted on a graph of efficiency versus the rate of frost penetration (as suggested by Penner,1972). This did not provide any relationship whatsoever. After analyzing six different relations it was discovered that a plot of E versus the square root of penetration rate ($\dot{X}$) multiplied by overburden pressure (P) produced a more acceptable correlation. The regression line from this relation provided an equation of the form:

$$E = a + b \sqrt{\dot{X}P} \qquad (24)$$

The plot of this relation for Agassiz silt is shown in Figure 21 and the a and b values were 0.227 and 0.018 respectively. The amount of segregational frost heave can be calculated from:

$$\Delta H = (0.227 + 0.018 \sqrt{\dot{X}P}) \times Q/L \times \Delta t \qquad (25)$$

in which:

ΔH = the increase in frost heave

Δt = the time increment

Q = the heat flow

L = the latent heat of fusion per unit volume of soil.

The frozen and unfrozen thermal conductivities and the latent heat of fusion of the soil mass must be either measured or estimated using accepted methods. The variables used as input are the temperature gradients immediately above and below the 0° C isotherm, the rate and depth of frost penetration , the applied pressure and time.

For Agassiz silt the statistical information (derived from eight observations) is as follows:

r = 0.775

CV = 144.5

90 % confidence interval for 'a' 0.184 - 0.270

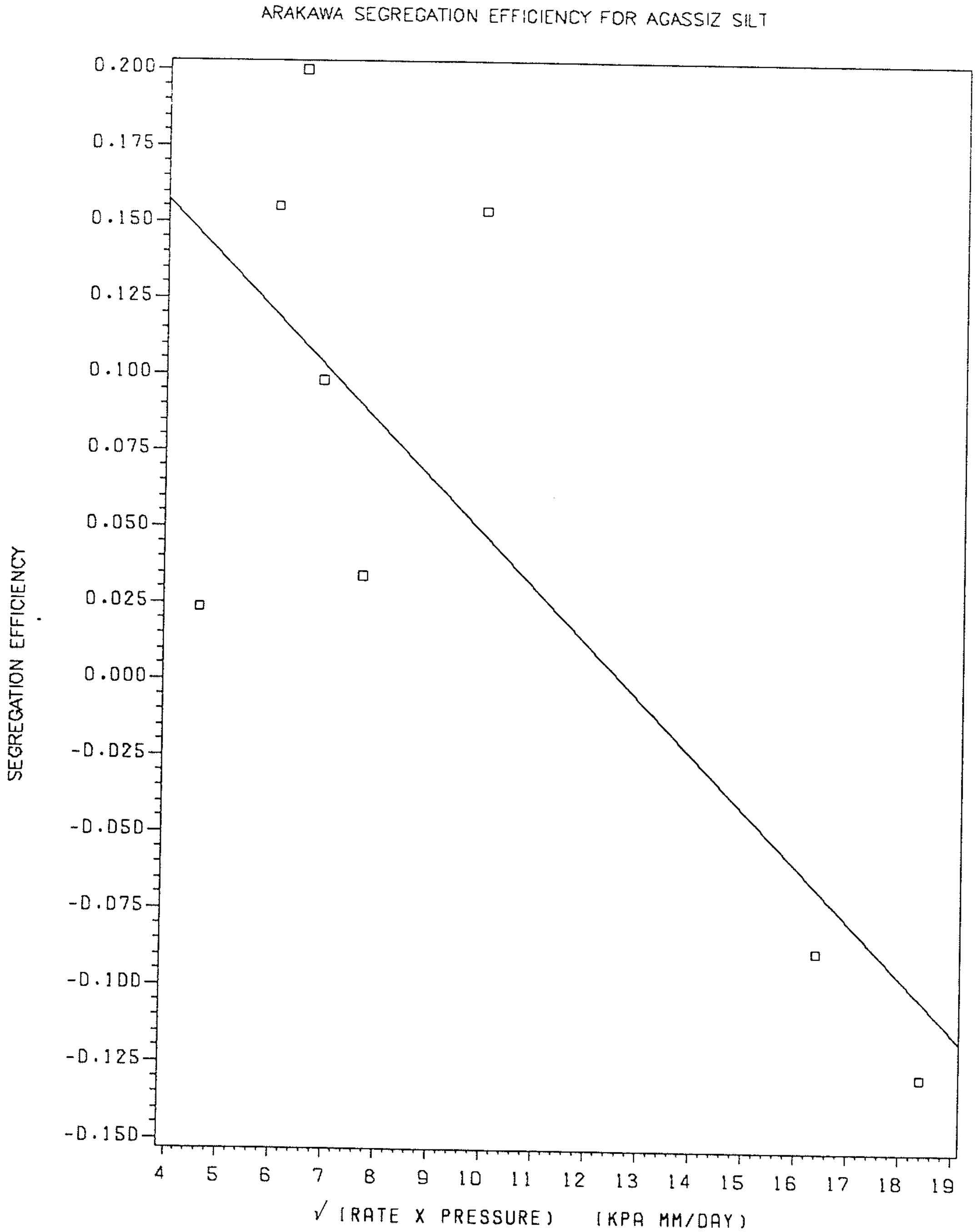

Figure 21: Plot of Arakawa's efficiency versus the square square root of frost penetration rate x overburden pressure

90 % confidence interval for 'b' 0.014 - 0.022

The coefficient of variation for the Arakawa efficiency model is the highest for any theory presented in this thesis. The confidence in obtaining representative values of both the 'a' and 'b' parameters is poor (roughly ±20 % of the mean).

4.2.5 Konrad and Morgenstern (1982)

Konrad and Morgenstern outlined a basic procedure for obtaining the segregation potential as a function of external pressure (Section 3.4). The segregation potential is defined as the flux of moisture moving towards the frost front divided by the temperature gradient in the partially frozen soil zone or "frozen fringe". A small number of laboratory controlled tests are all that is required to provide a definitive solution. A primary caution is that these tests must not be conducted under rapid rates of cooling. By failing to do this, erroneous results may be produced. Figure 22 illustrates how Konrad and Morgenstern's experimental results vary with the rate of cooling and the suction at the frost front.

Throughout the University of Manitoba tests there were a number of periods, particularily at the beginning of the experiments where the rate of cooling was greater than 0.01 °C/hr. Towards the later stages of the tests the rate of frost penetration was often rapid (greater than 50 mm/day)

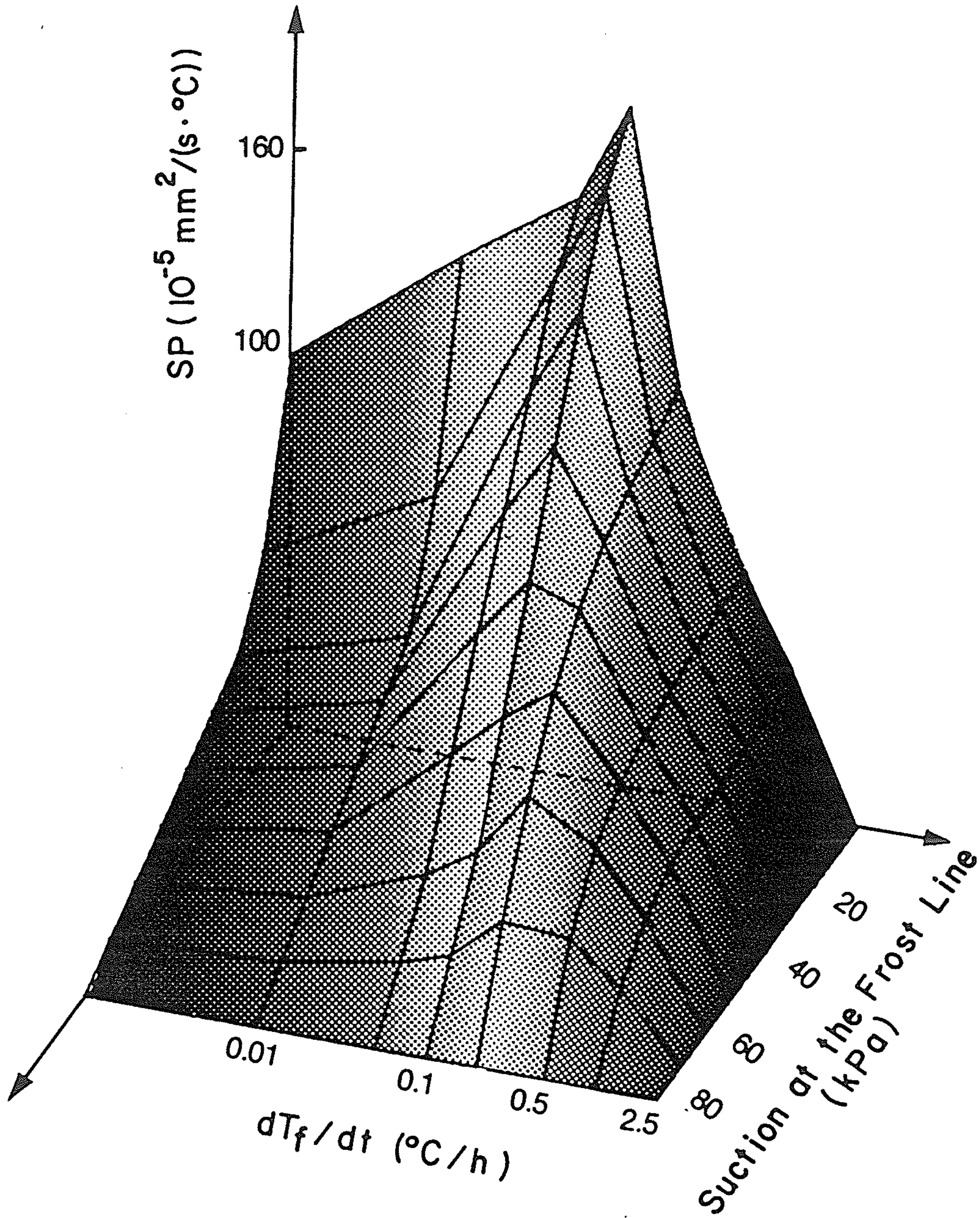

Figure 22: Characteristic frost heave surface for Devon silt (Konrad and Morgenstern 1982a)

and the overburden pressure increased with increased frost depth, while the rate of cooling remained low. In these instances negative calculated values of SP were frequently obtained. This suggests that an expulsion of moisture away from the freezing front was occurring. McRoberts and Morgenstern (1975) stated that this phenomenon occurs under conditions of increased pressure and the degree to which moisture is expelled depends upon the frost penetration rate.

The University of Manitoba tests were not all carried out on a small scale. The pressure exerted on the growing ice lens due to the weight of the frozen soil would become significant in a large scale test. The pressure exerted by the overlying material (Pe) was calculated and plotted against the evaluated segregation potential on a log-linear scale as described by Konrad and Morgenstern and is shown in Figure 23. Negative values of SP were ignored. The SP was determined by subtracting the theoretical heave due to expansion of insitu moisture from the total heave. This value would yield the moisture flow towards the freezing front which could in turn be divided by the measured temperature gradient at the zero degree isotherm. Only few values of SP were positive for the tests conducted on silty sand. The results for this soil type were nevertheless used in the analysis. Table 9 summarizes the values of SP_0 and 'a' required for use in the segregation potential equation:

$$SP = SP_0 \times \exp\{ -a \, Pe \} \qquad (16)$$

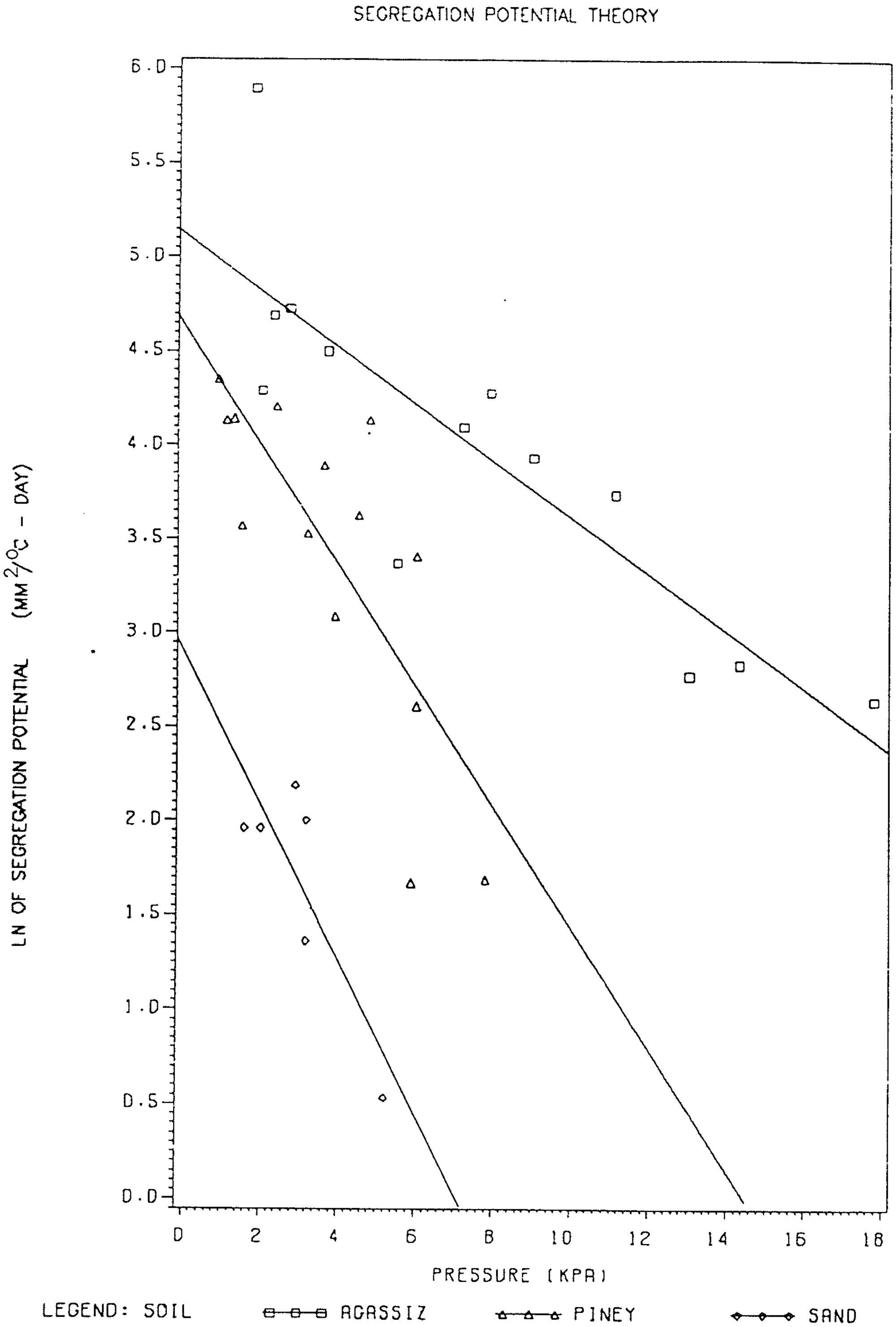

Figure 23: Plot of Konrad and Morgenstern's segregation potential versus overburden pressure

TABLE 9

Values of SP_0 and 'a' for Equation 16

Soil	SP_0 ($mm^2/°C$ day)	a (Kpa^{-1})
Agassiz Silt	168.1	0.151
Piney Silt	103.8	0.321
Silty Sand	18.3	0.412

The total frost heave can be calculated using:

$$\Delta H = (SP \times dTff/dx) \times 1.09\ \Delta t + 0.09\ \epsilon\ n\ \Delta X \quad (17)$$

where the variables required as input are the applied pressure (Pe), the temperature gradient in the frozen fringe (dTff/dx), the depth of frost penetration (X) and time (t).

The statistical information for the segregation potential model is shown in Table 10. The r values indicate that the fit was reasonable for all three soils. The 90 % confidence limits for Agassiz and Piney silts were within ±15 % of the SP_0 and 'a' values. The confidence limits for the silty sand were not reasonable since they were greater than ±25 % of both the SP_0 and 'a' values. The CV indicates that the regression line is the best fit for any of the models studied in this analysis.

TABLE 10

Statistical results for the segregation potential theory

Soil	r	CV	90 % confidence limits SP_0	a	Sample size
Agassiz	0.858	12.4	148.8 - 190.0	0.137 - 0.165	13
Piney	0.788	16.5	89.6 - 120.4	0.287 - 0.355	14
Sand	0.831	23.2	12.7 - 26.5	0.299 - 0.525	6

SP_0 and 'a' were obtained using only positive values of segregation potential. When the segregation potential is negative the total heave is less than the heave resulting from the freezing of in situ moisture. The negative values of segregation potential may indicate either that moisture is flowing away from the frost front or that the in situ moisture below the ice lens has reduced due to ice segregation. For tests on the silty sand the moisture was expelled away from the frost front during freezing since the total heave was often less than the calculated heave due to the freezing of in situ moisture. Negative values of segregation potential were calculated in each of the preliminary freezing tests for each soil type but the mechanism that causes this to occur is not clear. It is generally associated with rapid rates of frost penetration and high calculated values of overburden pressure. The process that causes a decrease in the calculated amount of segregated ice can not be predicted using this model since the value of SP from the equation : $SP = \exp(-a\ Pe)$, will never be negative.

The Konrad and Morgenstern model has been tested with considerable success by other authors (Nixon 1982, Rieke et al. 1983). The values of SP_0 and 'a' obtained for Piney silt, Agassiz silt, and silty sand can be compared with published values for other soils. Figures 24 and 25 (from Knutsson et al.,1985) illustrate how the values for the soils tested at the University of Manitoba compare with values for other soils. The value of SP_0 compares favourably while 'a' is roughly ten times higher than any other published value of 'a'.

Figure 24 illustrates that Rf is a good indicator for SP_0. Rf is determined from the grain size distribution and the liquid limit:

$$Rf = \frac{\% < 2\ \mu m \cdot \% < 74\ \mu m}{\% < 425\ \mu \cdot Wl} \times 100 \qquad (26)$$

Wl = Liquid limit of the fines fraction (%).

Silty sand has no Rf value since the liquid limit of the fines fraction was not or could not be measured. However this is not of concern to engineers since ice lensing rarely occurs in coarse grained soils. The magnitude of 'a' may be influenced not only by the grain size distribution but also by such factors as void ratio, initial moisture content and density.

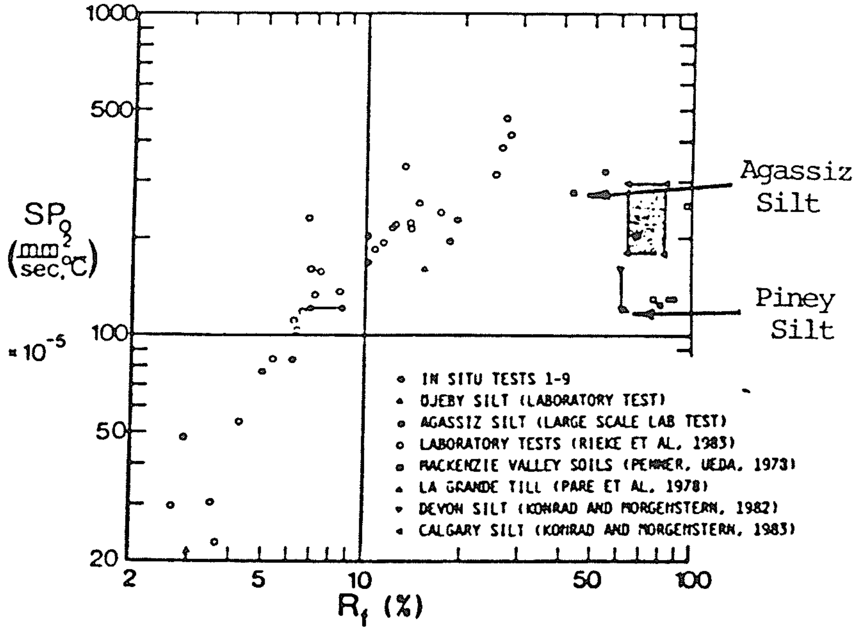

Figure 24: Rf versus published values of SP_0(from Knutsson et al.,1985)

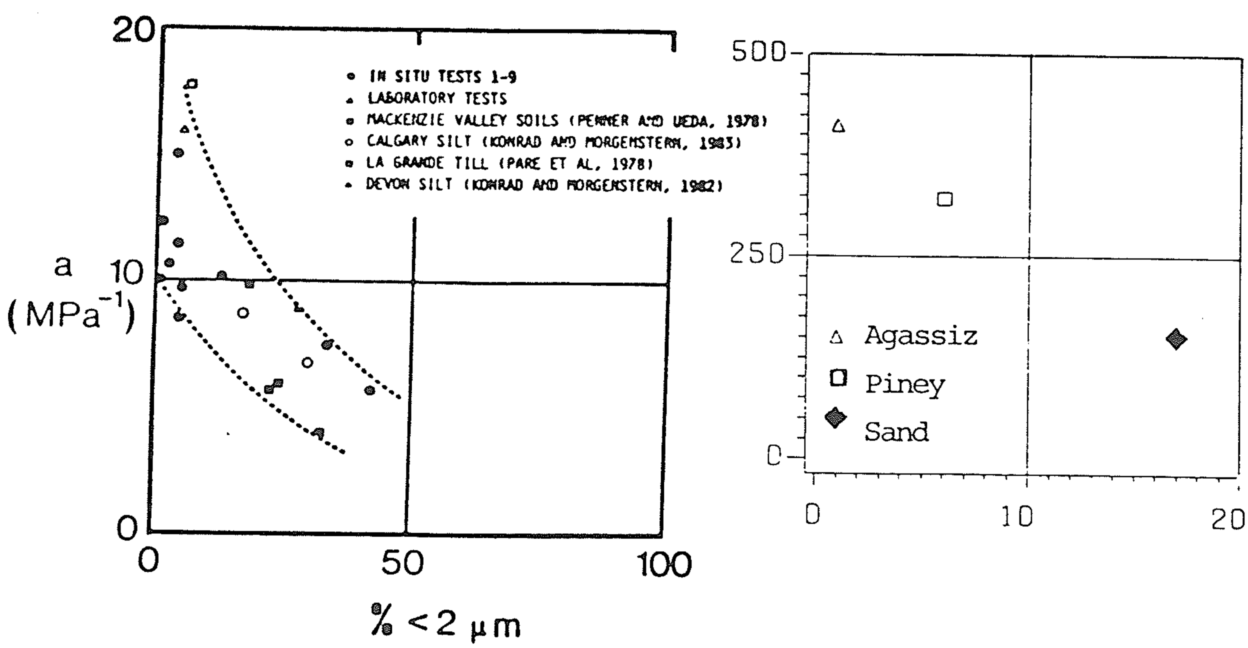

Figure 25: Values of 'a' versus percent clay content (from Knutsson et al.,1985, left figure)

Table 11 contains a complete summary of the frost heave prediction models used in the analysis.

TABLE 11 Summary of Frost Heave Prediction Models

Equations:		Parameters: Agassiz Silt	Piney Silt	Sand
Empirical;				
Sheriff, Ishibashi and Ding $H = F^{0.61}\, t^{0.83-0.063\theta}\, J$	(5)	F = 50	F = 12	F = 3
Ice Segregation Ratio; (ISR = H/X)				
Takashi, Yamamoto, Ohrai and Masuda $\Delta H = \frac{P_o}{Pe}\left(\sqrt{\frac{U_o}{\dot{X}}} - 1\right)\Delta X$	(11a)	P_o = 230.0 U_o = 113.7	P_o = 485 U_o = 83.7	P_o = 554 U_o = 61.5
Takashi et al. (alternate) $\Delta H = \frac{P_o}{Pe}\left(\sqrt{\frac{U_o}{\dot{X}}} - 1\right)(\Delta H + \Delta X)$	(11b)	P_o = 188 U_o = 138.7	P_o = 293 U_o = 114.6	P_o = 52.7 U_o = 63.8
Penner and Walton $H = (1 - \exp\{-R_o\, t/X\})\, X$	(13a)	R_o = 0.997	R_o = 3.078	R_o = 0.379
Knutson $H = w/100\ a\, FI^{-b}\, X$	(20)	a = 1.35 b = 0.174		
Pressure x Penetration Rate $\Delta H = a\,(\dot{X}Pe)^{-b}\,\Delta X$	(21a)	a = 22.20 b = 1.381	a = 2.80 b = 0.774	a = 0.296 b = 0.870
Pressure x Penetration Rate (alt.) $\Delta H = a\,(\dot{X}Pe)^{-b}\,(\Delta H + \Delta X)$	(21b)	a = 22.48 b = 1.378	a = 2.06 b = 0.712	a = 0.296 b = 0.862
Heat Flow; (Arakawa)				
$\Delta H = 1/L\,(a + b\sqrt{\dot{X}Pe}) \times (kf\ dTf/dx - ku\ dTu/dx)\Delta t + 0.09\ \epsilon\ n\ \Delta X$	(24a)	a = 0.227 b = 0.018		
Segregation Potential; (Konrad and Morgenstern)				
$\Delta H = SP_o \exp\{-a\, Pe\} \times dTff/dx \times 1.09\,\Delta t + 0.09\ \epsilon\ n\ \Delta X$	(17)	SP_o = 168.1 a = 0.151	SP_o = 103.8 a = 0.321	SP_o = 18.3 a = 0.412

H = Frost heave (mm)
X = Frost penetration (mm)
$\dot{X}$ = Frost penetration rate (mm/day)
Pe = Pressure at depth of frost penetration
dTff/dx, dTf/dx, dTu/dx = Temperature gradients in the frozen fringe, the frozen soil and unfrozen soil respectively (°C/mm)
kf, ku = Frozen and unfrozen thermal conductivities (kJ/hr m °C)
L = Latent heat of fusion (kJ/m^3)

t = Time (days)
n = Porosity
ϵ = A value relating to unfrozen moisture content (taken as 1 for all predictions)
F = % soil smaller than 0.02 mm by weight
θ = Temperature below 0°C
J $\doteq$ 0.8 when $\theta > 5$ or 0.4 + 0.08 θ when $\theta < 5$
w = % frozen water content (taken as the water content of unfrozen soil
FI = Freezing Index (°C-days)

Chapter V

FROST PENETRATION PREDICTIONS

The depth of frost penetration is a necessary component of most of the previously mentioned frost heave models. The frost depth can be either inputted directly or the depth of frost penetration and the soil temperature profile can be used to determine other input parameters (soil temperature gradients, frost penetration rates, overburden pressure on the ice lens). Empirical solutions and computer simulations for predicting the frost depth and soil temperature profile are quite common. The following three methods of calculating frost penetration were examined for use in the frost heave models. They were: the modified Berggren method; a finite difference solution outlined by Goodrich (1978); and a finite element method described by Wilson (1974).

1. The modified Berggren method is an extension of the Stefan equation which is based on the difference in interfacial energy at the phase change front ignoring heat flow below this front. This was modified by the introduction of a correction factor λ (Aldrich and Paynter 1953) which takes heat flow into account. The equation for frost depth is given by:

$$X = \lambda \sqrt{K F / L} \tag{27}$$

in which:

X = depth of frost penetration

K = average frozen and unfrozen thermal conductivity

F = freezing index

L = latent heat of fusion.

λ = correction factor taking heat flow into account

2. Wilson et al. (1974) provided a finite element model that utilized constant temperature gradient triangles and was based on the classical Neuman phase change problem. A finite element program based on this solution was developed by Shushkewich (1980).
3. Goodrich (1978) outlined a method of determining the temperature profile in a freezing (or thawing) soil by a one dimensional finite difference technique. This was accomplished by using a floating frozen to unfrozen interfacial boundary. The amount of frost penetration was calculated by equating the amount of latent heat given off during freezing to the heat flow at the interfacial boundary.

A comparison was made between the predicted values of frost penetration and the measured frost penetration in eight laboratory experiments. The eight experiments included five conducted on Agassiz silt, one on Piney silt, and two tests on silty sand. All but two tests were completed in the 800 mm by 600 mm square freezing tank. The remaining two tests were carried out in the 1.76 m by 2.40 m diameter tank using Agassiz silt. All eight tests were used as prediction tests in the frost heave analysis (see Table 2).

The measured surface and water temperatures and the thermal properties as derived from the measured moisture contents were used as input into the three previously mentioned methods. All three methods provided very poor correlations. A comparison of the predicted and measured heave in those models that required frost penetration predictions, would have no value if the frost depth prediction was poor. For this reason the initial soil temperatures, water temperatures and moisture contents were adjusted to yield predictions that were close to the measured frost depths. The surface temperatures used in the computer program were kept close to the measured values, but the initial soil temperatures and moisture contents were changed significantly in some instances. The amount that these values were changed is documented in Appendix A. Altering the initial soil temperature, the soil moisture content and the lower boundary or water temperature has a limited effect on the frost heave predictions. Knutson's β value and the frost heave due to the freezing of in situ moisture in the segregation efficiency and segregation potential models, will be affected to a small degree by changes in moisture content.

The frost penetration predictions using adjusted soil and temperature input are shown in figures 26 to 33. The modified Berggren method produced predictions that were as high as double the measured frost depths. Since the freezing index was not changed from the initial attempt the frost penetration predictions remained the same. The finite element model generated inconsistent results. The prediction of frost depth fluctuated excessively during each test. A steady increase in frost depth with time is required for the calculation of the rate of frost penetration. The inconsistency in the results may have been due to the rapid freezing rate or to a poor choice of the finite element grid. The finite difference model produced consistent results that closely modelled the actual frost penetration depth. The soil temperature profile was checked as well and was found to be predicted with acceptable accuracy. This method was therefore chosen for use in the frost heave prediction models that require frost penetration predictions.

The programs used to calculate the frost penetration and the frost heave are found in Appendix B.

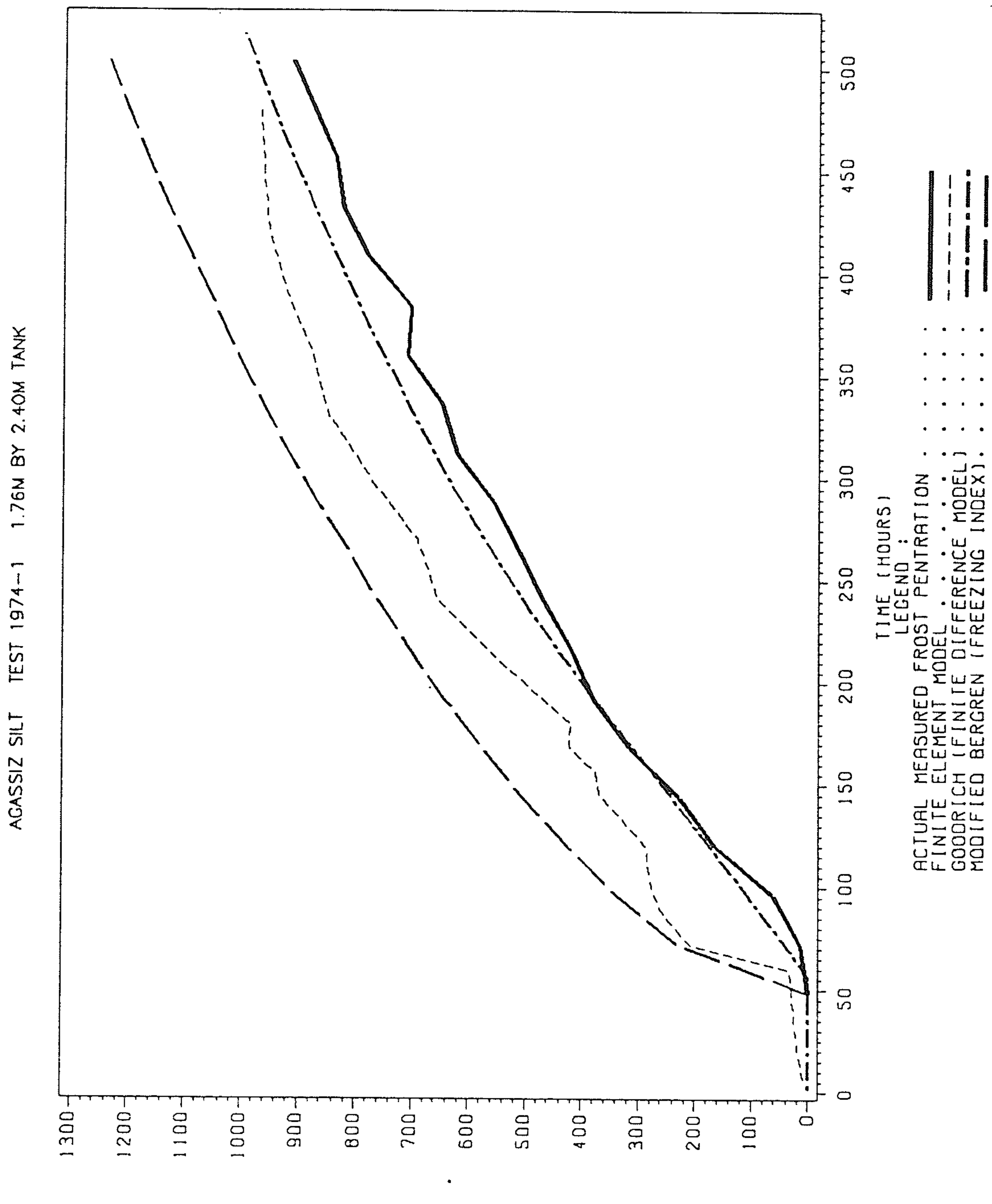

Figure 26: Frost penetration predictions for test 1974-1

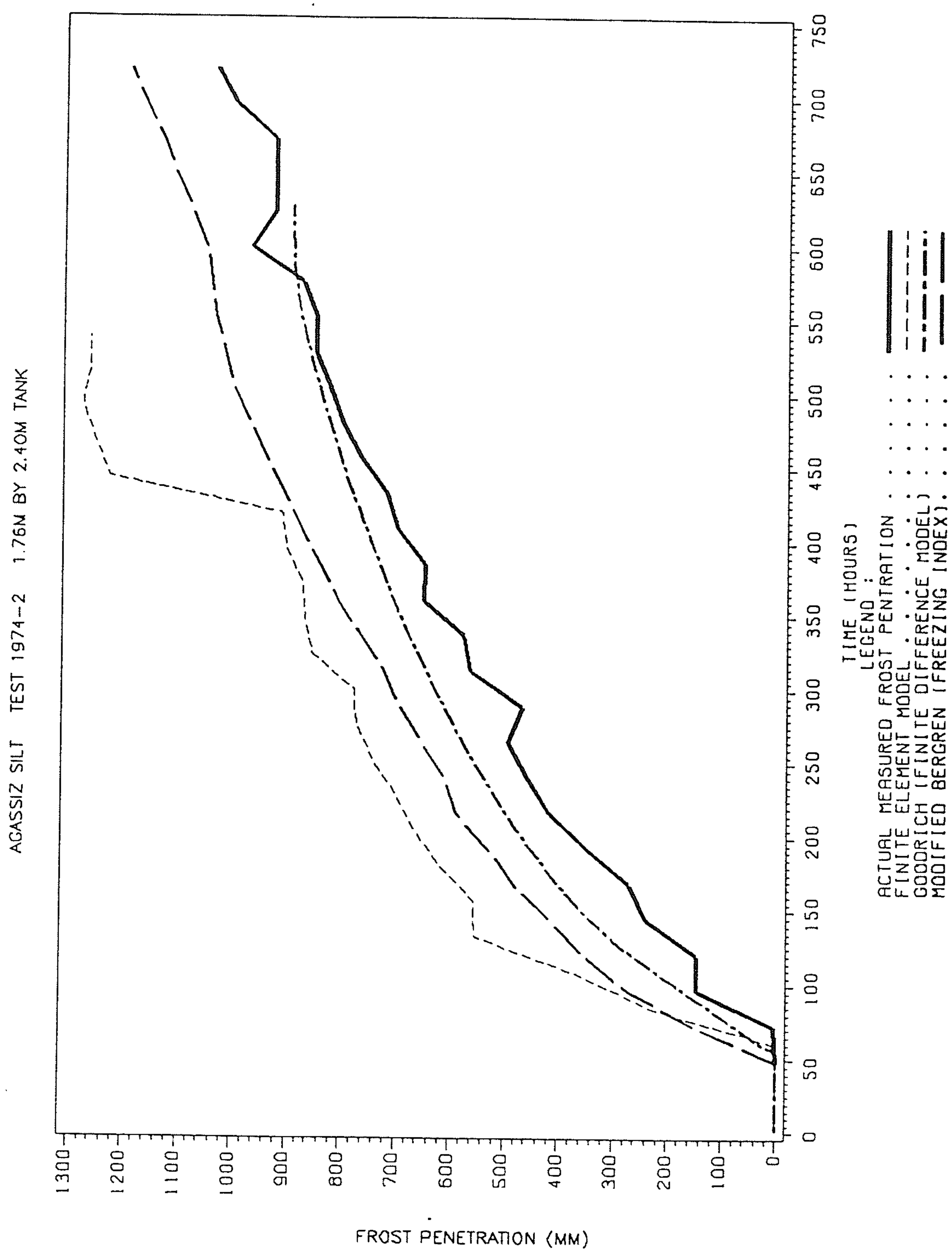

Figure 27: Frost penetration predictions for test 1974-2

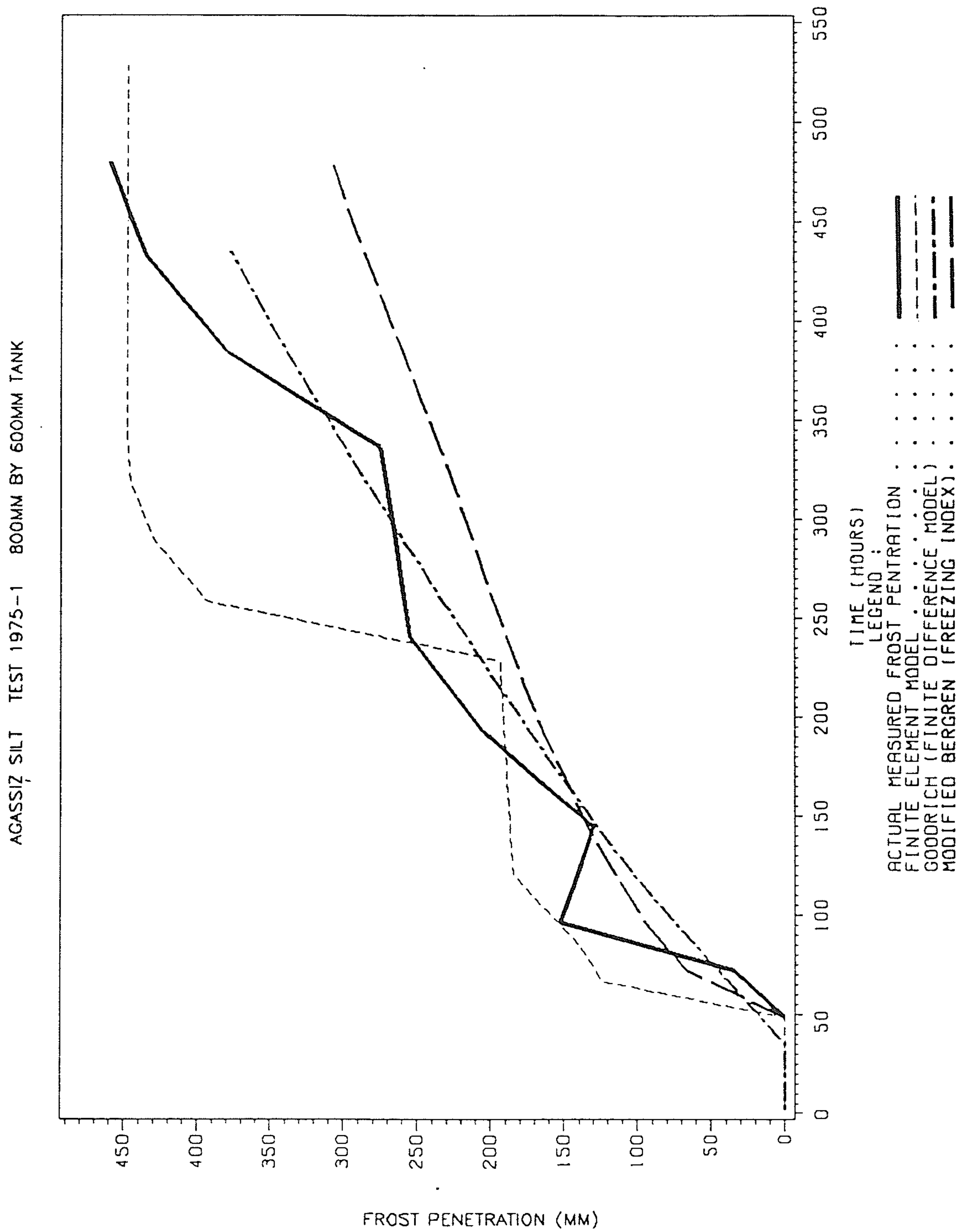

Figure 28: Frost penetration predictions for test 1975-1

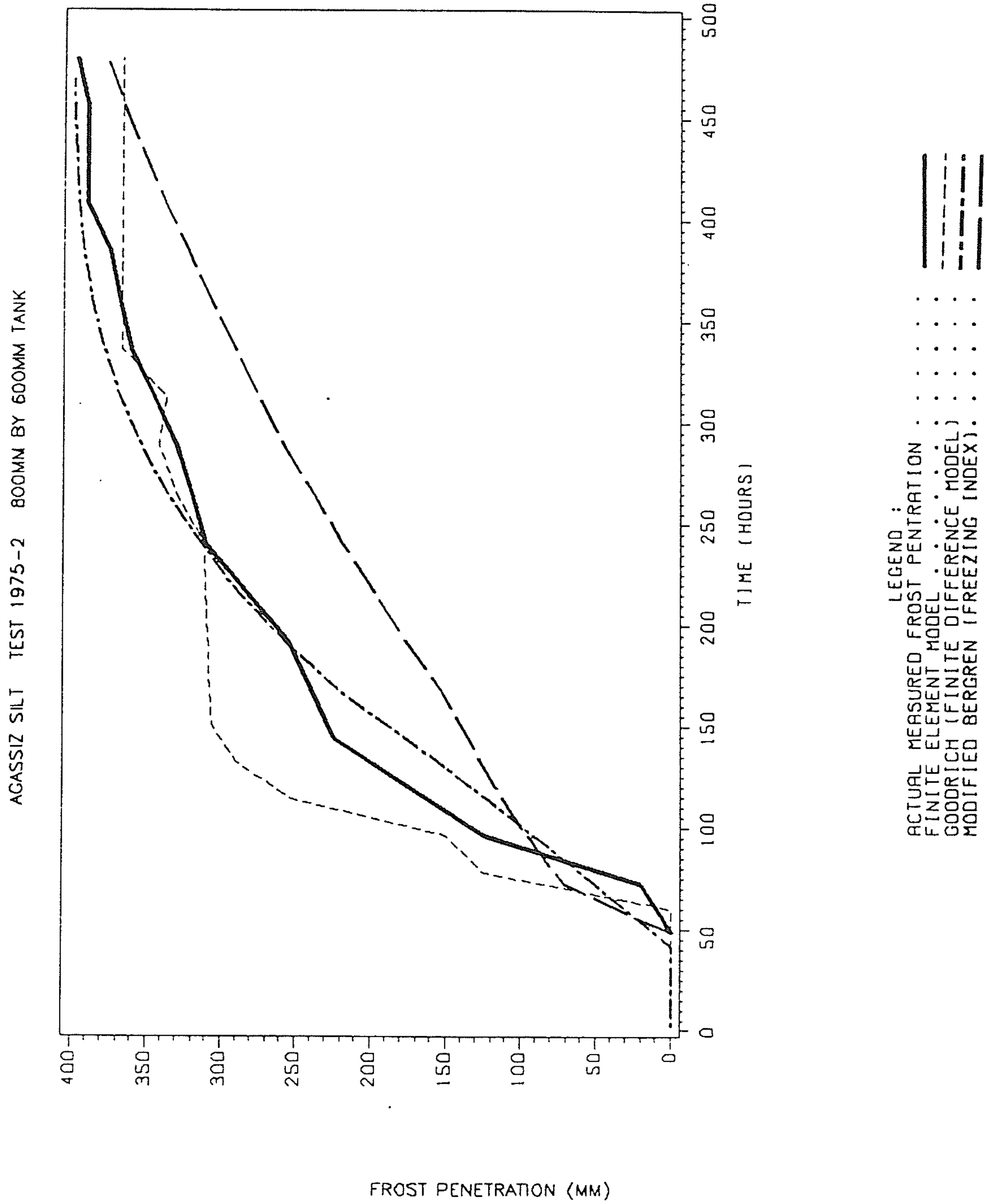

Figure 29: Frost penetration predictions for test 1975-2

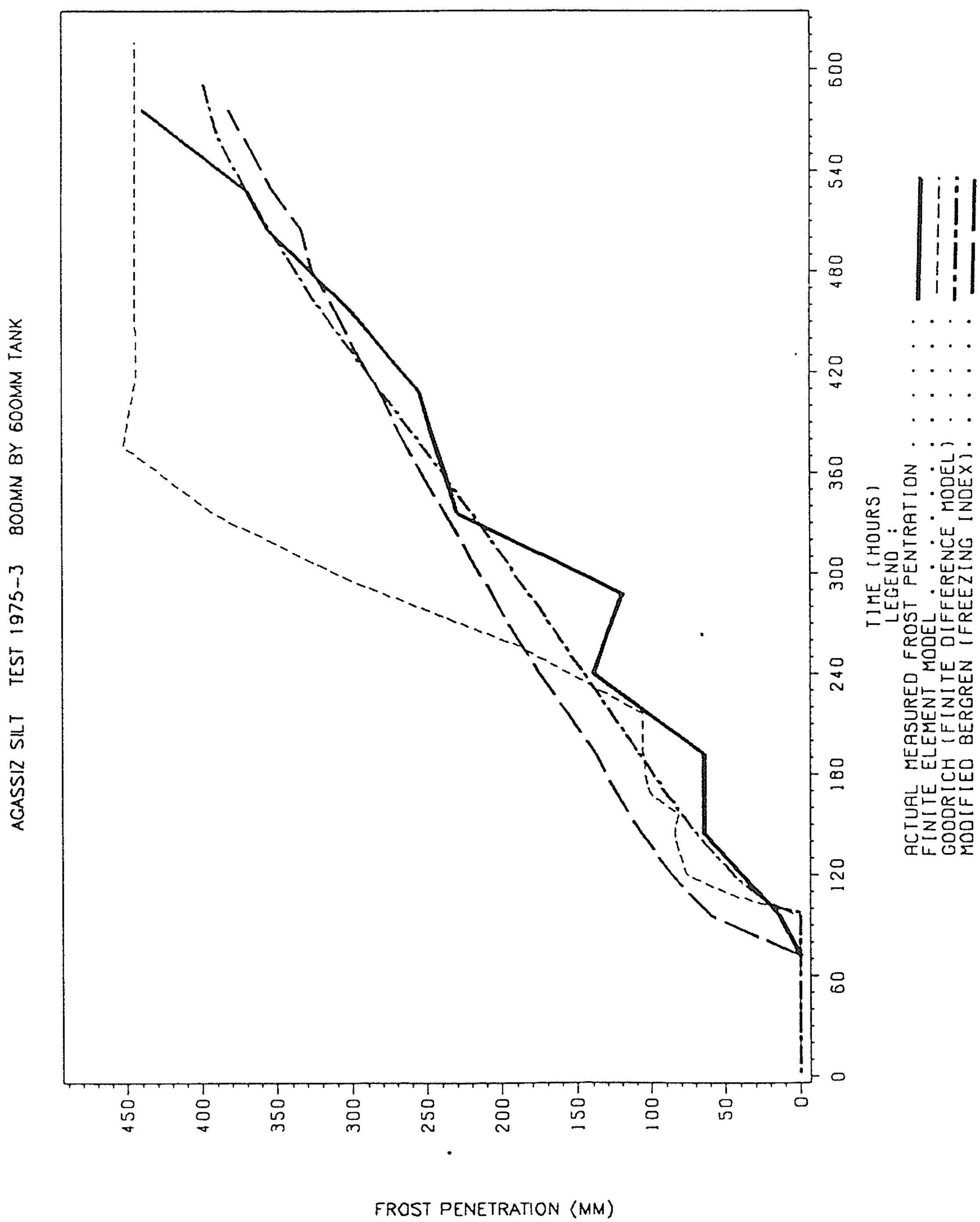

Figure 30: Frost penetration predictions for test 1975-3

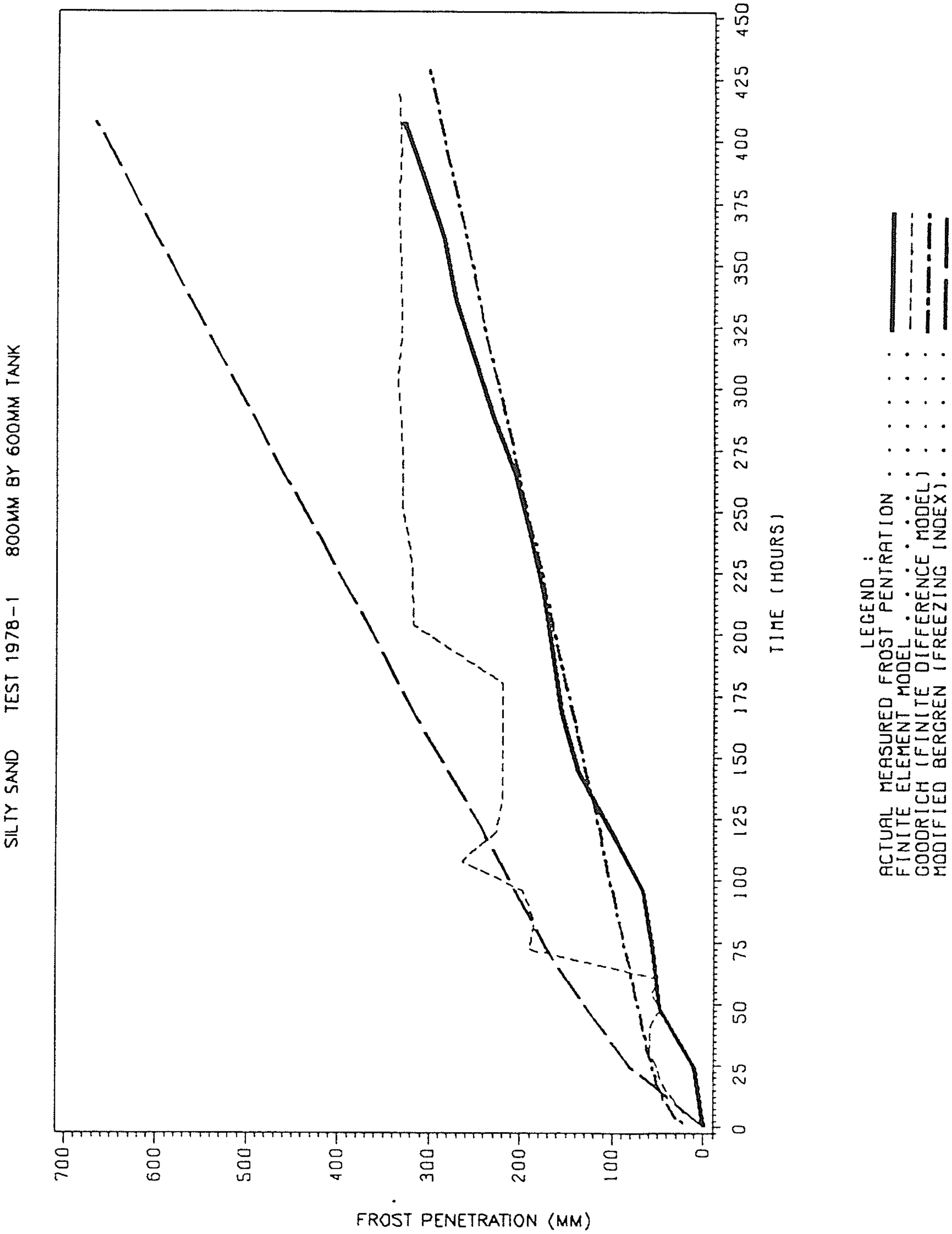

Figure 31: Frost penetration predictions for test 1978-1

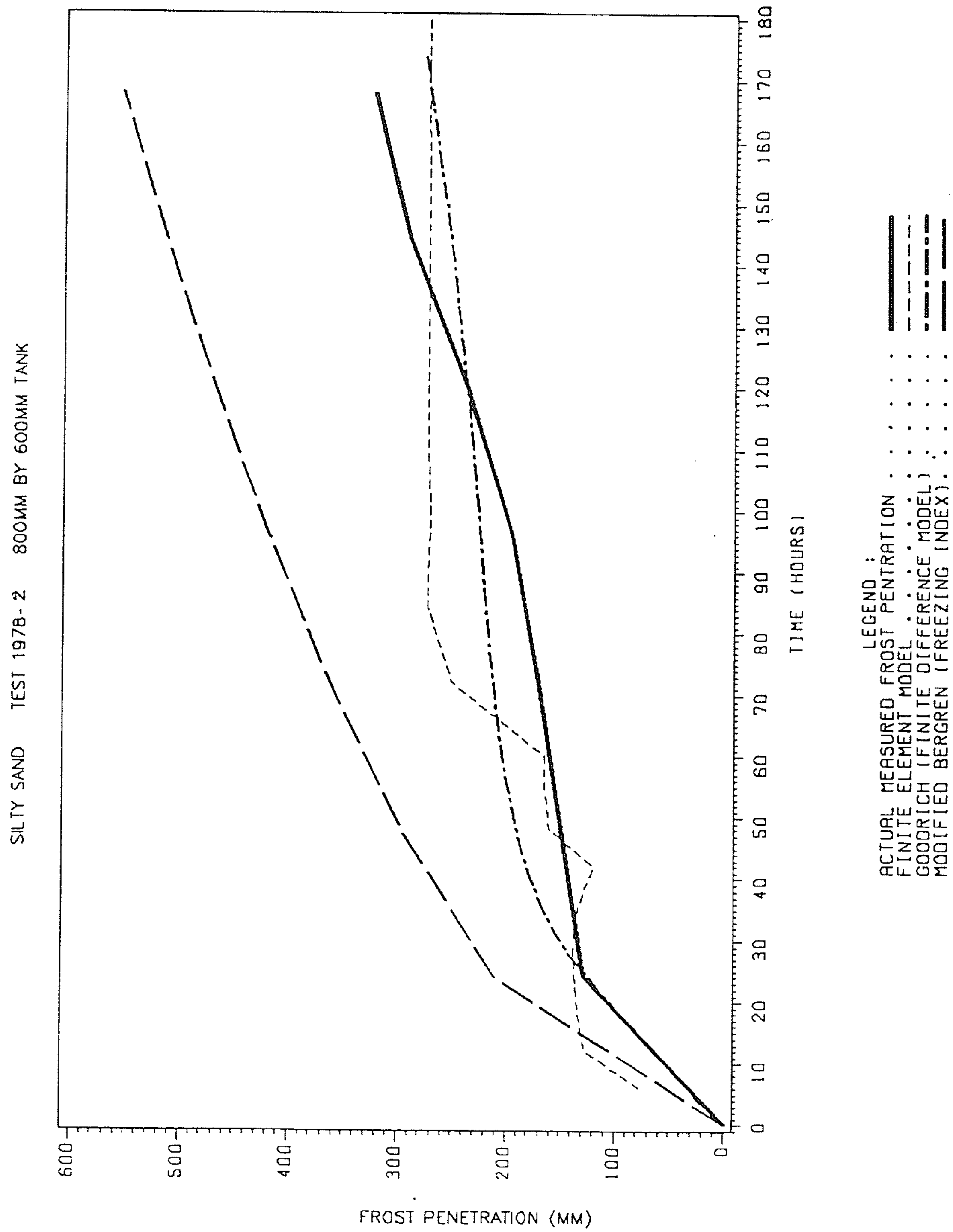

Figure 32: Frost penetration predictions for test 1978-2

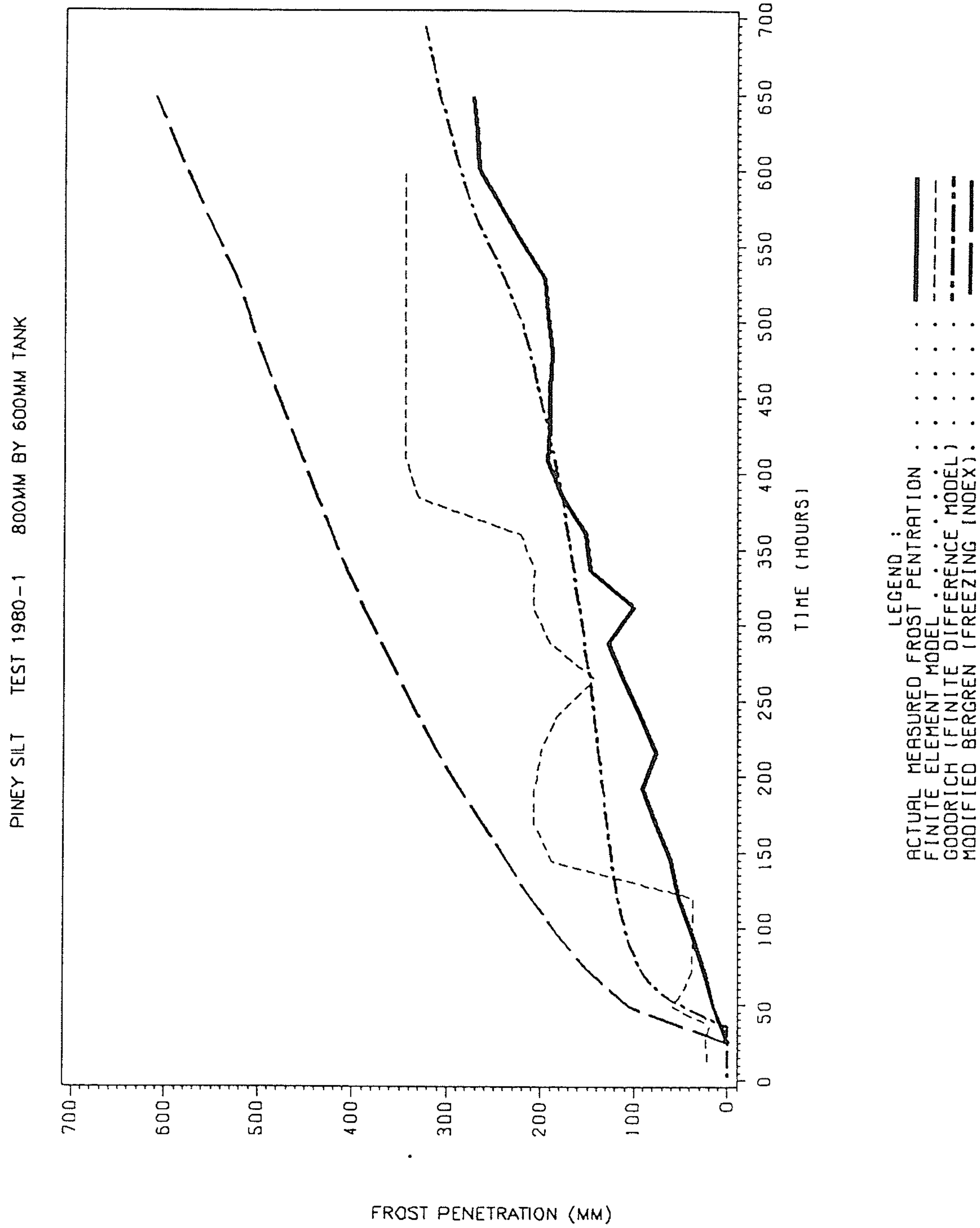

Figure 33: Frost penetration predictions for test 1980-1

Chapter VI

FROST HEAVE PREDICTIONS

6.1 INTRODUCTION

Nine frost heave models were used to predict the results of the twelve laboratory tests mentioned in section 4.1.3. All of the frost heave models have been summarized in Table 11.

Two approaches were used in the prediction of frost heave. The first approach used a calculated frost penetration depth as input into the frost heave models. The second approach used the measured depth of frost penetration to determine the amount of heaving. The input parameters affected by the depth of frost penetration are the frost penetration rate, the soil temperature gradients and the overburden pressure. Only the model by Sheriff et al. is unaffected by the approach chosen since it requires only surface temperature as input. The use of measured frost depth eliminates any error introduced by the frost depth calculation but the soil temperature gradients during most of the tests were unknown. They were estimated by assuming a linear distribution between the air temperature at the surface, zero degrees Celsius at the depth of frost penetration, and the water temperature at the base of the testing apparatus. The computer program which was used to predict the frost depth also estimated the temperature gradients in the vicinity of the frost front in both the frozen and unfrozen soils. This approach also offers the advantage of using time steps smaller than one day for each of the tests analyzed.

Both approaches were carried out using all nine frost heave models and, for the most part, on the same tests. Exceptions to this are noted in the following sections.

6.2 FROST HEAVE PREDICTIONS USING CALCULATED FROST DEPTH

The first approach to predicting the amount of frost heave used the frost penetration, frost penetration rate and temperature gradients as calculated by the finite difference method outlined by Goodrich (1978).

Nine frost heave tests were analyzed for the prediction comparison using this first approach. These nine tests were comprised of five tests on Agassiz silt, two tests on Piney silt and two tests on the silty sand. Two of the Agassiz silt tests were conducted in the 1.76 m by 2.40 m diameter apparatus and one test on Piney silt was conducted in the 100 mm by 125 mm diameter freezing cell. The remaining tests were carried out in the 800 mm by 600 mm square tank. A comparison of the measured frost heave and the predictions are plotted in Figures 34 to 42.

The calculation of the average percent error between the predicted and the measured frost heave was used to compare the various predictive models:

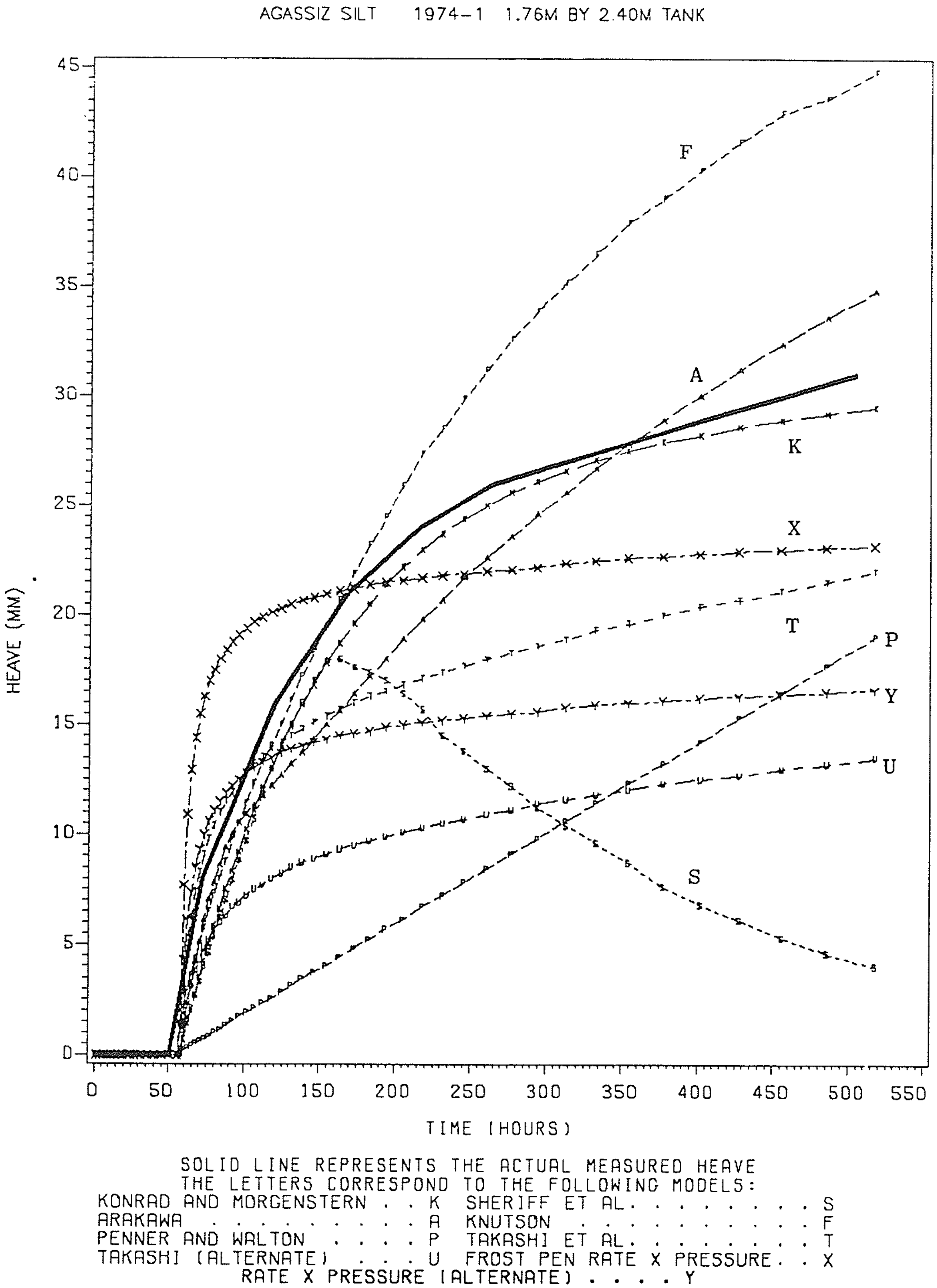

Figure 34: Frost heave predictions for test 1974-1 (using calculated frost depth)

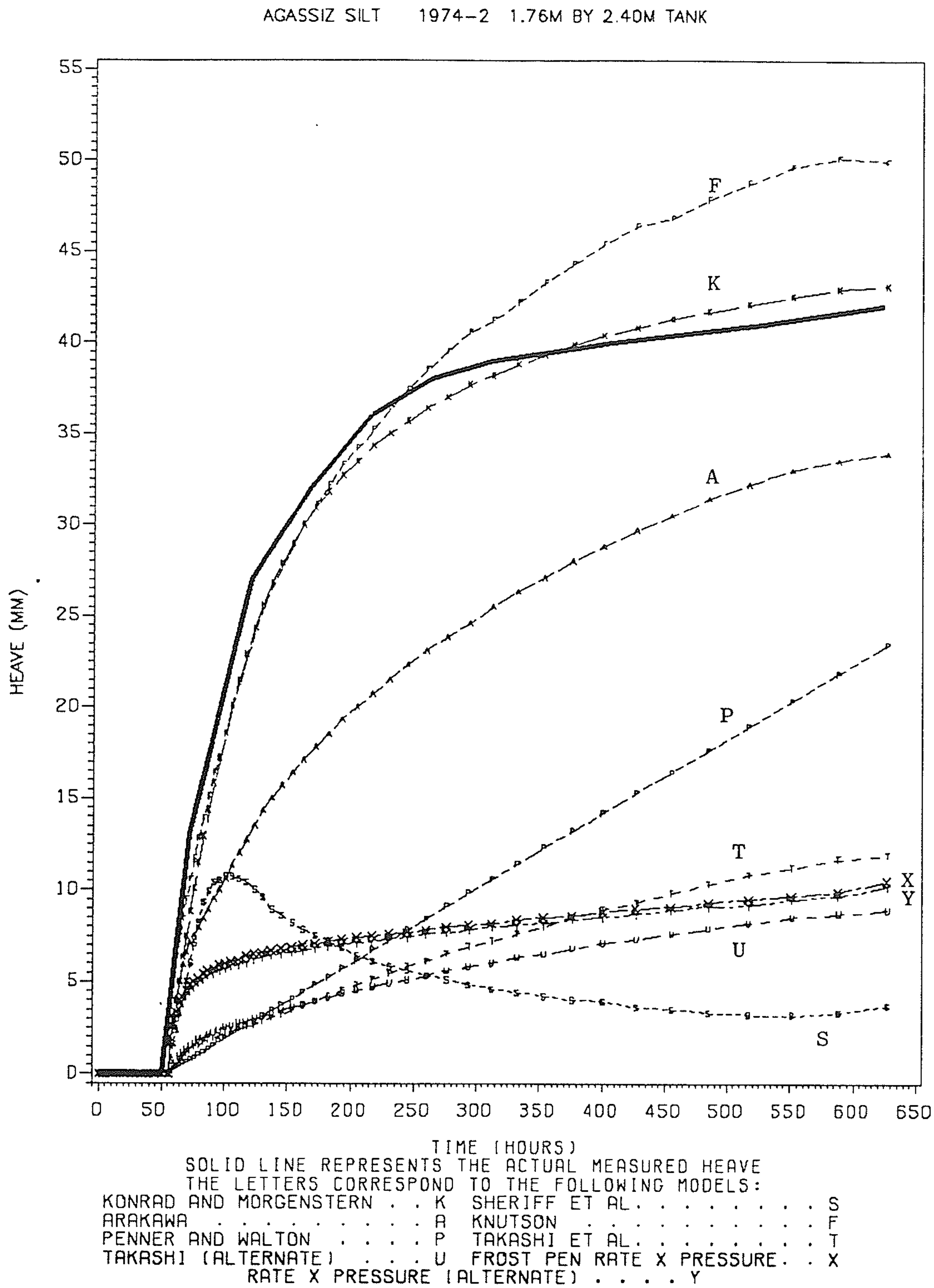

Figure 35: Frost heave predictions for test 1974-2 (using calculated frost depth)

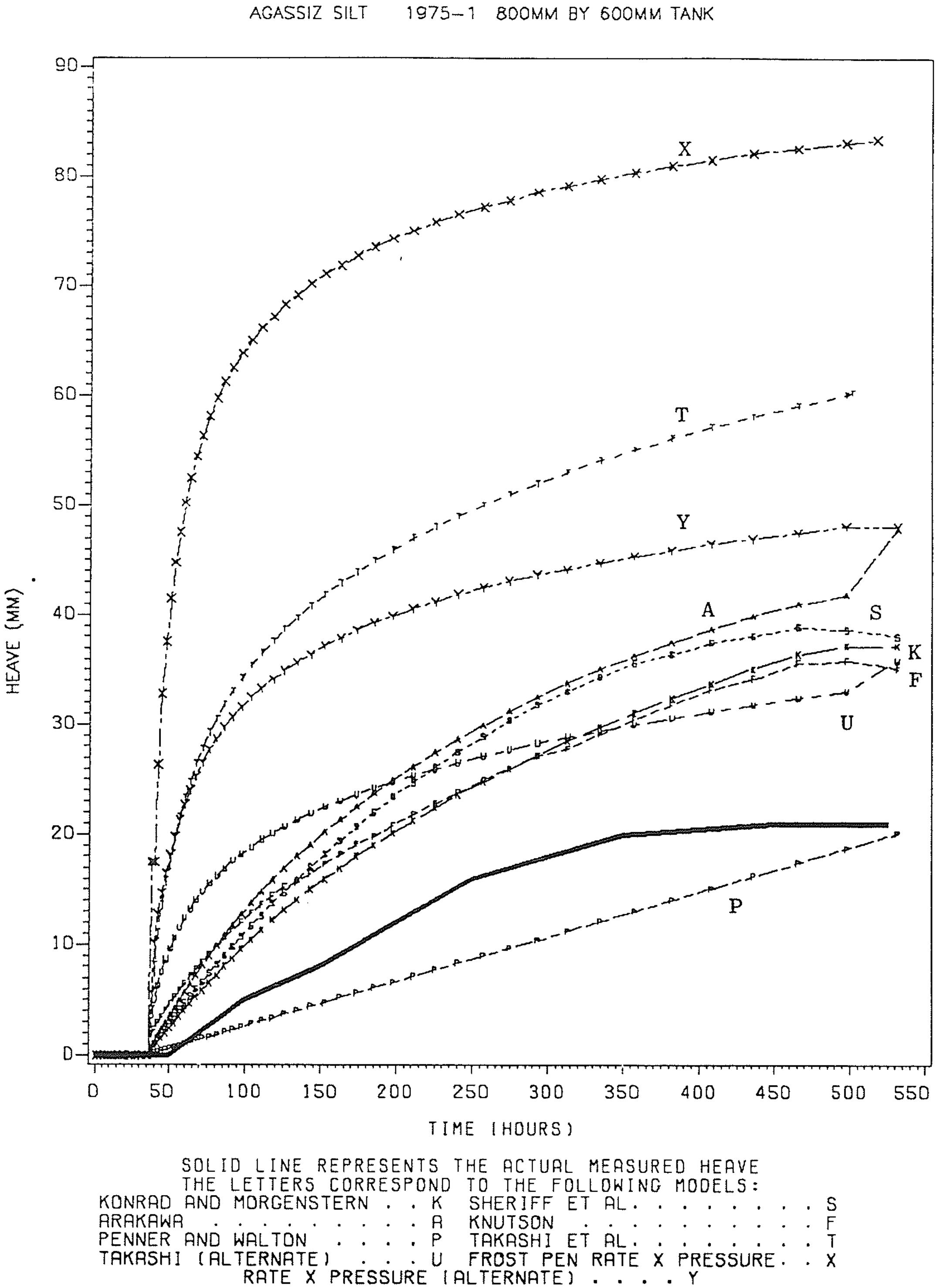

Figure 36: Frost heave predictions for test 1975-1 (using calculated frost depth)

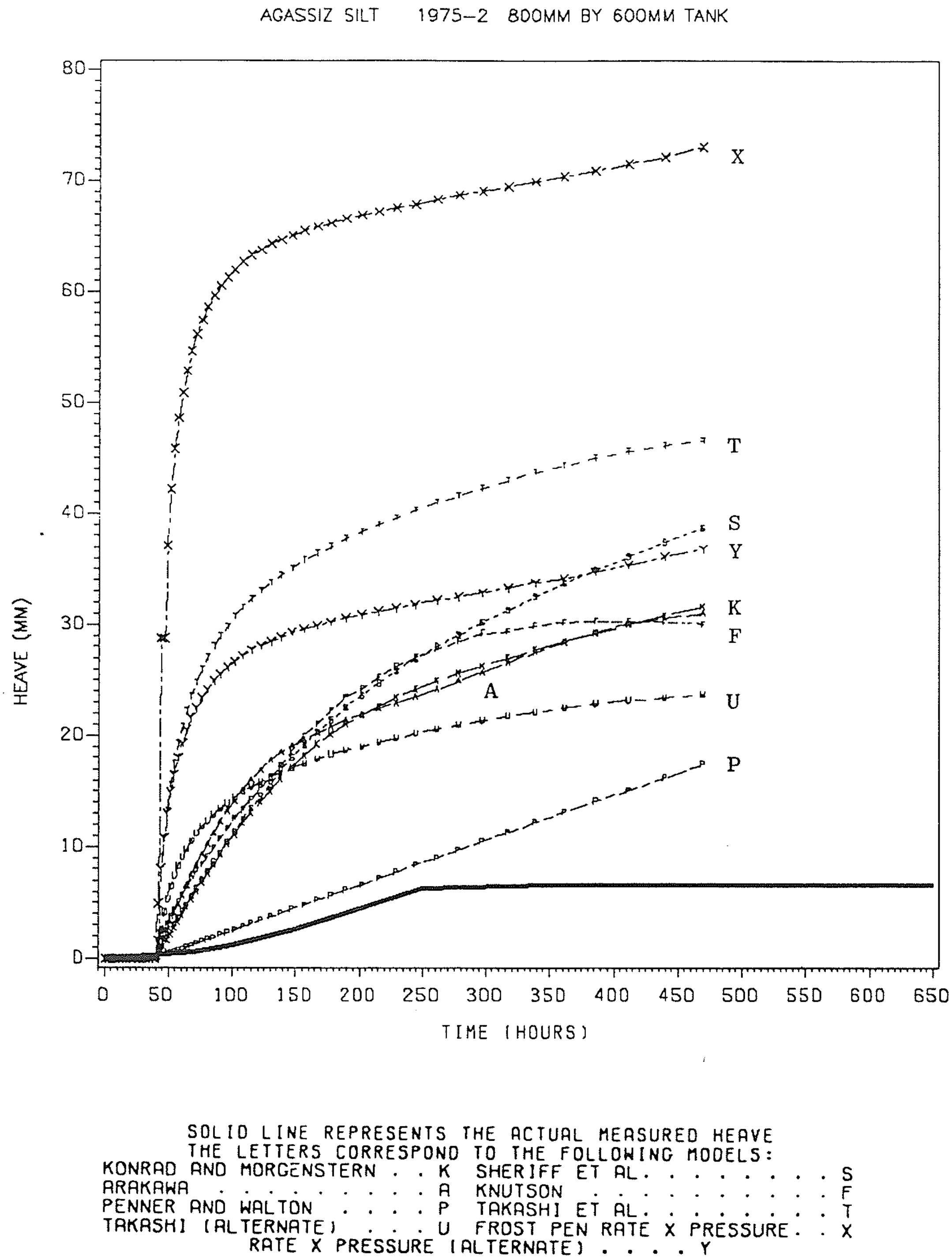

Figure 37: Frost heave predictions for test 1975-2 (using calculated frost depth)

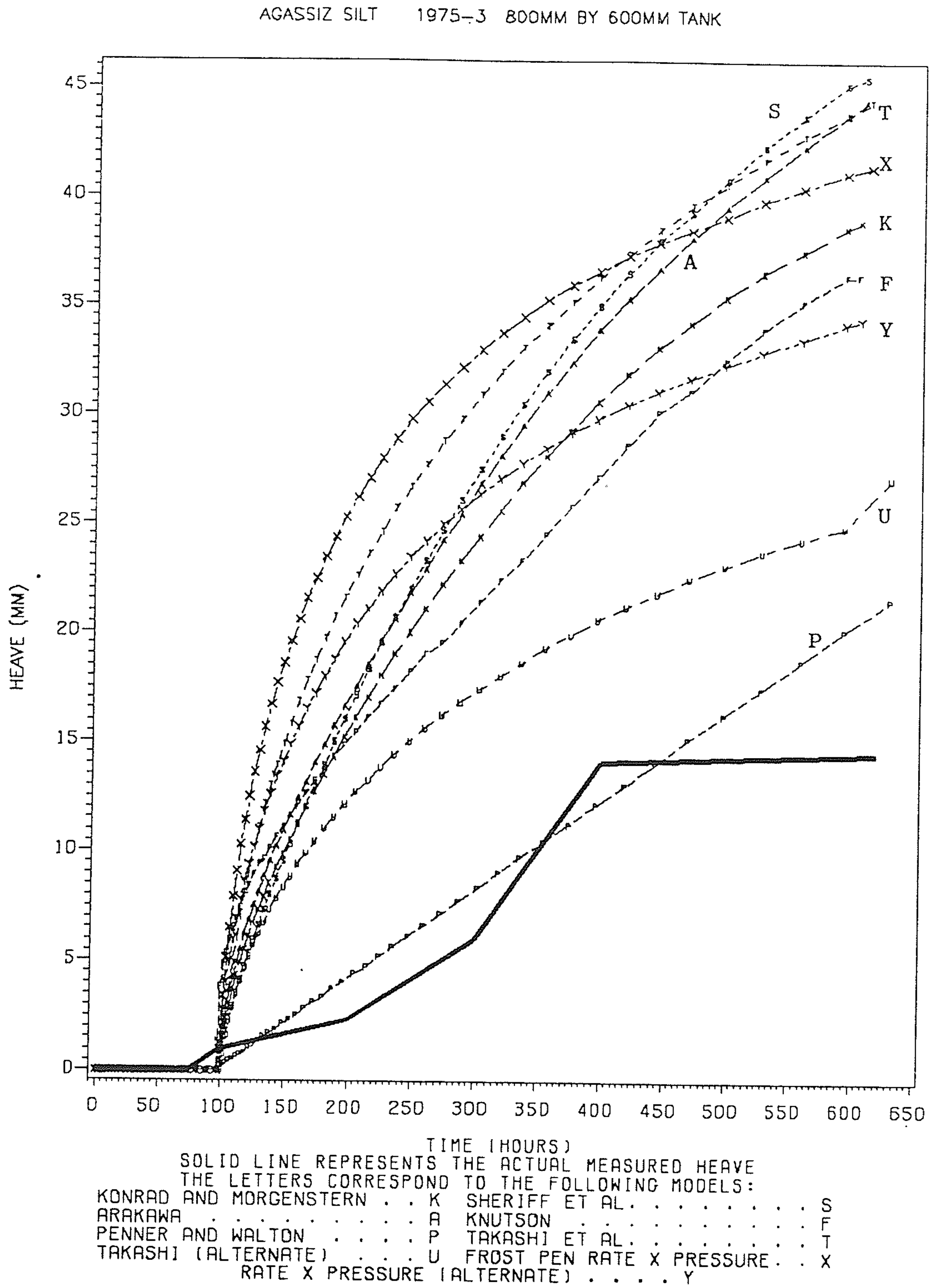

Figure 38: Frost heave predictions for test 1975-3 (using calculated frost depth)

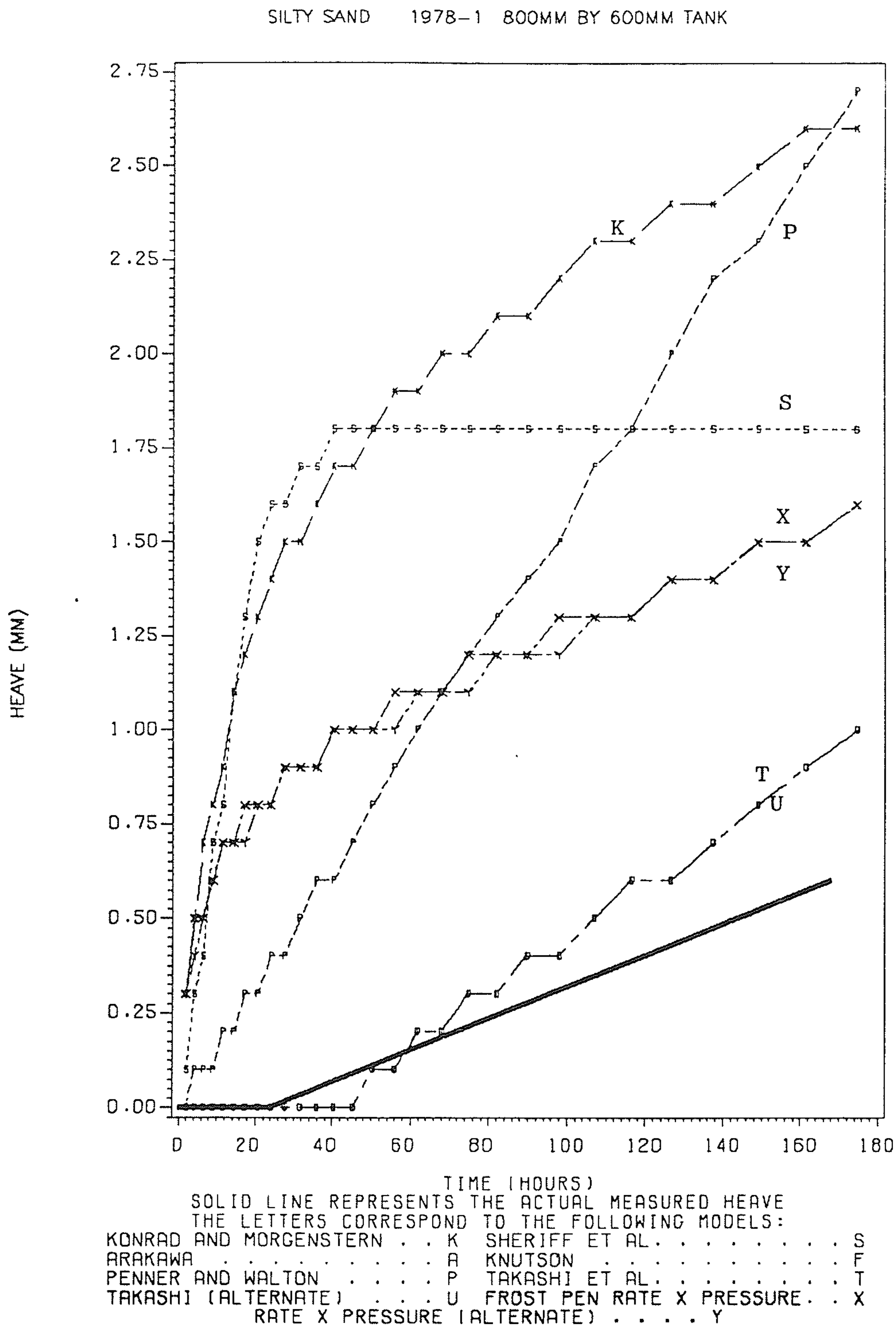

Figure 39: Frost heave predictions for test 1978-1 (using calculated frost depth)

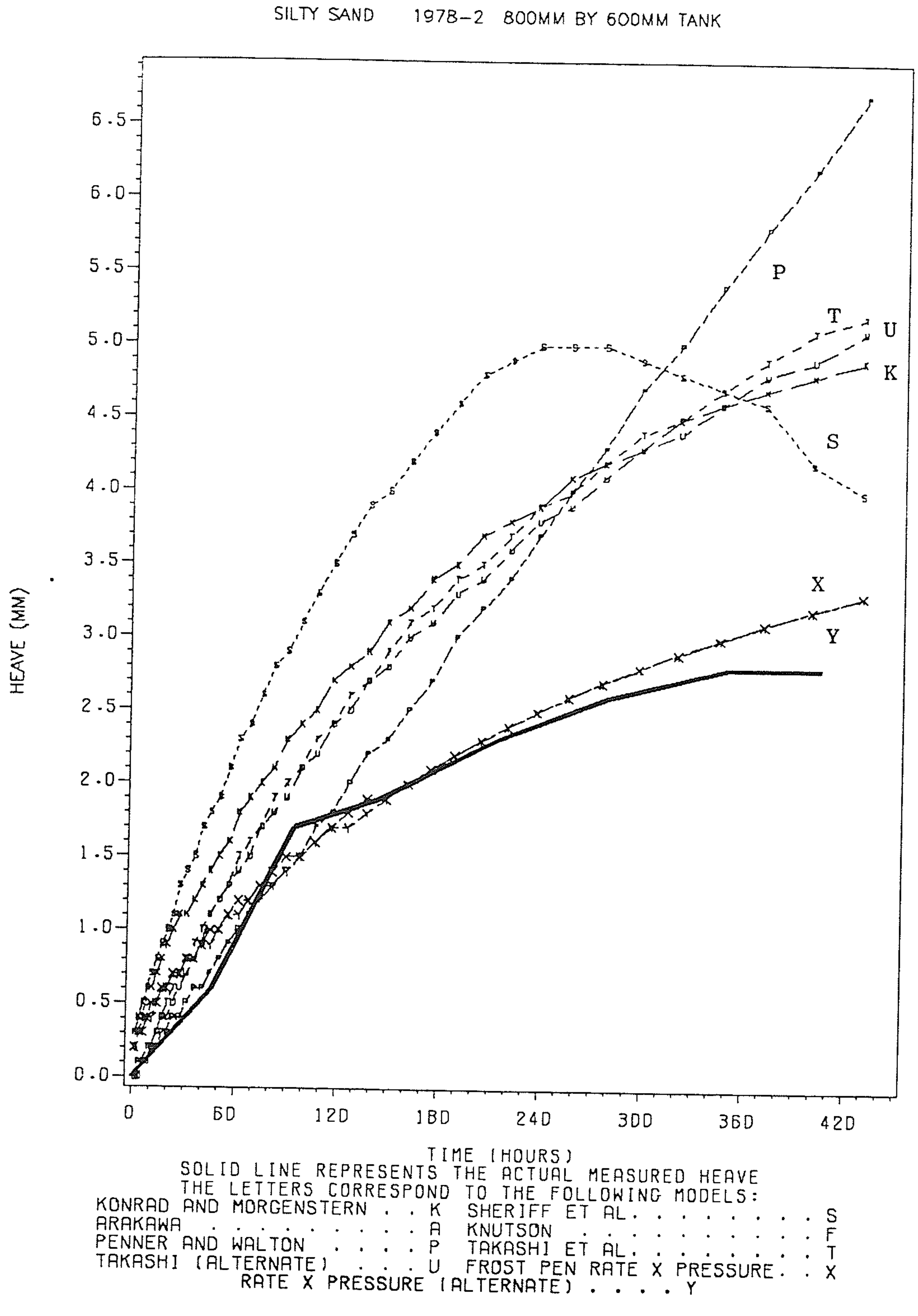

Figure 40: Frost heave predictions for test 1978-2 (using calculated frost depth)

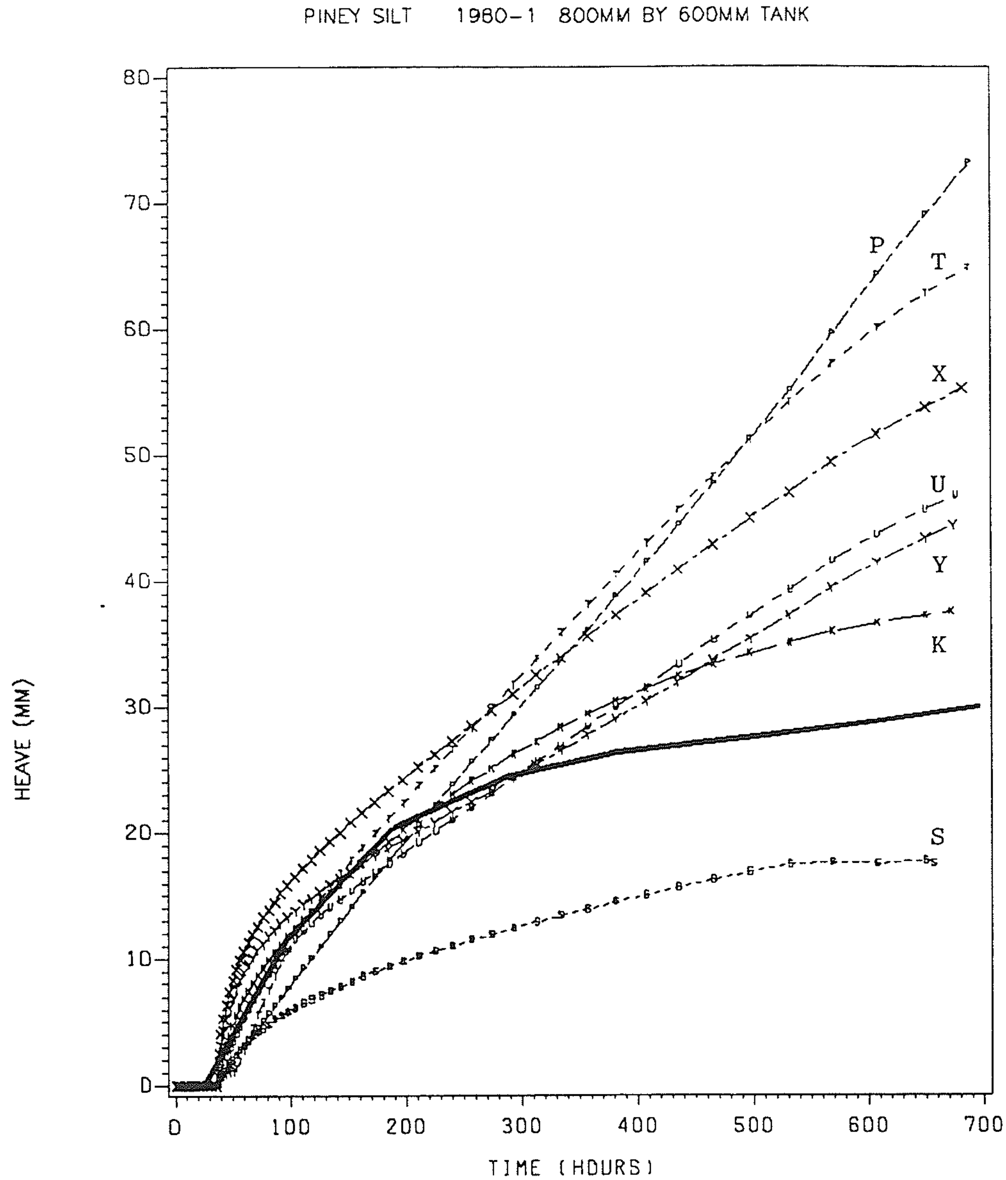

SOLID LINE REPRESENTS THE ACTUAL MEASURED HEAVE
THE LETTERS CORRESPOND TO THE FOLLOWING MODELS:

KONRAD AND MORGENSTERN . . K SHERIFF ET AL. . . . . S
ARAKAWA . . . . A KNUTSON . . . . F
PENNER AND WALTON . . . . . P TAKASHI ET AL. . . . . T
TAKASHI (ALTERNATE) . . . . U FROST PEN RATE X PRESSURE . . X
RATE X PRESSURE (ALTERNATE) . . . . Y

Figure 41: Frost heave predictions for test 1980-1 (using calculated frost depth)

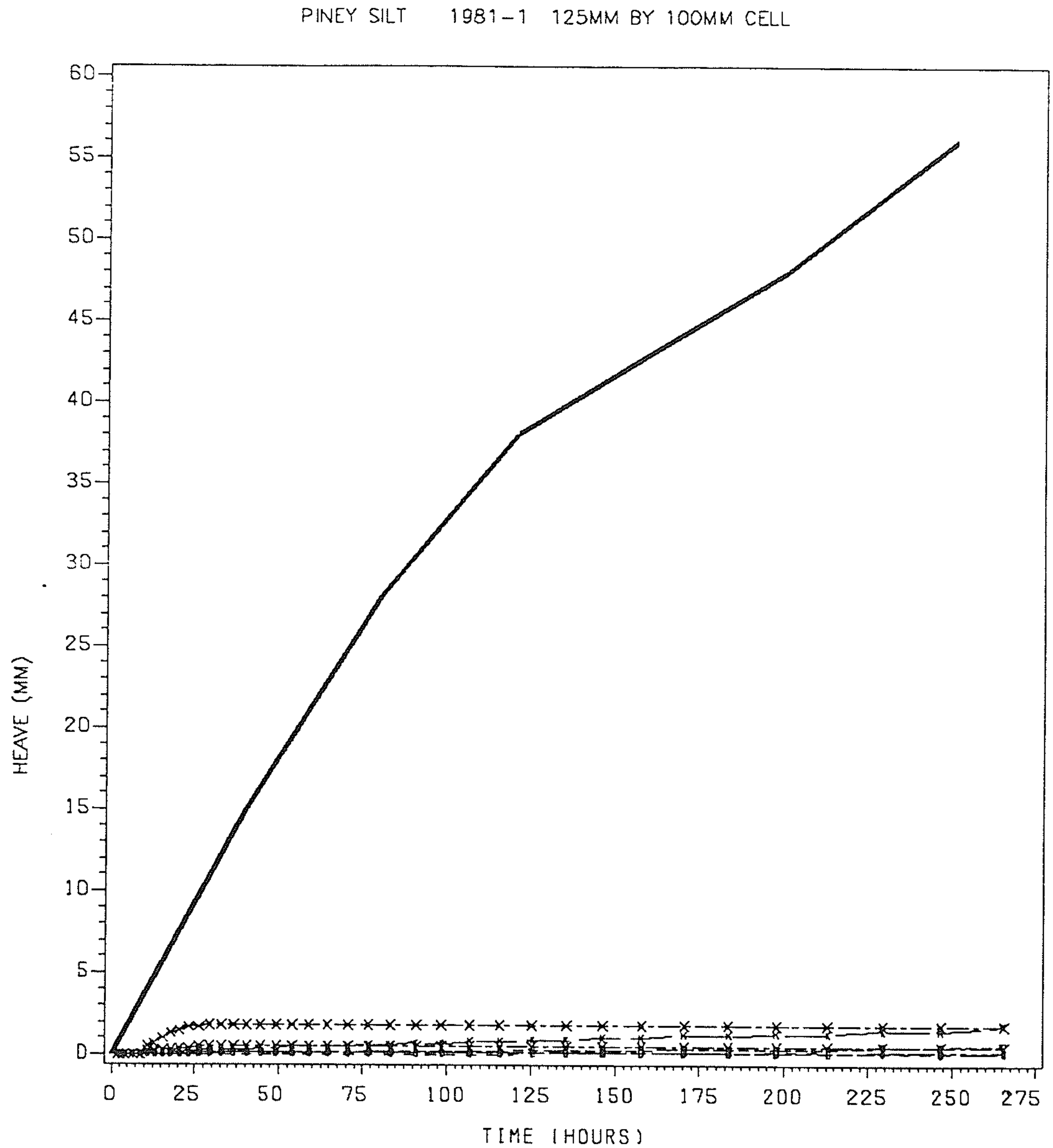

SOLID LINE REPRESENTS THE ACTUAL MEASURED HEAVE
THE LETTERS CORRESPOND TO THE FOLLOWING MODELS:

KONRAD AND MORGENSTERN . .	K	SHERIFF ET AL.	S
ARAKAWA	A	KNUTSON	F
PENNER AND WALTON	P	TAKASHI ET AL.	T
TAKASHI (ALTERNATE) . . .	U	FROST PEN RATE X PRESSURE . .	X

RATE X PRESSURE (ALTERNATE) . . . . Y

Figure 42: Frost heave predictions for test 1981-1 (using calculated frost depth)

$$\% \text{ Error} = \frac{1}{T} \left(\Sigma \frac{|\text{Actual} - \text{Predicted}|}{\text{Actual}} \Delta t \right) \times 100 \quad (28)$$

in which:

T = total time

Δt = time interval

Table 12 gives the percent error for each test while Table 13 shows the average percent error for all tests and for tests on a particular soil type. The results show that there is no one model which consistently predicts the frost heave accurately for every test. The Penner and Walton model provided the best overall average percent error (132 %) while the frost penetration rate times overburden pressure model provided the poorest correlation (891 %). The model given by Konrad and Morgenstern gave a very good prediction for tests 1974-1 and 1974-2 (11.1 % and 7.3 % respectively). This is significant since these were the only two large scale pit tests analyzed. The Konrad and Morgenstern model also gave the best prediction for test 1980-1 on Piney silt (19.5 %). For the Piney silt test using the 100 mm deep apparatus (1981-1) all of the nine models predicted less than 10 % of the total frost heave. The model by Takashi et al. provided the best results for tests on silty sand (64 % error).

TABLE 12 % Error for each test (using calculated frost depth)

	Test:								
Theory	1974-1	1974-2	1975-1 Agassiz Silt	1975-2	1975-3	1978-1 Silty sand	1978-2	1980-1 Piney silt	1981-1
1	28.1	82.5	3750.4	2244.6	451.0	1281.7	26.1	55.2	94.8
2	43.2	83.5	1611.8	921.7	324.0	1255.7	24.7	26.4	99.1
3	31.0	87.1	1768.1	2090.1	387.7	62.8	69.4	59.7	100.8
4	60.8	90.6	840.1	475.6	180.6	62.5	64.4	28.2	100.5
5	70.5	73.8	78.1	93.3	35.7	609.0	65.2	62.6	100.2
6	59.1	91.0	328.1	499.9	312.1	1679.5	121.2	53.4	100.6
7	11.1	7.3	262.9	444.1	284.7	1909.1	96.1	19.5	98.5
8	15.7	36.0	388.8	486.9	317.7	-	-	-	-
9	30.7	14.3	431.3	495.2	279.9	-	-	-	-

Theories:

1.Frost Penetration Rate x Pressure 2.Pen. Rate x Pressure (alternate) 3.Takashi et al.

4.Takashi et al. (alternate) 5.Penner and Walton 6.Sheriff et al.

7.Konrad and Morgenstern 8.Arakawa (Efficiency) 9.Knutson (Freezing Index)

TABLE 13

Average % error (calculated frost depth approach)

Model	Piney	Agassiz	Sand	Total
1	75.0	1311.3	653.9	890.5
2	62.8	596.8	640.2	487.8
3	80.3	672.8	66.1	406.3
4	64.4	329.5	63.5	211.5
5	81.4	70.3	337.1	132.1
6	77.0	258.0	900.4	360.5
7	59.0	202.0	1002.6	348.1
8	-	249.0	-	249.0
9	-	250.3	-	250.3

Legend: 1. Pen. rate x pressure 2. Rate x pressure (alt.)
3. Takashi et al. 4. Takashi (alternate)
5. Penner and Walton 6. Sheriff et al.
7. Konrad and Morgenstern 8. Arakawa
9. Knutson

6.3 FROST HEAVE PREDICTIONS USING MEASURED FROST DEPTH

Eleven of the frost heave prediction experiments used thermocouples placed at 25 or 50 mm intervals to measure the depth of frost penetration. The rate of frost penetration and the overburden pressure were calculated from the measured depths of frost penetration.

In addition to the nine tests analyzed using caclulated frost depths two laboratory tests on Piney silt and one additional test on the silty sand were analyzed using models 5 to 9 from Table 6. Only the depth of frost penetration was known for these tests and no temperature information was available and hence only Ice Segreation Ratio models could be used. The 125 mm by 100 mm diameter experiment on Piney silt was not used in this second approach since the depth of frost penetration was not measured, bringing the total number of tests analyzed using this approach to eleven. The frost heave predictions for the eleven tests using measured frost depth as input are plotted in Figures 43 to 53.

Table 14 gives the percent error calculated for each of the eleven tests while Table 15 shows the average percent error for all the tests and for tests on the same soil type. The percent error varied from a low of 8 % to a high of 4000 %. The average of the percent erors for all the tests were generally between 100 and 300 percent. The results are similar to the results from the first approach but the percent errors are generally smaller. There is a poorer correlation for the model by Konrad and Morgenstern which might be due to the assumptions regarding the temperature gradient in the frozen fringe. The model by Penner and Walton provided the lowest percent error for Agassiz silt (50 % error). The model by Sheriff et al. provided the lowest percent error for Piney silt (47 % error). The best results for the tests

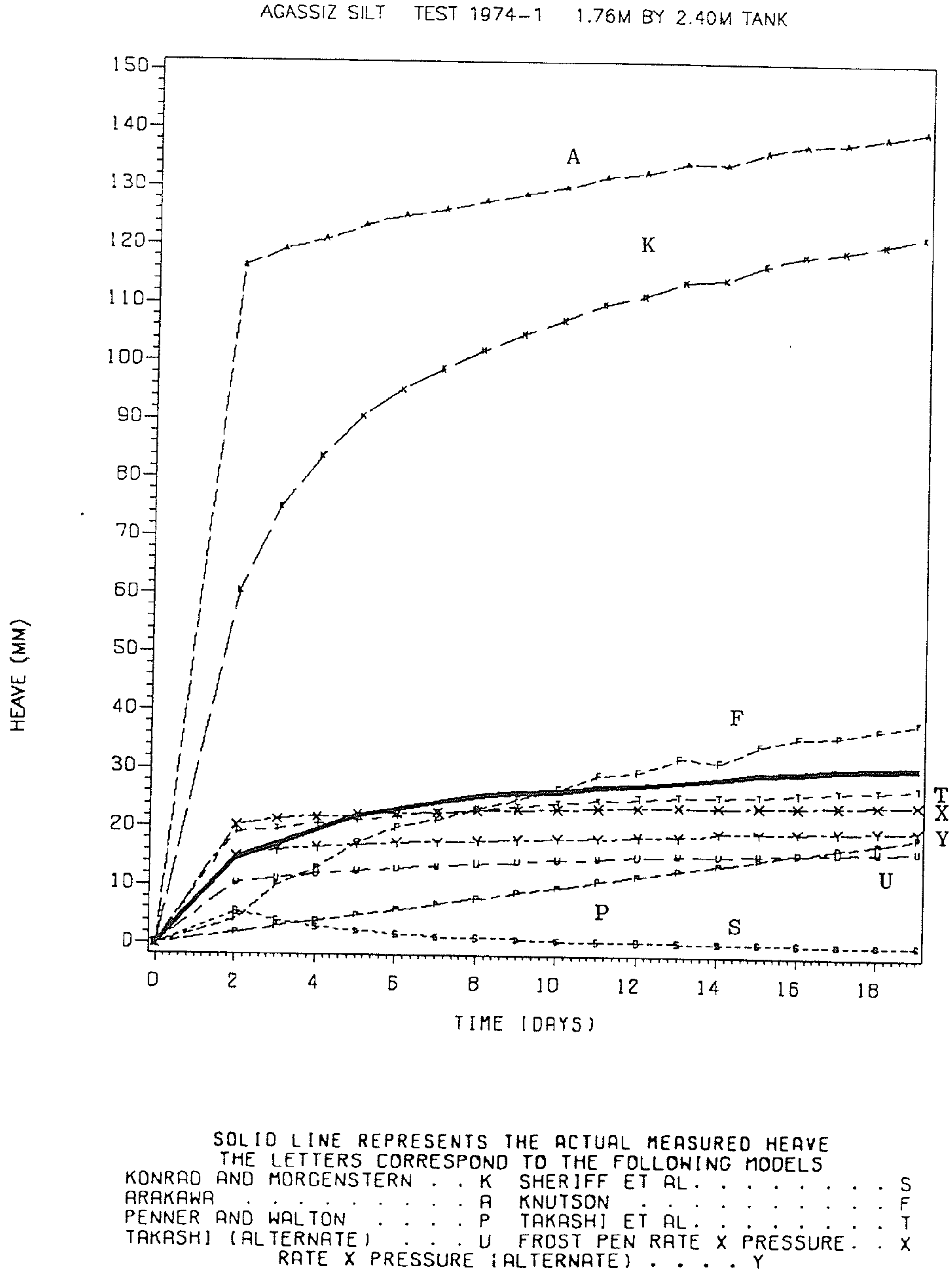

Figure 43: Frost heave predictions for test 1974-1 (using measured frost depth)

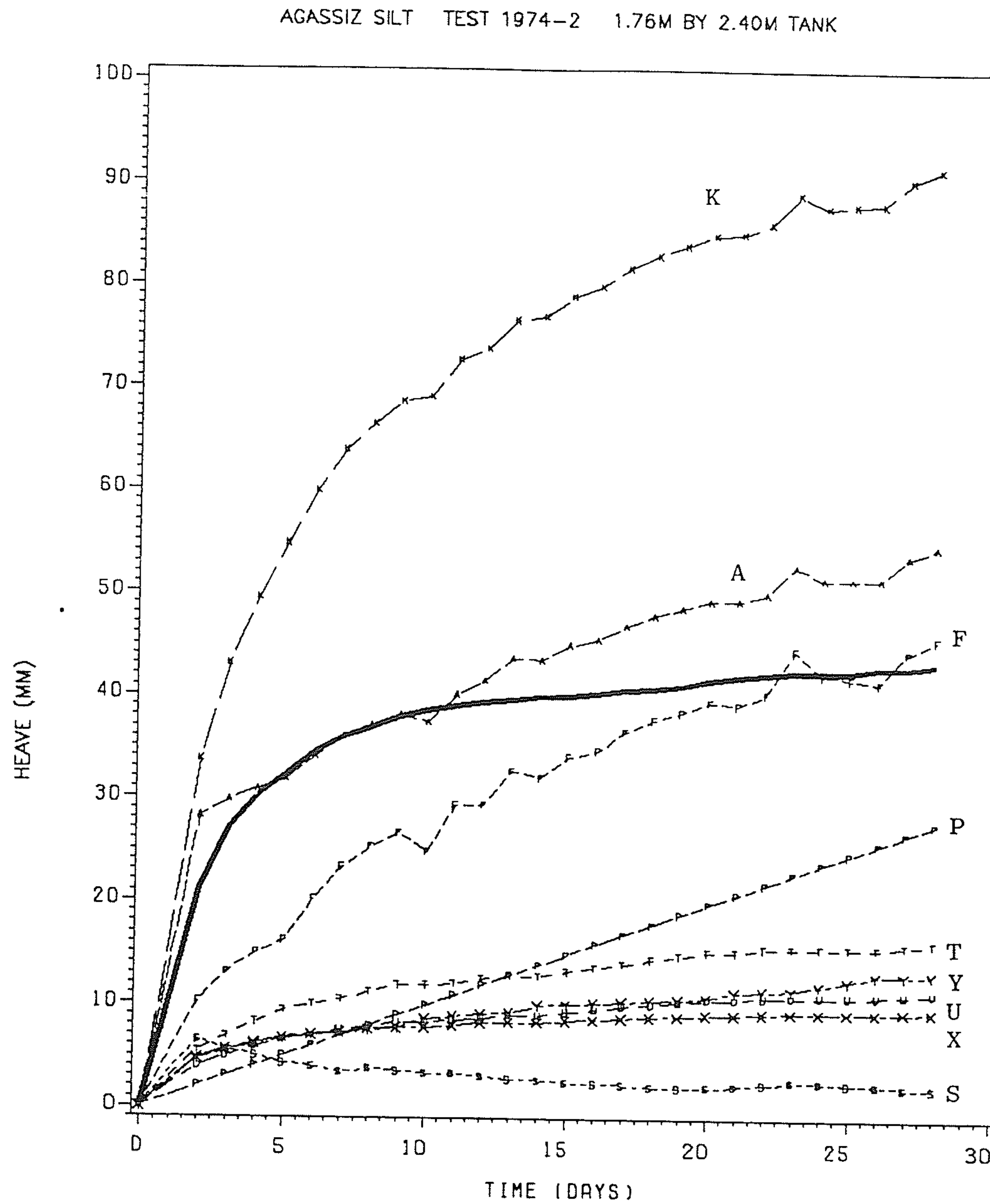

SOLID LINE REPRESENTS THE ACTUAL MEASURED HEAVE
THE LETTERS CORRESPOND TO THE FOLLOWING MODELS

KONRAD AND MORGENSTERN . . K SHERIFF ET AL. . . . . S
ARAKAWA . . . . A KNUTSON . . . . F
PENNER AND WALTON . . . . . P TAKASHI ET AL. . . . . T
TAKASHI (ALTERNATE) . . . . U FROST PEN RATE X PRESSURE . . X
RATE X PRESSURE (ALTERNATE) . . . . Y

Figure 44: Frost heave predictions for test 1974-2 (using measured frost depth)

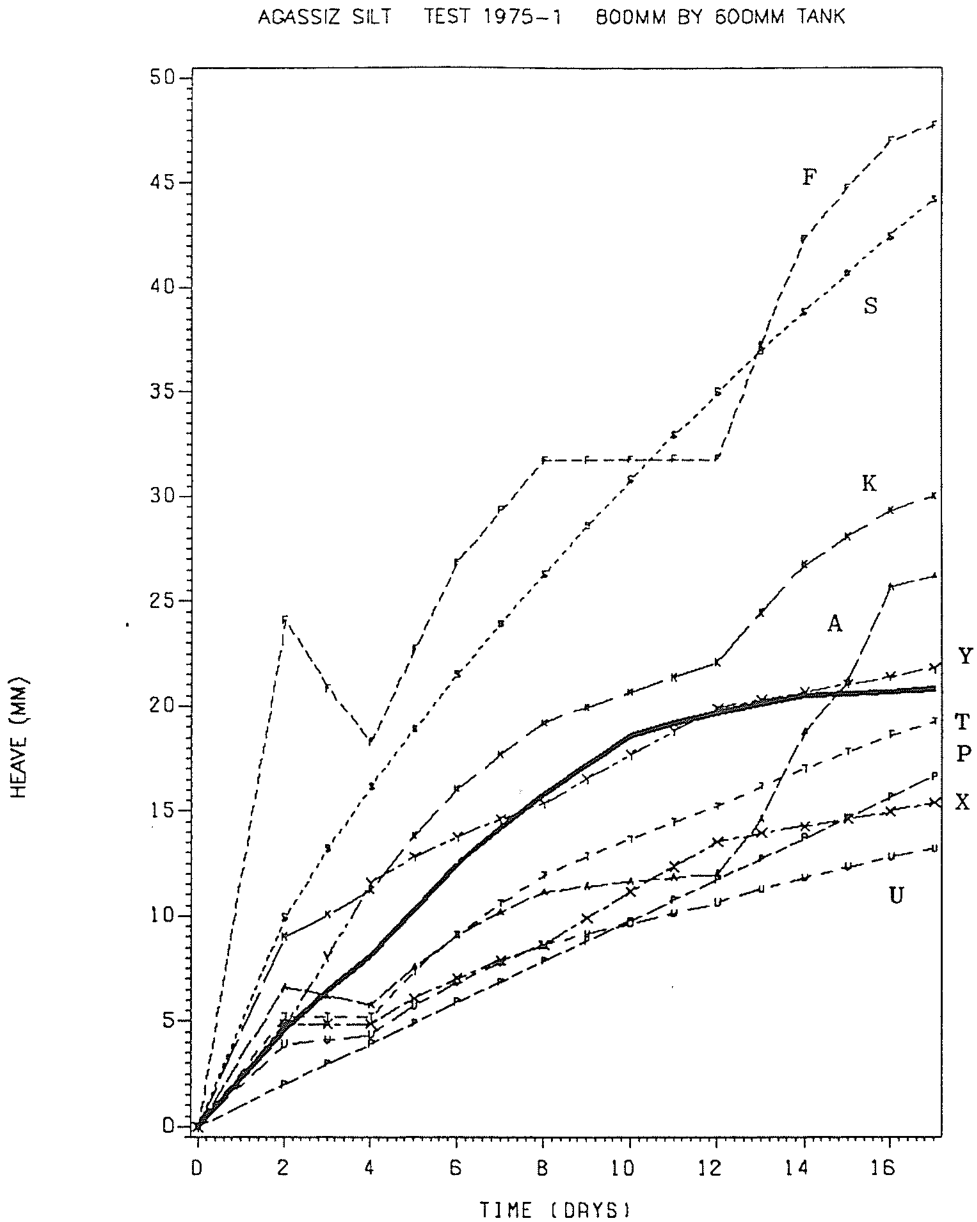

SOLID LINE REPRESENTS THE ACTUAL MEASURED HEAVE
THE LETTERS CORRESPOND TO THE FOLLOWING MODELS
KONRAD AND MORGENSTERN . . K SHERIFF ET AL. . . . . S
ARAKAWA . . . . A KNUTSON . . . . F
PENNER AND WALTON . . . . P TAKASHI ET AL. . . . . T
TAKASHI (ALTERNATE) . . . U FROST PEN RATE X PRESSURE . . X
RATE X PRESSURE (ALTERNATE) . . . . Y

Figure 45: Frost heave predictions for test 1975-1 (using measured frost depth)

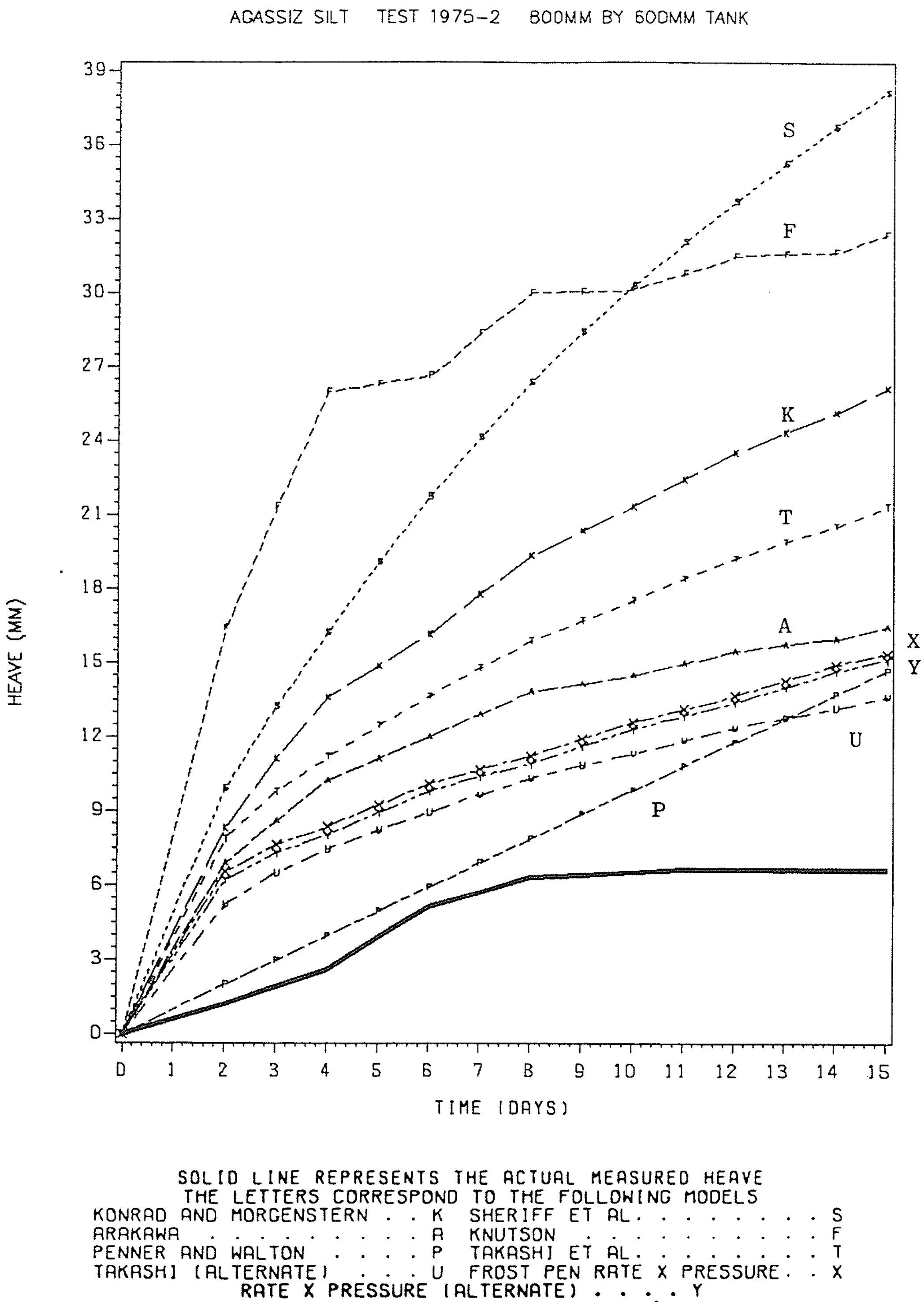

Figure 46: Frost heave predictions for test 1975-2 (using measured frost depth)

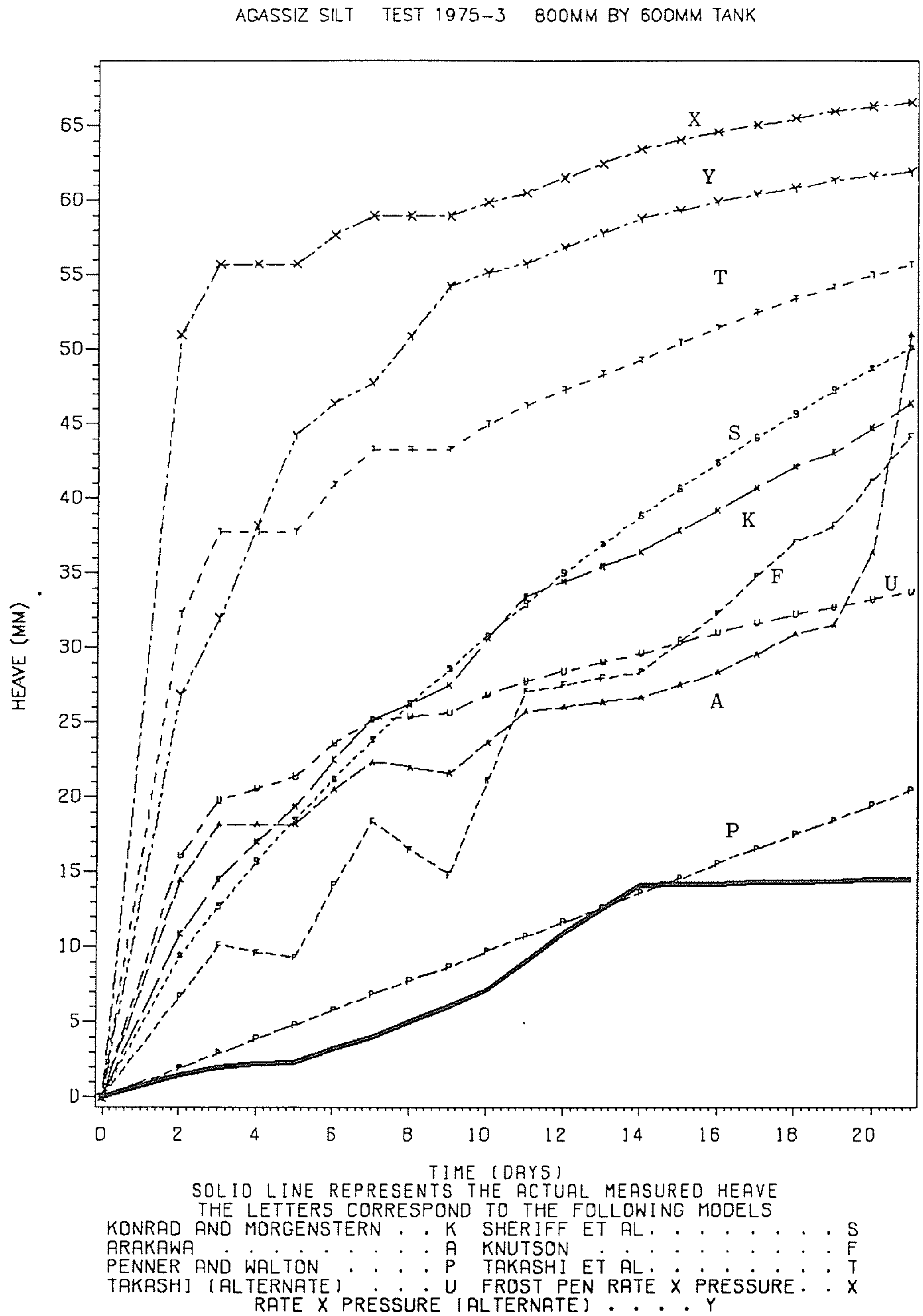

Figure 47: Frost heave predictions for test 1975-3 (using measured frost depth)

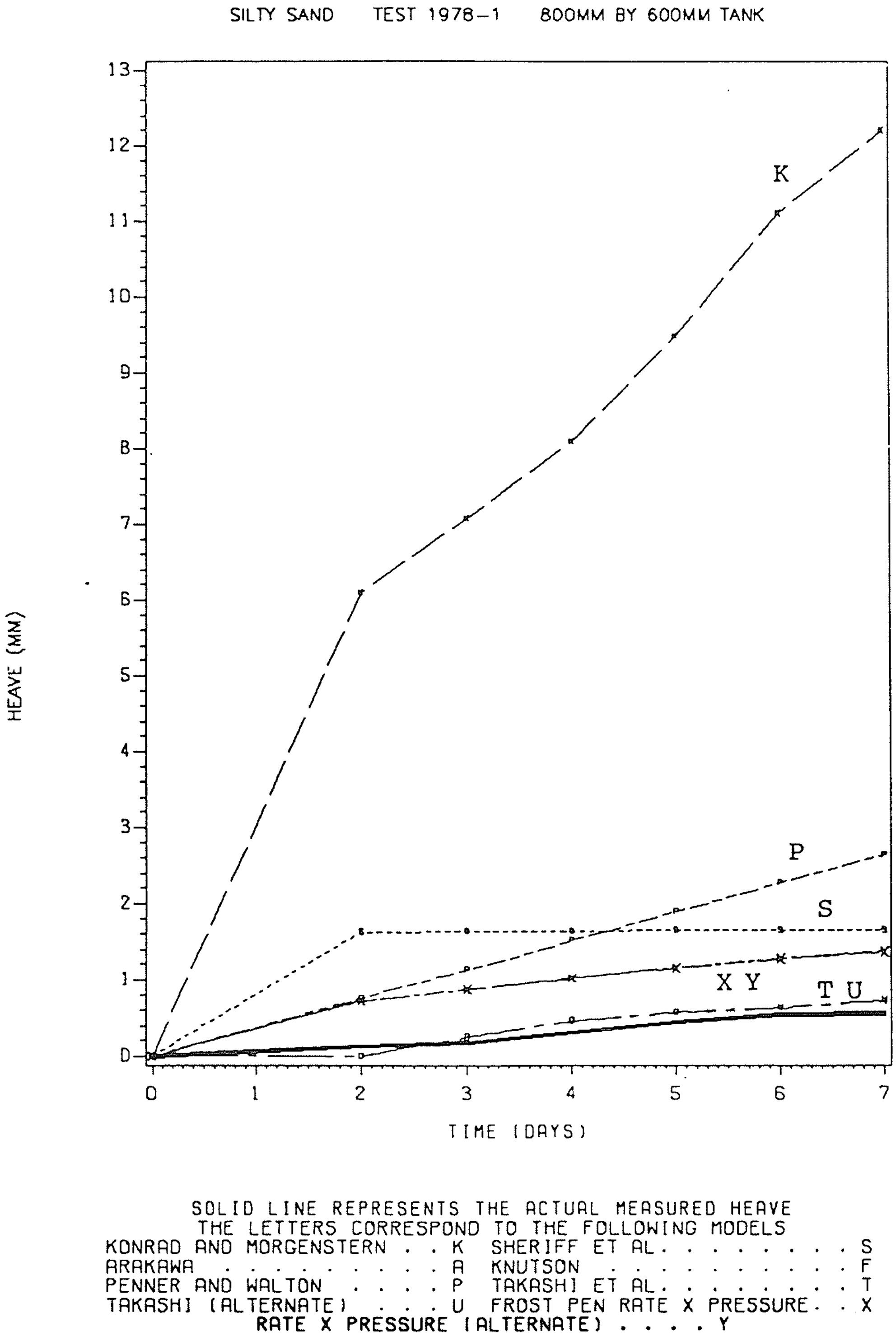

Figure 48: Frost heave predictions for test 1978-1 (using measured frost depth)

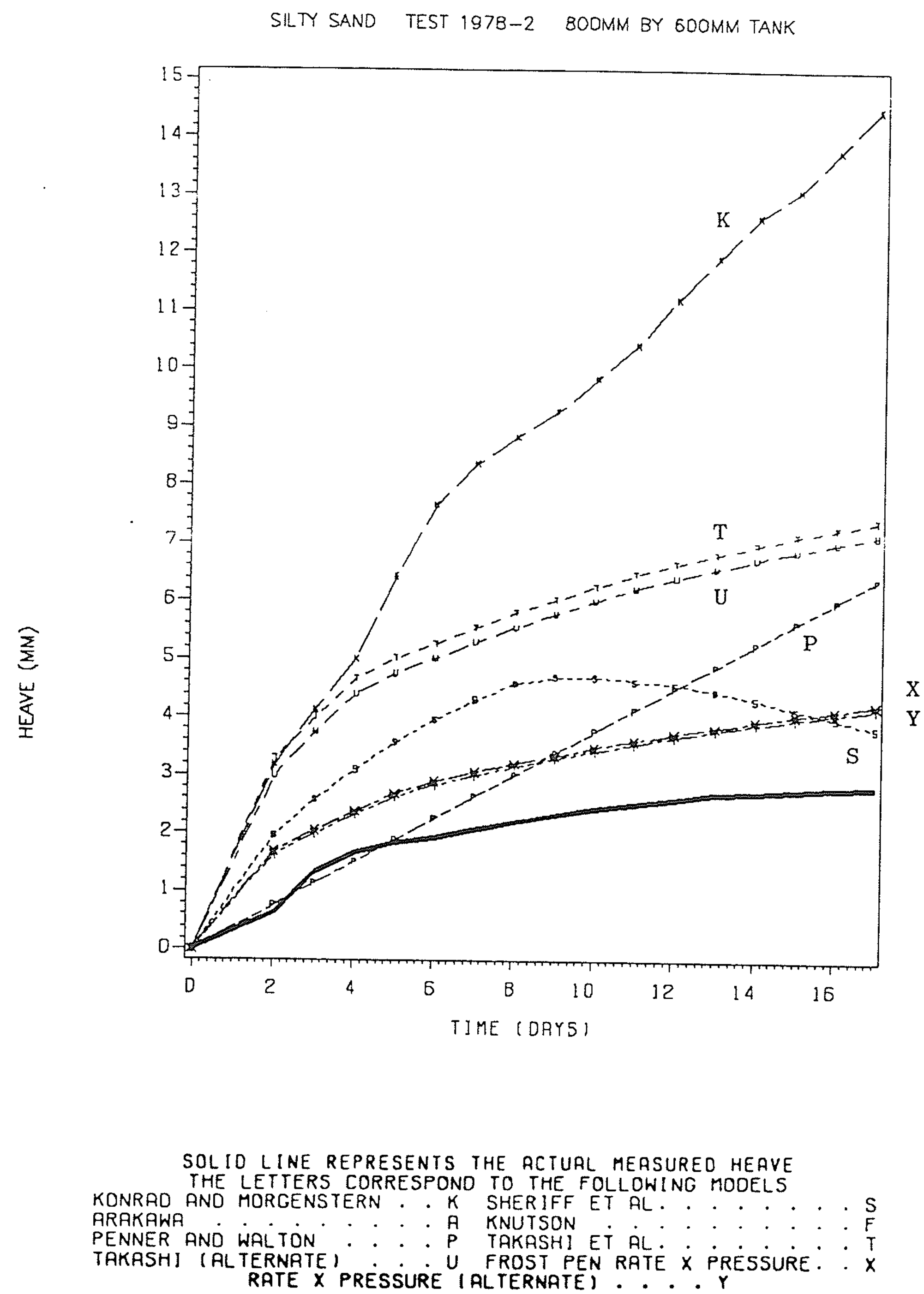

Figure 49: Frost heave predictions for test 1978-2 (using measured frost depth)

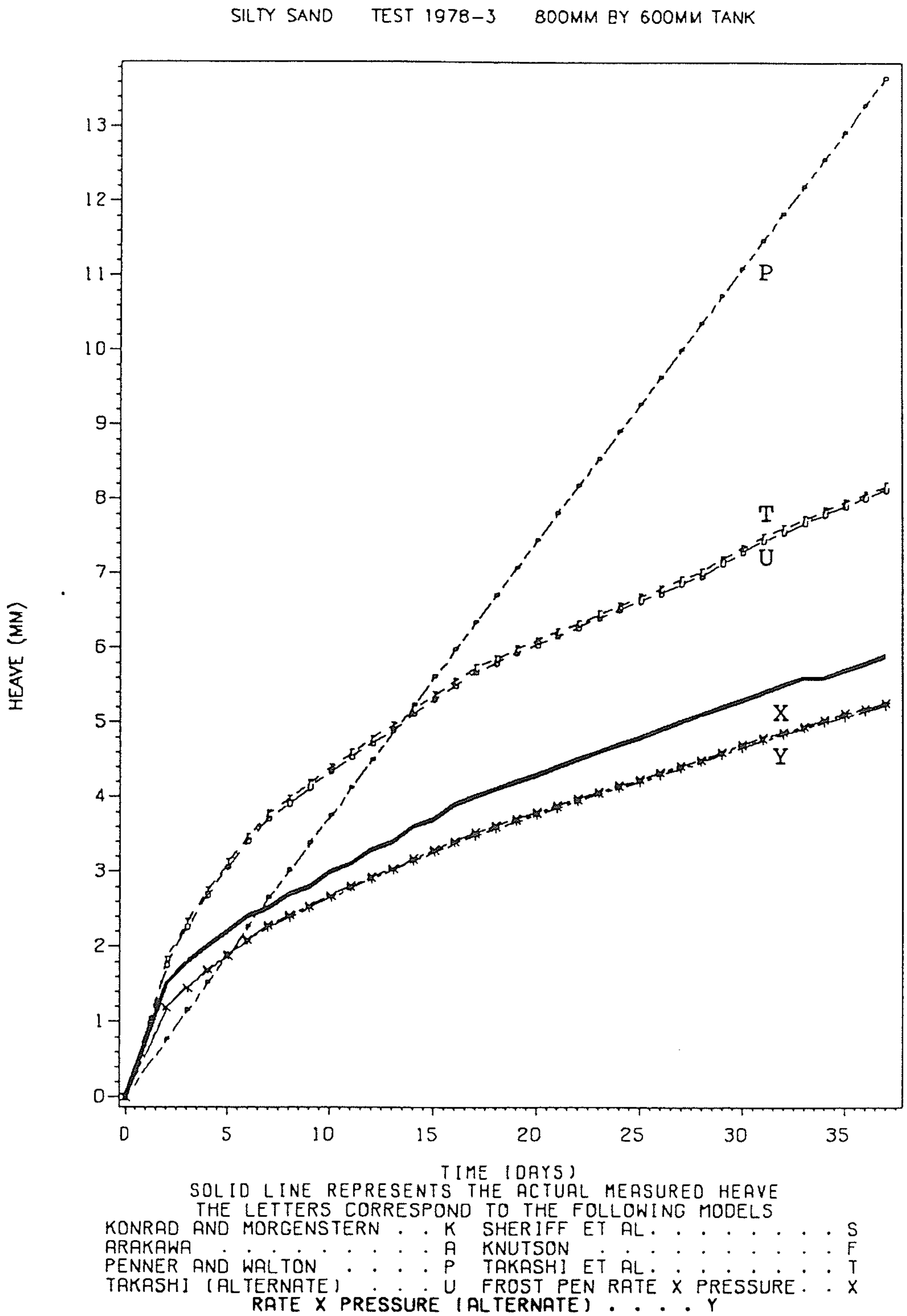

Figure 50: Frost heave predictions for test 1978-3 (using measured frost depth)

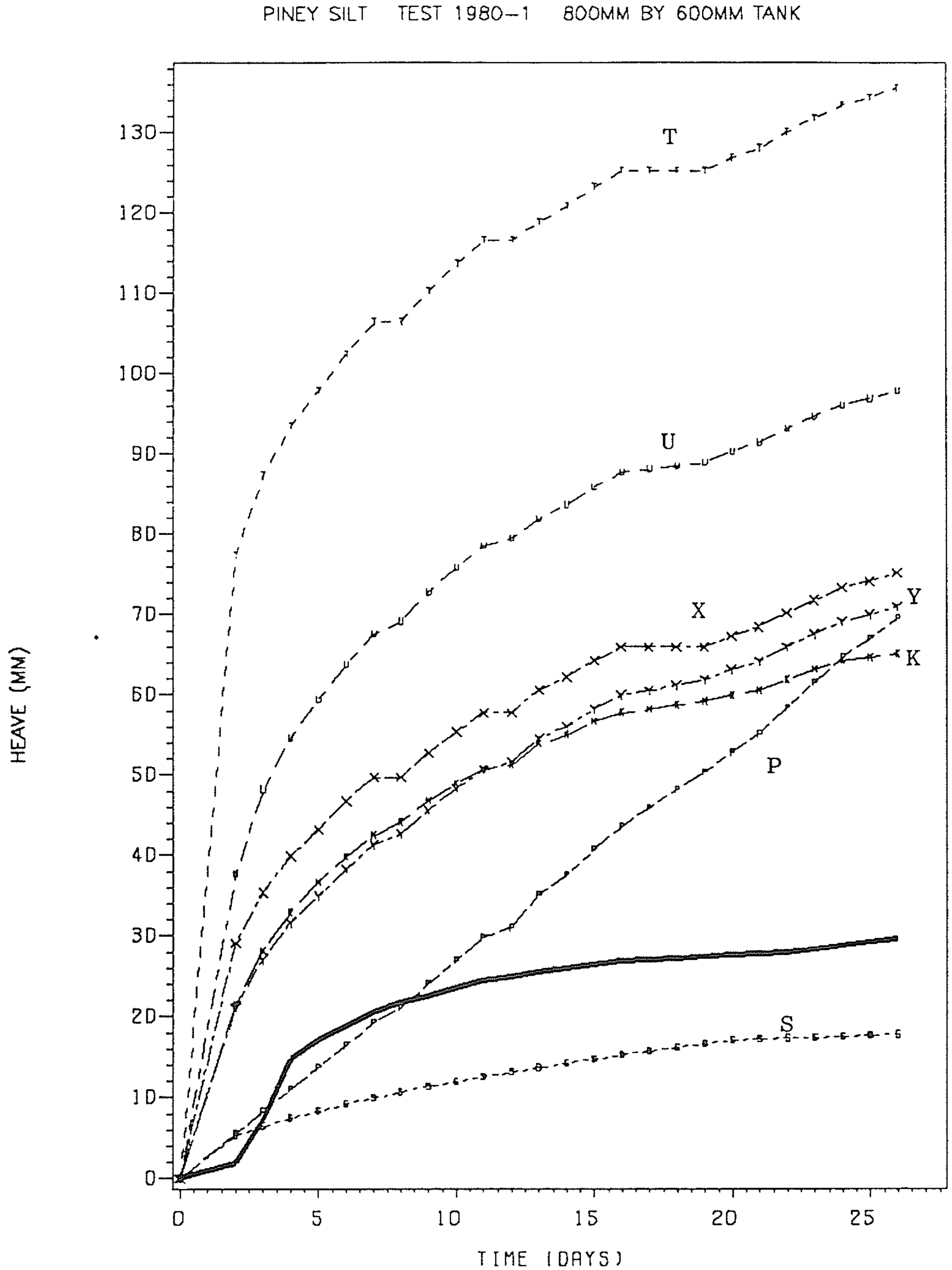

SOLID LINE REPRESENTS THE ACTUAL MEASURED HEAVE
THE LETTERS CORRESPOND TO THE FOLLOWING MODELS

KONRAD AND MORGENSTERN . . K SHERIFF ET AL. . . . . S
ARAKAWA . . . . A KNUTSON . . . . F
PENNER AND WALTON . . . . . P TAKASHI ET AL. . . . . T
TAKASHI (ALTERNATE) . . . . U FROST PEN RATE X PRESSURE. . X
RATE X PRESSURE (ALTERNATE) . . . . Y

Figure 51: Frost heave predictions for test 1980-1 (using measured frost depth)

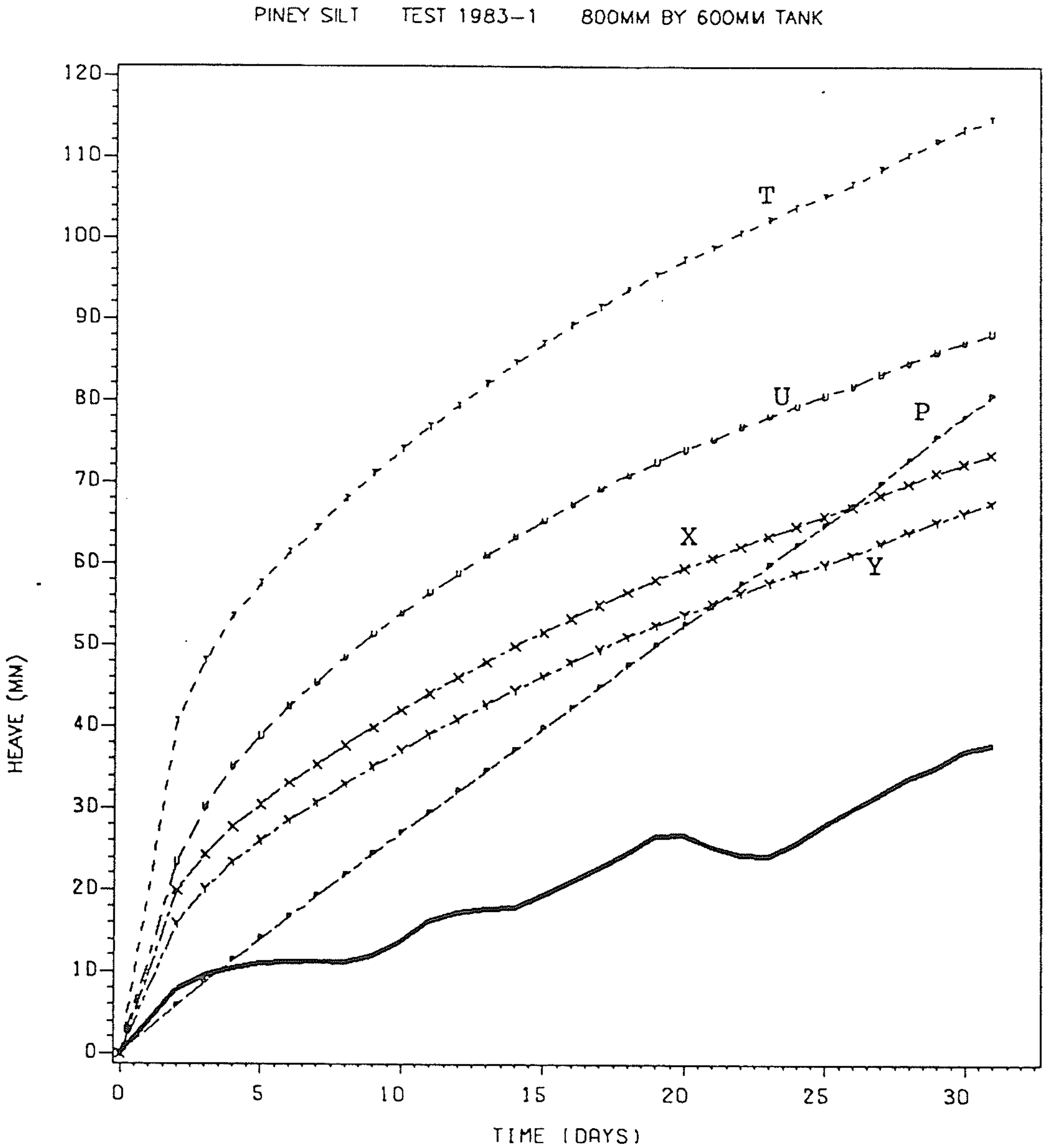

SOLID LINE REPRESENTS THE ACTUAL MEASURED HEAVE
THE LETTERS CORRESPOND TO THE FOLLOWING MODELS

KONRAD AND MORGENSTERN . .	K	SHERIFF ET AL.	S
ARAKAWA	A	KNUTSON	F
PENNER AND WALTON	P	TAKASHI ET AL.	T
TAKASHI (ALTERNATE) . . .	U	FROST PEN RATE X PRESSURE . .	X

RATE X PRESSURE (ALTERNATE) . . . . Y

Figure 52: Frost heave predictions for test 1983-1 (using measured frost depth)

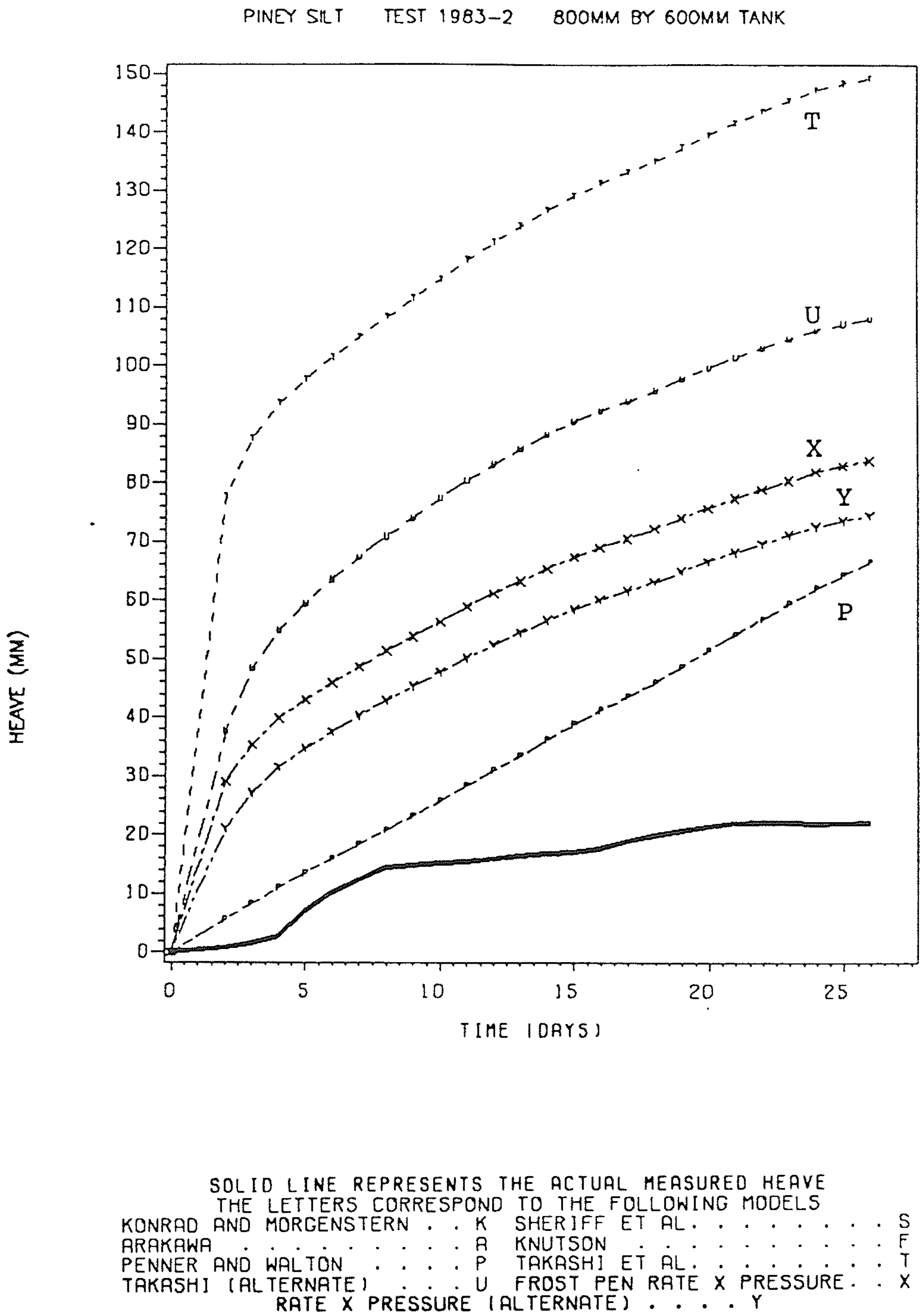

Figure 53: Frost heave predictions for test 1983-2 (using measured frost depth)

TABLE 14 % Error for each test (using measured frost depth)

Theory	Test: 1974-1										
	Agassiz Silt					Silty sand			Piney Silt		
	1974-1	1974-2	1975-1	1975-2	1975-3	1978-1	1978-2	1978-3	1980-1	1983-1	1983-2
1	14.7	76.1	31.6	142.1	991.1	225.8	51.1	11.5	201.6	150.2	520.6
2	26.0	72.9	8.0	134.5	732.7	227.2	48.2	12.3	157.2	122.6	402.0
3	10.2	64.9	20.0	222.3	678.7	38.3	171.3	39.9	545.1	327.6	1279.5
4	41.2	74.3	39.2	112.6	342.0	39.9	158.8	38.1	301.5	212.3	729.0
5	58.7	61.2	40.8	54.4	34.8	356.6	52.3	67.8	61.0	90.9	152.0
6	88.2	88.1	81.3	405.6	331.0	441.9	83.6	-	47.0	-	-
7	290.9	88.4	30.9	280.4	337.4	2516.2	301.6	-	154.3	-	-
8	402.3	12.5	24.9	174.6	303.6	-	-	-	-	-	-
9	18.3	19.9	121.6	505.8	206.5	-	-	-	-	-	-

Theories:

1.Frost Penetration Rate x Pressure 2.Pen. Rate x Pressure (alternate) 3.Takashi et al.

4.Takashi et al. (alternate) 5.Penner and Walton 6.Sheriff et al.

7.Konrad and Morgenstern 8.Arakawa (Efficiency) 9.Knutson (Freezing Index)

TABLE 15

Average % error (measured frost depth approach)

Model	Piney	Agassiz	Sand	Total
1	290.8	251.1	96.1	219.7
2	227.3	194.8	95.9	196.7
3	717.4	199.2	83.2	308.9
4	414.3	121.9	78.9	189.9
5	101.3	50.0	158.9	93.7
6	47.0	198.8	262.8	195.8
7	154.3	205.6	1408.9	500.0
8	-	183.6	-	183.6
9	-	174.4	-	174.4

Legend: 1. Pen. rate x pressure 2. Rate x pressure (alt.)
3. Takashi et al. 4. Takashi (alternate)
5. Penner and Walton 6. Sheriff et al.
7. Konrad and Morgenstern 8. Arakawa
9. Knutson

on silty sand were obtained by the Takashi et al. model (79 % error).

6.4 DISCUSSION OF THE COMPARISON

Although the Penner and Walton model produced the lowest average percent error, the predictions did not closely model the actual frost heave. When the Ice Segregation Ratio ($\Delta H/\Delta X$) is close to zero (it is usually less than 0.1) the Penner and Walton model implies that the frost heave will increase linearly with time. It also suggests that if the external pressure is zero then the rate of frost heave is independent of temperature. As can be seen from Figures 34 to 42 the actual frost heave rate was not constant but decreases with time. The measured frost heave however, is roughly approximated by Penner and Walton's linear relation. This suggests that although the theory will not provide a close fitting prediction it may provide an adequate short term approximation.

The accuracy of each model appears to be influenced by experimental procedure , apparatus and soil type. For instance, the frost heave in the large scale tests on Agassiz silt were very accurately predicted by Konrad and Morgenstern's model using calculated temperature gradients (Figures 34 and 35). For the smaller scale tests however, only the Penner and Walton prediction model was close (Figures 36 to 38). The freezing index model of Knutson and the Arakawa segregation efficiency model both predicted the heave of the large scale test on Agassiz silt with reasonable success but were inaccurate on the smaller scale experiments.

The Piney silt in the 100 mm freezing cell was compacted to optimum dry density whereas the material in the 800 mm freezing tank was loosely compacted. The actual heave in the smaller compacted sample was far higher than any of the seven predictions.

The type of material plays a role in the accuracy of each model. The Konrad and Morgenstern model provided the best predictions for the two large scale tests on Agassiz silt and for one of two tests on Piney silt but incurred no success with the predictions for the silty sands. The Penner and Walton model predictions were also better for the silts than for the sandy soil. The Takashi et al. model achieved only moderately successful results for Piney and Agassiz silt but supplied the best prediction model for the silty sand.

The model by Sheriff et al. produced its best predictions for Piney silt, which should be expected since Piney silt is similar to the type of material on which the model was based (material with a percent finer than 0.02 mm by weight between 6 and 21 %). The best prediction by this model on any soil type using measured surface temperature data was 47 % error. However this model has the advantage that frost heave prediction calculations can be carried out quickly by hand.

The solution from the penetration rate times pressure method generally had a slightly higher percent error than that of Takashi et al. and produced its best predictions for tests on the silty sand.

The frost heave predictions of the Ice Segregation Ratio models were more accurate when the alternate method of determining the frost penetration was used. This alternate method was defined as the depth of frozen soil below the upwardly heaving soil surface rather than below a fixed datum. As the frost depth approaches a constant elevation and the heat flow approaches steady state the predicted Ice Segregation Ratio will not approach infinity if the alternate method is applied. Continued heaving under near steady state conditions can be successfully calculated and the resulting accuracy are increased.

The Computer programs used to determine the frost heave for the approaches using both measured and predicted fost depth have been included in Appendix B.

Chapter VII

SUMMARY

No one prediction model provided a consistently accurate estimation of the frost heave for all the tests studied. However, the value of each model can be assessed from the discussion in chapter five by analyzing three points:

1. The ease of use of the prediction model;
2. The ability to confidently determine the frost heave parameters;
3. The accuracy of the predictions under varied experimental procedures or differing soil types.

Summarizing each model individually:

1. Konrad and Morgenstern (1982b). The segregation potential theory provided the best prediction for two large scale tests on Agassiz silt and for one of two tests on Piney silt. No success was experienced with the tests on the silty sand. The parameters for the two silts were determined with the greatest statistical confidence of any theory. The parameter SP_0 can be approximated using the Rf value and Figure 24. The 'a' parameter should be determined from freezing tests. The model does not apply to tests under rapid

rates of cooling and will not predict the expulsion of water away from the freezing front associated with coarse grained soils. The model does not work well if the temperature gradients are assumed to be linear. The model is recommended for the prediction of frost heave in silts and fine grained soils if the temperature gradient can be predicted.

2. Sheriff, Ishibashi and Ding (1977). This model did not produce good results. However calculations can be done quickly by hand and an acceptable rough value of predicted frost heave may be provided for silty sands.

3. Arakawa (1965). The segregation efficiency theory did not provide a good prediction for each of the tests in which it was used. There are three basic difficulties with the use of this model. Firstly, it is difficult to determine a function that will effectively describe the segregation efficiency. Arakawa's 'E' is not related only to the frost penetration ratio as suggested by Penner. Secondly, a good estimation of the unfrozen temperature gradient is difficult under experimental conditions and would be impractical under field conditions. Finally, it is difficult to accurately estimate the required thermal characteristics of the soil.

4. Knutson (1974). The determination of β as a function of the freezing index is the basic problem in the use

of this model. Although there was considerable error in determining this relationship for Agassiz silt, reasonably accurate predictions were still obtained in the large scale tests. This suggests that the model can be used with the ß values provided in Table 1 to produce a rough estimation of frost heaving under large scale or field conditions.

5. Penner and Walton (1979). This model predicted the frost heaving with the lowest overall percent error. However, it incorrectly predicted that the rate of frost heaving would be roughly constant for every test. Although the theory allows for any range of pressure to temperature ratio the model was only evaluated under a condition of zero external pressure. The initial frost heave rate 'R_0' was not determined with good statistical confidence for all of the three soils, but if this value were known then a good estimation of the short term frost heave should result.

6. Takashi, Yamamoto, Ohrai and Masuda (1978). The Ice Segregation Ratio adaption to Takashi et al.'s theory allows for the expulsion of water away from the frost front if the frost penetration rate and overburden pressure are sufficient. As a result it provides the best solution to the frost heaving in a sandy soil. This model is recommended for the prediction of frost heaving in a more coarse grained soil should such a

prediction be of engineering interest. A comparison fo the Takashi et al. model was made with one that related frost heave to the product of overburden pressure and frost penetration rate. The determination of the frost heave parameters for the Takashi et al. model were derived with greater statistical confidence than for the comparison model but with less confidence than for Konrad and Morgenstern's segregation potential theory. Also, the percent error of the prediction was generally less for the model presented by Takashi et al. than for the comparison model.

BIBLIOGRAPHY

Aldrich H.P. and Paynter H.M. 1953 Analytical Studies of Freezing and Thawing in Soils Arctic Constr. Frost Effects Laboratory Tech. Report 42., U.S. Army Corps. of Engineers

Arakawa K. 1966 Theoretical Studies of Ice Segregation in Soil Jour. of Glaciology, Vol. 6, No. 44, pp. 255-260

Beskow G. 1935 Soil Freezing and Frost Heaving with Special Application to Roads and Railroads The Swedish Geological Society, Series C, No. 375, 26th year, Book no. 3, Translated by J.O. Oserberg, published by Technical Institute, Northwestern University, 1974

Carlson L.E.,Ellwood J.R., Nixon J.F. and Slusarchuk W.A. 1982 Field Test Results of Operating a Chilled Buried Pipeline in Frozen Ground Proc. 4th Canadian Permafrost Conf., Calgary, pp. 475-480

Casagrande A. 1931 Discussion on Frost Heaving Hwy. Res. Brd. Proc., Vol. 11, Part 1, pp. 168-172

Chalmers B. and Jackson K.A. 1970 Experimental and Theoretical Studies of the Mechanism of Frost Heaving CRREL Research Rpt. 199, Hanover, NH

Chamberlain E.J. 1981 Frost Susceptibility of Soil - Review of Index Tests CRREL Monograph 81-2, Hanover, NH

Charleson D. 1981 Evaluation of Frost Susceptibility Criteria Master of Eng. thesis, Civil Eng. Dept., University of Manitoba

Domaschuk L. 1982 Frost Heave Forces on Embedded Structural Units Proc. 4th Canadian Permafrost Conf., Calgary, pp. 487-496

Domaschuk L. 1984 Frost Heave Resistance of Pipe Piles with Expanded Bases Proc. 3rd Int. Offshore Mechanics and Artic Eng. Symp., New Orleans, Vol. 3, pp. 58-63

Everett D.H. 1961 The Thermodynamics of Frost Action in Porous Solids Trans. Faraday Soc., Vol. 57, pp. 1541-1551

Freden S. 1965 Mechanism of Frost Heave and its Relation to Heat Flow Proc. 6th Int. Conf. SMFE, Vol. 1, pp. 41-45

Goodrich L.E. 1978 Efficient Numerical Technique for One-Dimensional Thermal Problems with Phase Change Int. Jour. of Heat and Mass Transfer, Vol 21., pp. 615-621

Guymon G.L., Berg R.L., Johnson T.C. and Hromodka T.V. 1981 Frost Action and Risk Assessment in Soil Mechanics Trans. Res. Brd., Trans. Res. Rec. 809, pp. 1-6

Holden J.T., Jones R.H. and Dudek S.J.M. 1981 Heat and Mass Flow Associated with a Freezing Front Eng. Geol., Vol. 18, pp. 153-164

Horiguchi K. 1978 The Effect of the Rate of Heat Removal on the Rate of Frost Heaving Eng. Geol., Vol. 13, pp. 63-71

Kaplar C.W. 1970 Phenomenon and Mechanism of Frost Heaving Hwy. Res. Brd., Hwy. Res. Rec. 304, pp. 1-13

Knutson F. 1973 Theory and Experience Regarding Frost Penetration and Frost Heaving Proc. OECD Symp.on Frost Action on Roads, Vol. 1, Paris, pp. 223-233

Knutsson S., Domaschuk L. and Chandler N. 1985 Analysis of Large Scale Laboratory and Insitu Frost Heave Tests (in publication) Proc. 4th Int. Symp. on Ground Freezing, Sapporo, Aug. 1985

Konrad J.M. and Morgenstern N.R. 1980 A Mechanistic theory of Ice Lens Formation in Fine Grained Soils Can. Geot. Jour., Vol. 17, pp. 473-486

Konrad J.M. and Morgenstern N.R. 1981 The Segregation Potential of a Freezing Soil Can. Geot. Jour., Vol. 18, pp. 482-491

Konrad J.M. and Morgenstern N.R. 1982a Prediction of Frost Heave in the Laboratory During Transient Freezing Can. Geot. Jour., Vol. 19, pp. 250-259

Konrad J.M. and Morgenstern N.R. 1982b Effects of Applied Pressure on Freezing Soils Can. Geot. Jour., Vol. 19, pp. 494-505

Loch J.P.G. 1977 Frost Heave Mechanism and the Role of the Thermal Regime in Heave Experiments on Norwegian Silty Soils Norwegian Road Research Laboratory, Meddelelse, nr. 50

Loch J.P.G. 1979 Influence of the Heat Extraction Rate on the Ice Segregation of Soils Frost 1 Jord, nr. 20, pp. 19-30

McRoberts E.C. and Morgenstern N.R. 1975 Pore Water Expulsion During Freezing Can. Geot. Jour., Vol. 12, pp. 130-141

Miller R.D. 1972 Freezing and Heaving of Saturated and Unsaturated Soils Hwy. Res. Brd., Hwy. Res. Rec. 393, pp. 1-11

Miller R.D. 1977 Lens Initiation in Secondary Heaving Proc. Int. Symp. on Frost Action in Soils, Luleå, Sweden, pp. 68-74

Nixon J.F. 1982 Field Frost Heave Predictions Using the Segregation Potential Concept Can. Geot. Jour., Vol. 19, pp. 526-529

Penner E. 1957 Soil Moisture Tension and Ice Segregation Hwy. Res. Brd., Bulletin No. 168, pp. 50-64

Penner E. 1972 Influence of Freezing Rate on Frost Heaving Hwy. Res. Brd., Hwy. Res. Rec. 393, pp. 56-64

Penner E. 1973 Frost Heaving Pressures in Particulate Materials Proc. OECD Symp. on Frost Action on Roads, Vol. 1, Paris, pp. 379-385

Penner E. and Ueda T. 1978 A Soil Frost Susceptibility Test and a Basis for Interpreting Heaving Rates Proc. 3rd Int. Conf. on Permafrost, Edmonton, Vol. 1, pp. 722-727

Penner E. and Walton T. 1979 Effects of Temperature and Pressure on Frost Heave Eng. Geol., Vol. 13, pp. 29-39

Reed M.A., Lovell C.W., Altschaeffl A.G. and Wood L.E. 1979 Frost Heaving Rate Predicted from Pore Size Distribution Can. Geot. Jour., Vol. 17, pp. 463-472

Rieke R.D., Vinson T.S. and Mageau D.W. 1983 The Role of Specific Surface Area and the Related Index Properties in the Frost Heave Susceptibility of Soils Proc. 4th Int. Conf. on Permafrost, Fairbanks, pp. 1066-1071

Saetersdaal R. 1980 Heaving Conditions by Freezing of Soils Eng. Geol., Vol. 18, pp. 291-305

Sheriff M., Ishibashi I. and Ding W-W. 1976 Heave of Silty Sands Proc. ASCE, Vol. 103, GT 3, pp. 185-195

Shushkewich K.W. 1980 A Geothermal Finite Element Program for Soil-Water-Ice Systems A report to the Civil Eng. Dept., University of Manitoba

Taber S. 1929 Frost Heaving Jour. of Geology, Vol. 37, pp. 428-461

Takagi S. 1977 Segregation Freezing as the Cause of Suction Force Proc. Int. Symp. on Frost Action in Soils, Luleå, Sweden, pp. 59-66

Takashi T., Yamamoto H., Ohrai T. and Masuda M. 1978 Effect of Penetration Rate of Freezing and Confining Stress on the Frost Heave Ratio of Soil Proc. 3rd Int. Conf. on Permafrost, Edmonton, Vol. 1, pp. 737-742

Wilson E., Bathe K. and Peterson F. 1974 Finite Element Analysis of Linear and Non Linear Heat Transfer Nuclear Engineering and Design, Vol. 29

Appendix A

SOILS INFORMATION

The grain size distributions for each of the three soil types are shown below:

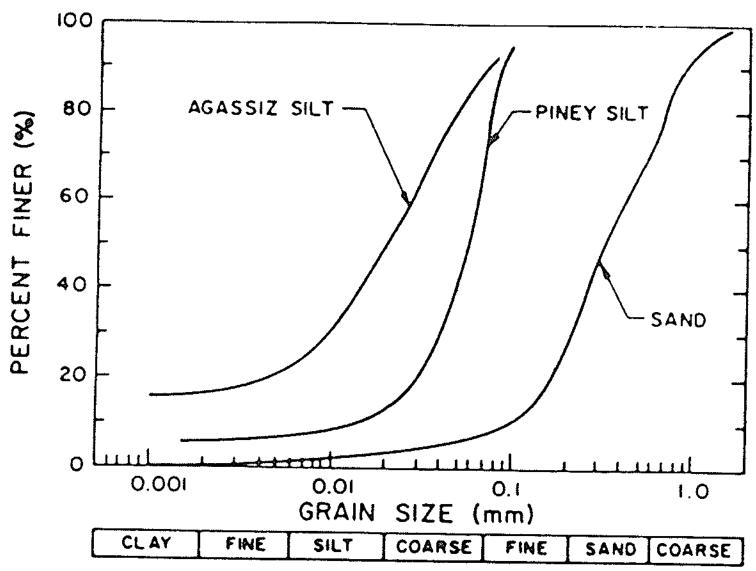

Soil Type	% Clay	% Silt	% Sand	Liquid Limit	Plastic Limit
Agassiz Silt	17	73	10	28	22
Piney Silt	6	64	30	18.5	-
Silty Sand	1	7	92	-	-

The dry densities and the soil moisture contents for each test are shown in the following table:

Test	1974-1	1974-2	1975-1	1975-2	1975-3	1978-1	1978-2	1980-1	1981-1
Moisture Content (%)	16.5	17.2	20*	22*	22*	19.6	19.6	24*	13
Dry Density (kN/m^3)	18.4*	18.2*	17.2	16.8	16.8	17.4*	17.4*	16.2	18.45

The values are taken as the average over the entire depth.

* indicates calculated values based on 100 % saturation and a specific gravity of 2.72.

More complete information of the soil properties and testing procedure for each test can be found in the following undergraduate and graduate reports:

i) Preliminary Tests

a) Agassiz silt

- Phelane D. "Frost Heave Model Study" 1979
- Piamsalee N., Lemke E. (data only) 1978

b) Piney silt

- Wachowich J.N. "Frost Heave of Short Piles" 1979
- Erickson D.J. "Frost Heave on Short Piles" 1980

c) Silty sand

- Hubbard B., Agar S. "Model Studies of Frost Heave Forces on Inclined Members" 1978

ii) Prediction Tests

a) Agassiz silt

- 1974-1, 1974-2 Larkin W.L.S. "Frost Heave Effects on a Tangent Tower Mast Footing" 1974
- 1975-1, 1975-2, 1975-3 Lau P-K "Frost Heave of Foundations and Pile Extraction Tests" 1975

b) Piney silt

- 1980-1 Erickson D.J. "Frost Heave on Short Piles" 1980
- 1981-1 Charleson D. "Evaluation of Frost Susceptibility Criteria" 1981

- 1983-1, 1983-2 Fong W. and Lai S.Y. "Frost Heave Resistance of Different Pile Bases" 1983

c) Silty sand

- 1978-1, 1978-2 Gerlach G.F. "Frost Heave of Short Piles" 1978
- 1978-3 reported by Wachowich J.N. "Frost Heave of Short Piles" 1979

SOIL INPUT INFORMATION FOR FROST DEPTH DETERMINATION

Test 1974-1

Hrs	Water Temp Meas	Water Temp Prgm	Surface Temp Meas	Surface Temp Prgm
100	*	15.0	-23	-5
200	*	15.0	-32	-15
400	*	15.0	-33	-24
600	*	15.0	-28	-32

% Water Content Meas-16.5
Prgm-16.5
Initial Soil Temperature:
Meas-(11-13) Prgm-15.0

Test 1974-2

Hrs	Water Temp Meas	Water Temp Prgm	Surface Temp Meas	Surface Temp Prgm
100	*	15.5	-20	-15
200	*	15.5	-20	-19
400	*	15.5	-22	-20
600	*	15.5	-6	-7
800	*	15.5	-27	-27

% Water Content Meas-17.2
Prgm-21.5
Initial Soil Temperature:
Meas-(11-17) Prgm-15.5

Test 1975-1

Hrs	Water Temp Meas	Water Temp Prgm	Surface Temp Meas	Surface Temp Prgm
0	14	3.5	14	1
100	2	3.0	-2	-2
200	2	2.3	-3	-4
400	0.5	1.0	-4	-7

% Water Content Meas-20
Prgm-26
Initial Soil Temperature:
Meas- * Prgm-15.0

Test 1975-2

Hrs	Water Temp Meas	Water Temp Prgm	Surface Temp Meas	Surface Temp Prgm
0	18	7.0	20	2
100	2	3.0	-2	-3
300	4	1.0	-4	-5.5
500	4	1.0	-5	-5.5

% Water Content Meas-22
Prgm-21.5
Initial Soil Temperature:
Meas- * Prgm-18.0

Test 1975-3

Hrs	Water Temp Meas	Water Temp Prgm	Surface Temp Meas	Surface Temp Prgm
0	21	23.0	23	20
100	5	5.0	-2	-1
300	3	2.3	-3	-4
500	1	0.6	-4	-5

% Water Content Meas-22
Prgm-26
Initial Soil Temperature:
Meas- * Prgm-20

Test 1978-1

Hrs	Water Temp Meas	Water Temp Prgm	Surface Temp Meas	Surface Temp Prgm
0	*	18	-13	-1
50	*	14	-13	-13
100	*	12	-13	-13
150	*	7.5	-13	-13

% Water Content:
Meas-(18-21) Prgm-19
Initial Soil Temperature:
Meas- * Prgm-18

Test 1978-2

Hrs	Water Temp Meas	Water Temp Prgm	Surface Temp Meas	Surface Temp Prgm
0	*	20.0	-2	-2
100	*	16.2	*	-5
300	*	8.7	*	-7
450	*	3.0	-14	-14

% Water Content:
Meas-(18-21) Prgm-19
Initial Soil Temperature:
Meas- * Prgm-10.0

Test 1980-1

Hrs	Water Temp Meas	Water Temp Prgm	Surface Temp Meas	Surface Temp Prgm
0	*	16	-5	10
200	*	14	-5	-5
500	*	3	-5	-5
700	*	1	-7	-7

% Water Content Meas-24
Prgm-22
Initial Soil Temperature:
Meas- * Prgm-16.0

<u>Notes</u>:
* indicates unavailable information
"Meas" indicates measured values
"Prgm" indicates values input into the computer program
Temperature information is in °C
Water Content is indicated in % by weight

Appendix B

COMPUTER PROGRAMS FOR CALCULATING FROST HEAVE AND FROST PENETRATION

FORTRAN PROGRAM FOR FROST PENETRATION AND METHOD 1 PREDICITONS

```
C
C     ***************************************************
C     *                                                 *
C     * THIS PROGRAM CALCULATES ONE DIMENSIONAL FROST   *
C     * PENETRATION BASED ON HEAT FLOW EQUILIBRIUM, AS  *
C     * EXPLAINED BY GOODRICH (1978),  AND IS MODIFIED  *
C     * TO INCLUDE NINE FROST HEAVE MODELS ;            *
C     *          1. PRESSURE X PENTRATION RATE          *
C     *          2. PRESSURE X PENETRATION RATE (ALT.)  *
C     *          3. TAKASHI ICE SEGREGATION RATIO       *
C     *          4. TAKASHI ET. AL. 1978 (ALTERNATE ISR) *
C     *          5. PENNER AND WALTON 1978 (ISR)        *
C     *          6. SHERRIF ET AL. 1976                 *
C     *          7. KONRAD AND MORGENSTERN 1982         *
C     *          8. ARAKAWA SEGREGATION EFFICIENCY      *
C     *          9. KNUTSON FREEZING INDEX              *
C     *         10. FROST PENETRATION ONLY              *
C     *                                                 *
C     ***************************************************
C
      REAL T(100),NT(100),KF(100),KU(100),K(100),CF(100),
     1CU(100),C(100),L(100),X(100),DX(100),HC(100),CN(100),
     2RHS(100),E(100),S(100),CUU(100),CFF(100),KUU(100),KFF(100)
     3,DFP(100),TT(100),HEAVE(100),AFH(100,9),BFH(100,9),DEPTH(100)
     4,WDENS(99),WFR(99),GD(99),W(99),UPT(25),LOT(25),TIM(25),AD(25)
     5,AH(25),AT(25),GA(3),FN(3),TF(100)
      INTEGER HEAD(18),MAT(100),START,H
      REAL DT,D,GAV,HAV,G,NG,LT,DTA,DTB,DTO,POB,GRT,LHEV,ISR,
     1SPO,HEAVES,HEAVEI,HEAVSL,HEVSL,GAMI,LATW,SUR,CC,CA,U,OT,
     2GAMW,TFAC,DTC,DELHEV,RATE,RATEH,FF,TAV,FI,EFF,HEAT,JAY,ACTUAL,
     3PERC,PERSUM,WPER,PTIME,PTOT,SHB
      INTEGER N,P,NM,B,NA,PA,PB,PC,NTI,THY,Q,TQ,NAP,NAPA,THEORY,R,SHA
      READ180,HEAD
  180 FORMAT(18A4)
      PRINT190,HEAD
  190 FORMAT('1',18A4)
      READ (5,200) NM,N,TQ,THEORY,NAPA,DTO,LT,TFAC,LATW,GAMW,SUR
      READ (5,210) (DEPTH(I),TF(I),MAT(I),I=1,N)
      READ (5,220) (CFF(J),CUU(J),KFF(J),KUU(J),GD(J),W(J),J=1,NM)
      TQ=TQ+1
      READ (5,280) (UPT(I),LOT(I),TIM(I),I=2,TQ)
      NAP=NAPA+1
      THY=0
      AT(1)=0.0
      AD(1)=0.0
      AH(1)=0.0
      READ (5,290) (AT(I),AD(I),AH(I),I=2,NAP)
      IF (THEORY.NE.10) WRITE (4,271) (AT(I),AH(I),THY,I=1,NAP)
      WRITE (6,230) (I,DEPTH(I),TF(I),MAT(I),I=1,N)
```

```
      GAMI=GAMW/1.09
      DO 2 I=1,NM
      L(I)=GD(I)*W(I)/100*LATW
      WFR(I)=GD(I)*W(I)/(100*GAMW)
    2 WDENS(I)=(1.0+W(I)/100)*GD(I)
      WRITE(6,235) (I,W(I),GD(I),WDENS(I),WFR(I),I=1,NM)
      WRITE (6,240) (J,CFF(J),CUU(J),KFF(J),KUU(J),L(J),J=1,NM)
      NA=N-1
      DO 5 I=1,NA
      J=MAT(I)
      CU(I)=CUU(J)
      CF(I)=CFF(J)
      KU(I)=KUU(J)
      KF(I)=KFF(J)
      WDENS(I)=WDENS(J)
      W(I)=W(J)
      L(I)=L(J)
    5 WFR(I)=WFR(J)
      DO 199 THY=1,THEORY
      IF (THEORY.EQ.10) WRITE(6,260) (DEPTH(I),I=1,N)
      DO 7 J=1,N
      X(J)=DEPTH(J)
    7 T(J)=TF(J)
      READ(5,301) (AFH(I,THY),BFH(I,THY),I=1,NM)
      DO 8 I=1,NA
      J=MAT(I)
      AFH(I,THY)=AFH(J,THY)
    8 BFH(I,THY)=BFH(J,THY)
      TAV=0.0
      FI=0.0
      B=0
      CA=0.0
      TT(1)=0.0
      RATE=0.0
      NTI=1
      HEAVE(1)=0.0
      DFP(1)=0.0
      HEVSL=0.0
      HEAVSL=0.0
      G=0.0
      H=1
      PERSUM=0.0
      PTIME=0.0
      S(1)=0.0
      S(N)=0.0
      START=0
      DT=DTO
      Q=1
      SHA=1
      TIM(1)=0.0
      UPT(1)=T(1)
      LOT(1)=T(N)
    9 DO 10 I=1,NA
      IF(T(I).GT.0.0) GOTO 20
```

```
      C(I)=CF(I)
   10 K(I)=KF(I)
      P=N
      GO TO 35
   20 P=I-1
      PC=P+1
      DO 30 I=PC,NA
      C(I)=CU(I)
   30 K(I)=KU(I)
   35 START=NTI
      IF (P.EQ.0) GOTO 38
      DT=DTO
   38 TAV=(-1*T(1)*DT+TAV*(TT(NTI)-TT(START)))/(TT(NTI)+DT-TT(START))
      IF (T(1).GT.0.0) TAV=0.0
      FI=FI-T(1)*DT
      IF (T(1).GT.0.0) FI=0.0
      E(1)=T(1)
      E(N)=T(N)
      NT(1)=T(1)
      NT(N)=T(N)
      U=1.0
      A=0
      DELHEV=0.0
      HEAVES=0.0
C
C     FROST DEPTH DETERMINATION
C
      DO 40 I=1,NA
      DX(I)=X(I+1)-X(I)
   40 CN(I)=K(I)/DX(I)
   41 DO 50 I=2,NA
      HC(I)=(C(I-1)*DX(I-1)+C(I)*DX(I))/DT
   50 RHS(I)=CN(I-1)*T(I-1)+(HC(I)-CN(I-1)-CN(I))*T(I)+CN(I)
     1*T(I+1)
   55 PA=P-1
      PB=P+2
      PC=P+1
      IF (PA.LT.2) GOTO 65
      DO 60 I=2,PA
      D=HC(I)+CN(I-1)+CN(I)-CN(I-1)*S(I-1)
      E(I)=(RHS(I)+CN(I-1)*E(I-1))/D
   60 S(I)=CN(I)/D
   65 I=N
   70 I=I-1
      IF (I.EQ.1) GOTO 90
      IF (I.LE.P+1) GOTO 80
      D=HC(I)+CN(I-1)+CN(I)-CN(I)*S(I+1)
      E(I)=(RHS(I)+CN(I)*E(I+1))/D
      S(I)=CN(I-1)/D
      GO TO 70
   80 IF (B.EQ.1) GOTO 82
      CA=0.0
      GA(1)=0.05*DX(P)
      GA(2)=0.95*DX(P)
```

```
      DO 98 J=1,30
      DO 97 I=1,3
      GAV=GA(I)
      HAV=DX(P)-GAV
   82 IF (P.LE.1) GOTO 85
      E(P)=(CN(P-1)*(T(P-1)+E(P-1))+(C(P-1)*DX(P-1)/DT+CF(P)
     1*GAV/DT-CN(P-1)-KF(P)/GAV)*T(P))/(C(P-1)*DX(P-1)/DT+CF(P)
     2*GAV/DT+KF(P)/GAV+CN(P-1)*(1-S(P-1)))
   85 IF (P.GE.NA) GOTO 88
      E(P+1)=(CN(P+1)*(T(P+2)+E(P+2))+(C(P+1)*DX(P+1)/DT+CU(P)
     1*HAV/DT-CN(P+1)-KU(P)/HAV)*T(P+1))/(C(P+1)*DX(P+1)/DT
     2+CU(P)*HAV/DT+KU(P)/HAV+CN(P+1)*(1-S(P+2)))
      NG=2*GAV-G
      RATE=(NG-G)/DT
      IF (B.EQ.1) GOTO 100
C
C     FALSE POSITION ITERATION
C
   88 FN(I)=KF(P)*(E(P)+T(P))/GAV+KU(P)*(E(P+1)+T(P+1))/HAV
     1+4*(GAV-G)/DT*L(P)
      IF (I.EQ.1) GOTO 95
      IF (I.EQ.3) GOTO 92
      IF (FN(2).LT.0.0) GOTO 96
      GA(3)=(GA(1)*FN(2)-GA(2)*FN(1))/(FN(2)-FN(1))
      GOTO 97
   92 FF=FN(2)*FN(3)
      A=1
      IF (FF.LT.0.0) GOTO 93
      GA(2)=GA(3)
      GOTO 94
   93 GA(1)=GA(3)
   94 CC=ABS(CA-RATE)
      IF (CC.LT.0.000001) GOTO 99
      CA=RATE
      GOTO 98
   95 IF (FN(1).LT.0.0) GOTO 97
      IF (A.EQ.1) GOTO 11
      GA(1)=GA(1)*.75
      GOTO 98
   11 GA(1)=GA(1)-0.0001
      GOTO 98
   96 IF (A.EQ.1) GOTO 102
      IF (P.EQ.NA) GA(2)=DX(P)-(DX(P)-GA(2))/2
      IF (P.LT.NA) GA(2)=0.1*DX(P)+GA(2)
      GOTO 98
  102 GA(2)=GA(2)+0.0001
      GOTO 98
   97 CONTINUE
   99 IF (ABS(FN(3)).LT.1.0) GOTO 101
   98 CONTINUE
  101 CONTINUE
      IF (NG.LE.DX(P))GOTO 100
      B=1
      DTA=(DX(P)-G)/(NG-G)*DT
```

```
      DTB=DT-DTA
      DTC=DT
      DT=DTA
      GAV=(DX(P)+G)/2
      HAV=DX(P)-GAV
      GO TO 41
C
C     FROST HEAVE PREDICTIONS
C
  100 IF (THEORY.EQ.10) GOTO 90
      IF (F.EQ.1.0) U=T(1)/(T(1)-OT)
      RATE=(NG-G)/(DT*U)*24000
      POB=(X(P)+GAV)*WDENS(P)+HEVSL*(GAMI-WDENS(P))+SUR
      HEAVEI=WFR(P)*(NG-G)*0.09
      GRT=-1*(T(P)+E(P))/(2*GAV)
      GRTU=(T(P+1)+E(P+1))/(2*HAV)
      GOTO (12,13,12,13,14,15,16,17,18),THY
   12 IF (RATE.LE.0.0) GOTO 90
      ISR=0.0
      IF (POB.LE.0.0) GOTO 83
      IF (THY.EQ.1) ISR=AFH(P,1)*((RATE*POB)**(-1*BFH(P,1)))
      IF (RATE.GE.BFH(P,3)) GOTO 83
      IF (THY.EQ.3) ISR=AFH(P,3)/POB*(SQRT(BFH(P,3)/(RATE))-1)
   83 DELHEV=ISR*(NG-G)
      HEAVES=DELHEV-HEAVEI
      GOTO 90
   13 DO 84 R=1,15
      RATEH=(NG-G+DELHEV)/(DT*U)*24000
      IF (RATEH.LE.0.0) GOTO 84
      ISR=0.0
      IF (POB.LE.0.0) GOTO 84
      IF (THY.EQ.2) ISR=AFH(P,2)*((RATEH*POB)**(-1*BFH(P,2)))
      IF (RATEH.GE.BFH(P,4)) GOTO 84
      IF (THY.EQ.4) ISR=AFH(P,4)/POB*(SQRT(BFH(P,4)/RATEH)-1)
   84 DELHEV=ISR*(GAV-G)*2
      HEAVES=DELHEV-HEAVEI
      GOTO 90
   14 ISR=1-EXP(-1*AFH(P,5)*(TT(NTI)+DT*U-TT(START))/(X(P)+NG-HEAVE(NTI)
     1)/24000)
      DELHEV=ISR*(X(P)+NG-HEAVE(NTI))-HEAVE(NTI)
      HEAVES=DELHEV-HEAVEI
      GOTO 90
   15 IF (TAV.GE.5.0) JAY=0.8
      IF (TAV.LT.5.0) JAY=0.4+TAV*0.08
      DELHEV=AFH(P,6)**0.61*((((TT(NTI)+DT*U-TT(START))/24)**(0.83-0.063
     1*TAV))*JAY/1000-HEAVE(NTI)
      HEAVES=DELHEV-HEAVEI
      GOTO 90
   16 IF (RATE.LE.0.0) GOTO 90
      SPO=AFH(P,7)
      IF (POB.LE.0.0) GOTO 86
      SPO=GRT*AFH(P,7)*EXP(-1.0*BFH(P,7)*POB)*0.000001
   86 HEAVES=SPO*1.09*DT*U/24
      DELHEV=HEAVES+HEAVI
```

```
      GOTO 90
   17 IF (RATE.LT.0.0) GOTO 90
      IF (POB.LE.0.0) POB=0.0
      HEAT=KF(P)*GRT-KU(P)*GRTU
      EFF=AFH(P,8)-BFH(P,8)*SQRT(RATE*POB)
      HEAVES=EFF*HEAT/L(P)*DT*U
      IF (HEAVES.LT.0.0) HEAVES=0.0
      DELHEV=HEAVES+HEAVEI
      GOTO 90
   18 ISR=W(P)/100.0*AFH(P,9)*(1/FI)**BFH(P,9)
      DELHEV=ISR*(X(P)+NG-HEAVE(NTI))-HEAVE(NTI)
      HEAVES=DELHEV-HEAVEI
   90 CONTINUE
C
C     NODAL TEMPERATURE CALCULATION
C
      NT(P+1)=E(P+1)
      IF (PB.GE.N) GOTO 115
      DO 110 I=PB,NA
  110 NT(I)=S(I)*NT(I-1)+E(I)
  115 IF (P.EQ.0) GOTO 158
      F=0
      I=P
      NT(P)=E(P)
  120 I=I-1
      IF(I.LE.1) GOTO 130
      NT(I)=S(I)*NT(I+1)+E(I)
      GOTO 120
  130 IF (B.NE.1) GOTO 140
      C(P)=CF(P)
      K(P)=KF(P)
      NG=NG-DX(P)
      P=P+1
  140 DO 150 I=1,N
  150 T(I)=NT(I)
      NTI=NTI+1
      DFP(NTI)=X(P)+NG+DELHEV
      TT(NTI)=TT(NTI-1)+DT
      HEVSL=HEAVES+HEVSL
      HEAVE(NTI)=HEAVE(NTI-1)+DELHEV
      IF (B.NE.3) GOTO 155
      NTI=NTI-1
      DFP(NTI)=DFP(NTI+1)
      HEAVE(NTI)=HEAVE(NTI+1)
      TT(NTI)=TT(NTI+1)
  155 IF (B.EQ.1) DT=DTB
      IF (B.EQ.3) DT=DTC
      IF (B.EQ.3) B=0
      IF (B.EQ.1) B=3
      G=NG+DELHEV
      DO 157 I=PC,N
  157 X(I)=X(I)+DELHEV
      IF (B.EQ.1) G=G-DELHEV
      IF (B.EQ.1) X(P)=X(P)+DELHEV
```

```
      GOTO 159
  158 NTI=NTI+1
      DFP(NTI)=0.0
      HEAVE(NTI)=0.0
      DO 156 I=1,N
  156 T(I)=NT(I)
      TT(NTI)=TT(NTI-1)+DT
      CC=0.0
      F=1
      OT=T(1)
  159 IF (THEORY.EQ.10) WRITE(6,265) TT(NTI),(T(I),I=1,N)
      IF (AT(H+1).EQ.0.0) GO TO 166
      IF (TT(NTI).GT.AT(H+1)) H=H+1
  166 ACTUAL=AH(H)+(AH(H+1)-AH(H))/(AT(H+1)-AT(H))*(TT(NTI)-AT(H))
      IF (ACTUAL.LE.0.0) GOTO 163
      IF (SHA.EQ.1) SHB=NTI-1
      SHA=2
      PERC=ABS(HEAVE(NTI)-ACTUAL)/ACTUAL*100
      PERSUM=PERC*DT+PERSUM
      WPERC=PERSUM/(TT(NTI)-TT(SHB))
      IF(PERC.LE.20.0) PTIME=PTIME+DT
      PTOT=PTIME/(TT(NTI)-TT(SHB))*100.0
  163 IF (TT(NTI).GT.LT) GOTO 160
      IF (B.EQ.0) DT=DT*TFAC
  161 IF (TT(NTI).LT.TIM(Q+1)) GOTO 162
      Q=Q+1
      GOTO 161
  162 T(1)=UPT(Q)+(UPT(Q+1)-UPT(Q))/(TIM(Q+1)-TIM(Q))*(TT(NTI)-TIM(Q))
      T(N)=LOT(Q)+(LOT(Q+1)-LOT(Q))/(TIM(Q+1)-TIM(Q))*(TT(NTI)-TIM(Q))
      IF (P.EQ.0) GOTO 9
      GOTO 38
  160 WRITE(6,270) THY,(TT(I),DFP(I),HEAVE(I),I=2,NTI)
      IF (THEORY.EQ.10) WRITE(4,272) (TT(I),DFP(I),HEAVE(I),I=2,NTI)
      IF (THEORY.NE.10) WRITE(4,271) (TT(I),HEAVE(I),THY,I=2,NTI)
  175 WRITE(6,302) PTOT,WPERC
  199 IF (THEORY.EQ.10) GOTO 198
  271 FORMAT(10X,F8.1,F12.4,I3)
  272 FORMAT(10X,F8.1,2F12.4)
  198 WRITE(6,300) (AT(I),AD(I),AH(I),I=2,NAP)
  200 FORMAT(5I5/2F10.3,F5.1,3F10.3)
  210 FORMAT(2F10.3,I5)
  220 FORMAT(4F10.3/2F10.2)
  230 FORMAT(20H NODAL INFORMATION ;///
     1       32H  NODE   DEPTH   TEMP   MATERIAL/
     2       32H -------------------------------//
     3       (I5,F10.3,F6.1,I7))
  235 FORMAT(///18H SOIL PROPERTIES ;///
     1   48H             MOISTURE     DRY       BULK     WATER/
     2   51H MATERIAL    CONTENT %    DENSITY   DENSITY  FRACTION/
     3  51H ---------------------------------------------------//
     4   (I5,F13.2,F12.1,F10.1,F10.2))
  240 FORMAT(///26H SOIL THERMAL PROPERTIES ;///
     1       46H MATERIAL    CF      CU      KF      KU      L/
     2       51H ---------------------------------------------------//
```

```
     3          (I5,4X,4F8.2,F10.1))
 260 FORMAT(25H1TEMPERATURE DISTRIBUTION///
     1       40H TIME                                DEPTH//
     2       (7X,15F8.3/))
 265 FORMAT(F7.2/7(7X,15F8.3/))
 270 FORMAT(40H1FROST PENETRATION AND HEAVE -THEORY NO.I3///
     1       32H   TIME     FROST          FROST/
     2       32H            PENETRATION    HEAVE/
     3       32H ------------------------------/
     4       (F8.1,2F12.4))
 280 FORMAT(3F10.3)
 290 FORMAT(2F10.3,F10.5)
 300 FORMAT(///44H ACTUAL FROST DEPTH AND FROST HEAVE VALUES ;///
     1       32H   TIME     FROST          FROST/
     2       32H            PENETRATION    HEAVE/
     3       34H --------------------------------//
     4       (F8.0,F12.3,F12.5))
 301 FORMAT(2F10.3)
 302 FORMAT(//31H % TIME AT LESS THAN 20 % ERROR,F10.2//
     1         16H AVERAGE % ERROR,F10.2)
      STOP
      END
```

INPUT:

Step 1: Heading (18A4) (HEAD)

Step 2: (5I5)
Number of materials (NM)
Number of nodes (N)
Number of temperature changes (TQ)
Number of prediction theories (THEORY)
Number of measured input data (NAPA)

Step 3: (2F10.3,F5.1,3F10.3)
Initial time increment (TPO)
Time for end of test (LT)
Factor for increasing the size of the time increment (TFAC)
Latent heat of water (LATW)
Density of water (GAMW)
External surface pressure (SUR)

Step 4: (2F10.3,I5) N cards
Nodal Depth (DEPTH)
Initial nodal temperature (TF)
Material no. directly below node (MAT)

Step 5: (4F10.3)
Unfrozen and frozen heat capacity (CUU) (CFF)
Unfrozen and frozen thermal conductivity (KUU) (KFF)

Step 6: (2F10.2)
Dry Density (GD)

Percent moisture content (W)
(Repeat steps 5 and 6 NM times)

<u>Step</u> <u>7</u>: (3F10.3) TQ cards
New upper boundary temperature (UPT)
New lower boundary temperature (LOT)
Time of temperature change (TIM)

<u>Step</u> <u>8</u>: (2F10.3,F10.5) NAPA cards
Time of frost heave and frost depth measurement (AT)
Measured frost depth (AD)
Measured frost heave (AH)

<u>Step</u> <u>9</u>: (2F10.3) THEORY cards
First frost heave parameter for each theory (AFH)
Second frost heave parameter for each theory (BFH)
(Repeat for each material)

The units used may be English or metric but must be compatable. Suggested units are: (metres hours °C kJ kN KPa) or (feet hours °F-32° BTU's lbs lbs/ft^2).

FORTRAN PROGRAM FOR METHOD 2 PREDICITONS

```
C
C     *****************************************************
C     *                                                   *
C     *  THIS PROGRAM PREDICTS FROST HEAVE IF THE FROST   *
C     *  PENETRATION AND/OR SURFACE TEMPERATURES ARE KNOWN  *
C     *  WITH RESPECT TO TIME                             *
C     *                                                   *
C     *****************************************************
C
      REAL AFH(9),BFH(9),HEAVE(50),H(50,9),HL(9),HS(9),POB(9)
     1,POBL(9),PAV(9),PSUM(9),WPERC(9),PTIME(9),PTOT(9)
      INTEGER HEAD(18)
      REAL WFR,KU,KF,L,BOTTEM,DEPTH,DELX,DL,WDENS,DDENS,MC,DELH,ISR
     1,TOTAL,Q,E,FI,RATIO,TS,STE,GAMMA,ETA,TEMP,RAT,DELHS,XL,XR,XM,GAMA
     2,HEV,HEAV,J,TW,TEMW,WTIME,HIN,PERC
      INTEGER THEORY,TIME,F
      FN(GAMMA)=STE/1.7725*(EXP(-1*(GAMMA**2))/ERF(GAMMA)-BOTTEM/TS*
     1EXP(-1*(RAT)*(GAMMA**2))/ERFC(SQRT(RAT)*GAMMA))-GAMMA
      READ105,HEAD
      READ110,THEORY,DDENS,MC
      IF (THEORY.LE.6) GOTO 5
      READ120,L,KU,KF,BOTTEM,TOTAL
    5 READ130,(AFH(I),BFH(I),I=1,THEORY)
      TEMW=0.0
      WTIME=0.0
      F=2
      HEAV=0.0
      HEV=0.0
      TIME=0
      DL=0.0
      TS=0.0
      DO 8 I=1,9
      POBL(I)=0.0
      HS(I)=0.0
      HL(I)=0.0
    8 CONTINUE
      WRITE(4,161)TIME,HEV,(HS(I),I=1,THEORY)
      WDENS=DDENS*(1+MC/100)
      WFR=(WDENS-DDENS)/9.81
   10 TIME=TIME+F
      READ140,DEPTH,HEAVE(TIME),TEMP
      IF (DEPTH.EQ.-1) GOTO 100
      DELX=DEPTH-DL
      RATE=DELX/F
      DO 15 I=1,THEORY
      POB(I)=(DEPTH*WDENS+HS(I)*9.0)/1000.0
      PAV(I)=(POB(I)+POBL(I))/2
   15 POBL(I)=POB(I)
      HI=WFR*DEPTH*0.09
      DL=DEPTH
```

```
C
C     PRESSURE * RATE MODEL
C
      IF (DELX.LE.0.0)ISR=0.0
      IF (DELX.LE.0.0) GOTO 17
      ISR=AFH(1)*((RATE*PAV(1))**(-1*BFH(1)))
   17 DELH=ISR*DELX
      H(TIME,1)=HL(1)+DELH
      HL(1)=H(TIME,1)
      IF (RATE.LE.0.0) RATE=0.0
      DELH=0.1
C
C     ALTERNATE PRESSURE * RATE MODEL
C
      DO 20 I=1,10
      ISR=AFH(2)*(((RATE+DELH)*PAV(2))**(-1*BFH(2)))
   20 DELH=ISR*(RATE*F+DELH)
      H(TIME,2)=HL(2)+DELH
      HL(2)=H(TIME,2)
C
C     TAKASHI ET AL. MODEL
C
      IF (DELX.LE.0) ISR=0.0
      IF (DELX.LE.0) GOTO 22
      ISR=AFH(3)/PAV(3)*(SQRT(BFH(3)/RATE)-1)
   22 H(TIME,3)=ISR*DELX+HL(3)
      IF (H(TIME,3).LT.0.0) H(TIME,3)=0.0
      HL(3)=H(TIME,3)
      DELH=0.1
C
C     ALTERNATE TAKASHI ET AL. MODEL
C
      DO 30 I=1,10
      ISR=AFH(4)/PAV(4)*(SQRT(BFH(4)/(RATE+DELH))-1)
   30 DELH=ISR*(RATE*F+DELH)
      H(TIME,4)=DELH+HL(4)
      IF (H(TIME,4).LT.0.0) H(TIME,4)=0.0
      HL(4)=H(TIME,4)
C
C     PENNER & WALTON MODEL
C
      ISR=1-EXP(-1*AFH(5)*TIME/DEPTH)
      H(TIME,5)=ISR*DEPTH
      IF (THEORY.EQ.5) GOTO 90
C
C     SHERIFF ET AL. MODEL
C
      TEMW=TEMP*TIME+TEMW
      WTIME=TIME+WTIME
      TW=TEMW/WTIME
      TS=(TS*(TIME-1)+TEMP*F)/TIME
      IF (TS.GE.5.0) J=0.8
      IF (TS.LT.5.0) J=(0.4+TS*0.08)
      H(TIME,6)=(AFH(6)**0.61)*(TIME**(0.83-0.063*TS))*J
```

```
      IF (THEORY.EQ.6) GOTO 90
C
C     KONRAD & MORGENSTERN MODEL
C
   41 SPO=AFH(7)*EXP(-1*BFH(7)*PAV(7))
      DO 42 I=1,15
      DELHS=SPO*TW/(DEPTH+HEV)*F
   42 HEV=DELHS+HS(7)+HI
      HS(7)=DELHS+HS(7)
      H(TIME,7)=HS(7)+HI
      IF (THEORY.EQ.7) GOTO 90
C
C     ARAKAWA EFFICIENCY MODEL
C
      IF (DELX.LE.0) DELHS=0.0
      IF (DELX.LE.0) GOTO 50
      E=AFH(8)-BFH(8)*SQRT(RATE*PAV(8))
      DO 45 I=1,20
      Q=KF*TW/(DEPTH+HEAV)-KU*BOTTEM/(TOTAL-DEPTH)
      DELHS=E*Q/L*24E6*F
   45 HEAV=DELHS+HS(8)+HI
      IF (DELHS.LT.0.0) DELHS=0.0
   50 HS(8)=HS(8)+DELHS
      HIN=-1*HI
      IF (HS(8).LT.HIN) HS(8)=HIN
      H(TIME,8)=HS(8)+HI
      IF (THEORY.EQ.8) GOTO 90
C
C     KNUTSON FREEZING INDEX MODEL
C
      FI=TEMP*F*24+FI
      ISR=MC/100.0*AFH(9)*((1/FI)**BFH(9))
      H(TIME,9)=ISR*DEPTH
   90 DO 95 I=1,6
   95 HS(I)=H(TIME,I)-HI
      IF (TIME.EQ.2) PRINT150,HEAD
      F=1
      PRINT160,TIME,HEAVE(TIME),(H(TIME,I),I=1,THEORY)
      DO 99 I=1,THEORY
      PERC=ABS(HEAVE(TIME)-H(TIME,I))/HEAVE(TIME)*100.0
      PSUM(I)=PERC*F+PSUM(I)
      WPERC(I)=PSUM(I)/TIME
      IF (PERC.LE.20.0) PTIME(I)=PTIME(I)+F
   99 PTOT(I)=PTIME(I)/TIME*100.0
      WRITE(4,161)TIME,HEAVE(TIME),(H(TIME,I),I=1,THEORY)
      GOTO 10
  105 FORMAT(18A4)
  110 FORMAT(I3,2F5.1)
  120 FORMAT(5F10.2)
  130 FORMAT(2F10.3)
  140 FORMAT(F10.1,F10.2,F10.1)
  150 FORMAT('1',18A4//
     144H TOTAL HEAVE (MEASURED AND PREDICTED) (MM) :///
     258H   DAY     ACTUAL     ISR        ISR      TAKASHI    TAKASHI  ,
```

```
     3         49H PENNER &    SHERIFF  KONRAD &    ARAKAWA    KNUTSON/
     458H           HEAVE               ALTERNATE              ALTERNATE,
     5         26H WALTON                MORG./
     658H__________________________________________________________,
     7         50H____________________________________________________/)
 160 FORMAT(' ',/I5,10F10.2)
 161 FORMAT(I5,10F10.2)
 100 PRINT170,(PTOT(I),I=1,THEORY)
     PRINT180,(WPERC(I),I=1,THEORY)
 170 FORMAT(//14H TIME AT 20 % ,9F10.2)
 180 FORMAT(//14H AVE % ERROR  ,9F10.2)
     STOP
     END
```

INPUT:

Step 1: Heading (18A4) (HEAD)

Step 2: (I3,2F5.1)
Number of prediction theories (THEORY)
Dry density of the soil kN/m^3 (DDENS)
Soil moisture content % (MC)

Step 3: (5F10.2)
Latent heat of fusion per unit volume of soil kJ/m^3 (L)
Unfrozen thermal conductivity kJ/hr m °C (KU)
Frozen thermal conductivity kJ/hr m °C (KF)
Lower boundary temperature °C (BOTTEM)
Total depth of the sample mm (TOTAL)

Step 4: (2F10.3) Repeat THEORY times
First frost heave prediction parameter (AFH)
Second frost heave prediction parameter (BFH)

Step 5: (F10.1,F10.2,F10.1)
Measured depth of frost penetration mm (DEPTH)
Measured surface heave mm (HEAVE)
Measured surface temperature °C (TEMP)
(Repeat step 5 for values measured every day of the test beginning day number 2)

Step 6: (F10.1)
Place -1.0 at end of data

Frost heave parameters for both Method 1 and Method 2 were derived using a frost penetration rate measured in mm/day; pressure measured in KPa; temperature gradient measured in °C/mm; and freezing index measured in °C days.